

Utah State University

DigitalCommons@USU

All Graduate Theses and Dissertations

Graduate Studies

5-2015

Catalytic Pyrolysis of Olive Mill Wastewater Sludge

Hamza Abdellaoui
Utah State University

Follow this and additional works at: <https://digitalcommons.usu.edu/etd>

 Part of the [Environmental Engineering Commons](#)

Recommended Citation

Abdellaoui, Hamza, "Catalytic Pyrolysis of Olive Mill Wastewater Sludge" (2015). *All Graduate Theses and Dissertations*. 4468.

<https://digitalcommons.usu.edu/etd/4468>

This Thesis is brought to you for free and open access by the Graduate Studies at DigitalCommons@USU. It has been accepted for inclusion in All Graduate Theses and Dissertations by an authorized administrator of DigitalCommons@USU. For more information, please contact digitalcommons@usu.edu.



CATALYTIC PYROLYSIS OF OLIVE MILL WASTEWATER SLUDGE

by

Hamza Abdellaoui

A thesis submitted in partial fulfillment
of the requirements for the degree

of

MASTER OF SCIENCE

In

Biological Engineering

Approved:

Foster A. Agblevor, PhD
Major Professor

Isaa Hamud, MS, PE
Committee member

Ronald Sims, PhD
Committee member

Mark Mclellan, PhD
Vice President for Research
and Dean of the School of
Graduate Studies

UTAH STATE UNIVERSITY
Logan, Utah

2015

Copyright © Hamza Abdellaoui 2015

All Rights Reserved

ABSTRACT

Catalytic Pyrolysis of Olive Mill Wastewater Sludge

by

Hamza Abdellaoui, Master of Science

Utah State University, 2015

Major professor: Dr. Foster Agblevor
Department: Biological Engineering

Olive mill wastewater sludge (OMWS) is the solid residue that remains in the evaporation ponds after evaporation of the majority of water in the olive mill wastewater (OMW). OMWS is a major environmental pollutant in the olive oil producing regions. Approximately 41.16 wt. % of the OMWS was soluble in hexanes (HSF). The fatty acids in this fraction consist mainly of oleic and palmitic acid. Catalytic pyrolysis of the OMWS over red mud and HZSM-5 has been demonstrated to be an effective technology for converting this waste material into fuel. Red mud-catalyzed pyrolysis gave higher organics yields than the HZSM-5 catalysis. The viscosity as well as the oxygen content of the catalytic pyrolysis oils were significantly lower than those of the non-catalytic oil. The reaction pathways of red mud and HZSM-5 were different. The catalytic pyrolysis of the HSF gave an acidic oil with low viscosity and high energy content, and was nitrogen and sulfur free, whereas the catalytic pyrolysis of the solid residue after hexanes extraction (SR) gave an oil with higher viscosity, close to neutral pH, lower energy content, and had

high nitrogen content and traces of sulfur.

(153 pages)

PUBLIC ABSTRACT

Catalytic Pyrolysis of Olive Mill Wastewater Sludge

Hamza Abdellaoui

From 2008 to 2013, an average of 2,821.4 kilotons/year of olive oil were produced around the world. The waste product of the olive mill industry consists of solid residue (pomace) and wastewater (OMW). Annually, around 30 million m³ of OMW are produced in the Mediterranean area, 700,000 m³ year⁻¹ in Tunisia alone. OMW is an aqueous effluent characterized by an offensive smell and high organic matter content, including high molecular weight phenolic compounds and long-chain fatty acids. These compounds are highly toxic to micro-organisms and plants, which makes the OMW a serious threat to the environment if not managed properly. The OMW is disposed of in open air evaporation ponds. After evaporation of most of the water, OMWS is left in the bottom of the ponds. In this thesis, the effort has been made to evaluate the catalytic pyrolysis process as a technology to valorize the OMWS. The first section of this research showed that 41.12 wt. % of the OMWS is mostly lipids, which are a good source of energy. The second section proved that catalytic pyrolysis of the OMWS over red mud and HZSM-5 can produce green diesel, and 450 °C is the optimal reaction temperature to maximize the organic yields. The last section revealed that the HSF was behind the good fuel-like properties of the OMWS catalytic oils, whereas the SR hindered the bio-oil yields and quality.

ACKNOWLEDGMENTS

I'd like to thank my major professor, Dr. Foster A. Agblevor, for his continuous support, patience, and tough love for all of his students. I'd like to thank my committee members, Dr. Ronald Sims and Mr. Isaa Hamud, for their support and willingness to be a member of my committee. I shouldn't forget to thank Dr. Seung-Soo Kim for his advice and help with the GC/MS analysis of my samples. I would like to express my appreciation for Utah State University for making it possible for me and other international students to pursue our higher education in the U.S.A, and the Biological Engineering staff for their unconditional help and advice. Thank you all.

I also would like to thank my wife, Tatiana Drugova, for her unconditional love and support. I wouldn't have made it without her. I'd like to thank the Abdellaoui family for their support and for believing in me. Last but not least, to all my colleagues in the Bioinnovation center, thank you for your help whether it was technical or psychological.

Hamza Abdellaoui

CONTENTS

	Page
ABSTRACT.....	iii
PUBLIC ABSTRACT	v
ACKNOWLEDGMENTS	vi
LIST OF TABLES	xii
LIST OF FIGURES	xv
CHAPTER	
1. LITERATURE REVIEW	1
1.1. History of olive fruit	1
1.2. Manufacturing process of olive oil	1
1.2.1. Cold press batch process	2
1.2.2. Centrifugation continuous process.....	2
1.2.2.1. Three-phase process.....	3
1.2.2.2. Two-phase process.....	3
1.3. Worldwide generation of olive mill wastewater.....	5
1.4. Olive mill industry waste product handling.....	6
1.5. Management and handling of the olive mill wastewater	8
1.5.1. Composition and characteristics of the OMWW	8
1.5.2. Direct application of the OMWW.....	9

1.5.3. Processing of the OMWW	9
1.6. Recovery/production of high-added-value products from the OMWW	10
1.7. Pyrolysis: a potential thermochemical process for the valorization of OMWW	12
1.7.1. Pyrolysis.....	12
1.7.2. Fast pyrolysis	14
1.8. Applications of the fast pyrolysis bio-oil.....	15
1.9. Application of bio-oil for energy/power generation	17
1.10. Problem statement.....	20
1.11. Research hypothesis.....	20
1.12. Research goals and objectives	21
1.13. References.....	21
2. CHARACTERIZATION OF THE OLIVE MILL WASTEWATER SLUDGE.....	29
Abstract.....	29
2.1. Introduction.....	30
2.2. Materials and methods	31
2.2.1. Materials	31
2.2.2. Methods.....	32
2.2.5. Moisture	32
2.2.4. Ash	32

2.2.5. Volatile organic matter and fixed carbon.....	33
2.2.6. Ultimate analysis.....	34
2.2.7. Higher heating value	35
2.2.8. pH.....	35
2.2.9. Sequential extraction.....	35
2.2.10. Hexanes extraction of the OMWS	36
2.2.11. Optimal extraction time	36
2.2.12. Elemental composition of the HSF and the SR	37
2.2.13. Gas chromatography/mass spectroscopy	37
2.2.14. Saponification value.....	38
2.3. Results and discussion	39
2.3.1. Proximate analysis of the OMWS.....	39
2.3.2. Ultimate analysis of the OMWS	40
2.3.3. Solvent extraction of the OMWS.....	41
2.3.4. GC/MS analysis of the HSF and the ESF	48
2.3.5. Saponification value of the HSF	54
2.4. Conclusions.....	54
2.5. References.....	55
3. CATALYTIC PYROLYSIS OF OLIVE MILL WASTEWATER SLUDGE	58
Abstract	58

3.1. Introduction.....	59
3.2. Experimental.....	60
3.2.1. Feedstock	60
3.2.2. Catalysts.....	61
3.2.3. Pyrolysis of olive mill wastewater sludge	61
3.2.4. Gas analysis	64
3.2.5. Bio-oils characterization	64
3.3. Results and discussion	65
3.3.1. Catalyst characterization.....	65
3.3.2. Pyrolysis yields	66
3.3.2.1. Fast pyrolysis of the OMWS	66
3.3.2.2. Effect of catalyst on the pyrolysis products distribution	68
3.3.2.3. Effect of reaction temperature on the performance of the catalysts	69
3.3.3. Characterization of the pyrolysis oils	70
3.3.4. Pyrolysis gas product composition	89
3.4. Conclusions.....	100
3.5. References.....	101
4. CATALYTIC PYROLYSIS OF OLIVE MILL WASTEWATER SLUDGE	
FRACTIONS	104
Abstract	104

4.1. Introduction.....	105
4.2. Experimental.....	107
4.2.1. Materials	107
4.2.2. Catalytic pyrolysis of the OMWS fractions and extra virgin olive oil	107
4.2.3. Gas analysis	108
4.2.4. Bio-oil characterization.....	108
4.3. Results and discussion	110
4.3.1. Pyrolysis yields	110
4.3.2. Bio-oils characterization	113
4.3.3. Pyrolysis gas product composition	126
4.4. Conclusions.....	133
4.5. References.....	133
5. SUMMARY AND CONCLUSIONS	135

LIST OF TABLES

Table	Page
1 Comparison of the olive oil manufacturing processes (Aragon and Karagouni, 2000)	5
2 Example of material balance of the olive mill industry waste product (Toscano and Montemurro, 2012)	7
3 Typical product yields (dry wood basis) obtained by different modes of pyrolysis of wood (modified from (Bridgwater, 2000))	14
4 Proximate and ultimate analysis of the OMWS.....	42
5 Elemental composition of the HSF and the SR	46
6 ¹³ C NMR integration for the HSF and EVOO	47
7 Composition of the hexanes soluble fraction determined by GC/MS	50
8 Composition of the 95 vol% ethanol soluble fraction determined by GC/MS ..	52
9 Saponification value and saponifiables yield (wt.%) of the hexanes soluble fraction	54
10 Properties of the red mud and the HZSM-5.....	66
11 Product yields distribution for the catalytic/conventional pyrolysis of the OMWS	72
12 Properties of the ESP bio-oils for the catalytic/conventional pyrolysis of the OMWS	73

13	Elemental composition of the ESP oils from the conventional/catalytic pyrolysis of the OMWS at 450 °C.....	74
14	Gas product composition (mole % of total gases) from the conventional/catalytic pyrolysis of the OMWS over red mud and HZSM-5	91
15	Gas product composition (wt. %, dry basis) from the conventional/catalytic pyrolysis of the OMWS over red mud and HZSM-5.....	94
16	Products yield from the cracking of water over regenerated red mud under carbon monoxide atmosphere	95
17	Gas product composition from the cracking of water over regenerated red mud under carbon monoxide atmosphere	96
18	Product yield distribution from the conventional/catalytic pyrolysis of the OMWS fractions at 450 °C and using three times the minimum fluidization velocity.....	115
19	Characteristics of the ESP bio-oils from the conventional/catalytic pyrolysis of the OMWS fractions at 450 °C and using three times the minimum fluidization velocity.....	116
20	Integration of the ¹³ C NMR spectra of bio-oils from the conventional/catalytic pyrolysis of the HSF	121
21	Integration of the ¹³ C NMR spectra of bio-oils from the conventional/catalytic pyrolysis of the solid residue	125
22	Integration of the ¹³ C NMR spectrum of the ESP oils from the regenerated red mud catalyzed pyrolysis of the HSF and the EVOO at 450 °C	125

23 Gas product composition (wt. %) for the conventional/catalytic pyrolysis of the OMWS fractions and EVOO at 450 °C, using three times the minimum fluidization velocity	131
---	-----

LIST OF FIGURES

Figure	Page
1 Thermogravimetric analysis (TGA) and differential thermal analysis (DTA) of OMWS under nitrogen gas (L/min).	41
2 Yields of various OMWS extractives.....	43
3 Yield of HSF as a function of extraction time.....	44
4 ¹³ C NMR spectra of the HSF fraction extracted from the OMWS for one hour using (a) Soxhlet extraction and (b) boiling extraction.	45
5 ¹³ C NMR of the (a) HSF and (b) the extra virgin olive oil.	48
6 Chromatogram from the GC/MS analysis of the hexanes soluble fraction of the OMWS.....	50
7 Chromatogram from the GC/MS analysis of the 95 vol% ethanol soluble fraction of the OMWS.....	51
8 FT-IR spectra of the bio-oils from the (a) non-catalytic, (b) red mud catalyzed, and (c) HZSM-5 catalyzed pyrolysis of OMWS mixture at 450 °C.	77
9 ¹ H NMR spectra for the bio-oils from the (a) non-catalytic, (b) red mud catalyzed, and (c) HZSM-5 catalyzed pyrolysis of OMWS-wood biochar mixture at 450 °C.	80
10 ¹ H NMR spectra for the bio-oils from the (a) non-catalytic, (b) red mud catalyzed, and (c) HZSM-5 catalyzed pyrolysis of OMWS-wood biochar mixture at 400 °C.	81

11	¹ H NMR spectra for the bio-oils from the (a) non-catalytic, (b) red mud catalyzed, and (c) HZSM-5 catalyzed pyrolysis of OMWS-wood biochar mixture at 500 °C.	82
12	¹³ C NMR spectra of the ESP oil from the catalytic pyrolysis at 450 °C of the OMWS over (a) fresh red mud, (b) calcined red mud, and (c) regenerated red mud.	86
13	¹³ C NMR spectra of the ESP oil from the catalytic pyrolysis at 400 °C of the OMWS over (a) fresh red mud, (b) calcined red mud, and (c) regenerated red mud.	88
14	¹³ C NMR spectra of the ESP oil from the catalytic pyrolysis at 500 °C of the OMWS over (a) fresh red mud, (b) calcined red mud, and (c) regenerated red mud.	90
15	FTIR spectrum for the liquid in condenser one from the water-gas-shift reaction on regenerated red mud under CO atmosphere.	98
16	CO/CO ₂ ratio for the conventional and catalytic pyrolysis of the OMWS at 450 °C.	100
17	¹ H NMR spectra of the HSF ESP oil from the (a) fast pyrolysis, (b) catalytic pyrolysis over regenerated red mud, (c) and catalytic pyrolysis over HZSM-5	118
18	¹ H NMR spectra of the SR ESP oil from the (a) fast pyrolysis, (b) catalytic pyrolysis over regenerated red mud, (c) and catalytic pyrolysis over HZSM-5.	119

19	¹³ C NMR spectra of the HSF ESP oil from the (a) fast pyrolysis, (b) catalytic pyrolysis over regenerated red mud, (c) and catalytic pyrolysis over HZSM-5.....	122
20	¹³ C NMR spectra of the SR ESP oil from the (a) fast pyrolysis, (b) catalytic pyrolysis over regenerated red mud, (c) and catalytic pyrolysis over HZSM-5.....	124
21	¹³ C NMR of the ESP oil from the regenerated red mud catalyzed pyrolysis of the (a) HSF and (b) the EVOO at 450 °C.....	126
22	CO/CO ₂ ratio of the conventional/catalytic pyrolysis of the HSF	132
23	CO/CO ₂ ratio of the conventional and catalytic pyrolysis of the SR	132

CHAPTER 1

LITERATURE REVIEW

1.1. History of olive fruit

Olive is an Asia Minor originated wild fruit. It was spread by the Phoenicians to the Mediterranean countries in the 16th century through the Greek isles. The Greeks were the first to cultivate the olive trees, which were introduced to their mainland between the 12th and the 14th century. By 1560, the olive tree was being cultivated in the New World (“International olive council,” 1959). Numerous are the reasons behind the commitment of several civilization to the cultivation of olives. On the first hand, olive trees can grow on their own without the need of fertilizer, they can live for decades and still produce olive fruits. In addition, olive fruits are known to have several therapeutic, nutritional and cosmetic benefits (“Herbs-Treat and Taste,” 2010).

1.2. Manufacturing process of olive oil

There are two main processes used by olive mill industry to produce olive oil: (1) the cold press batch process, (2) and the centrifugation continuous process. The continuous centrifugation process can be divided into two subcategories; the three-phase process and the two-phase process.

1.2.1. Cold press batch process

The cold press process is the traditional way of extracting olive oil from the olive fruits using mechanical pressure. The first step of this process consists on crushing the olive fruits to form a paste. The paste is spread on fiber mats, the mats are then piled and placed in the press.

As pressure is applied to the paste, the oil percolation is enhanced by running water on the sides of the mats. The oil is then separated from water by decantation or by mean of vertical centrifugation. In addition to the low operation cost, the cold press process produces a relatively dry solid waste (pomace), which is easy to handle. However, the traditional method is labor-intensive and time consuming.

Moreover, the oil produced by this process is at a great risk of being contaminated due to non-properly cleaned mats and/or oxidation (Vossen, 2007).

1.2.2. Centrifugation continuous process

In order to increase the efficiency of the olive extraction process and reduce the exposure of the paste to the air, modern decanters were adopted. These decanters are large centrifuges that allow the separation of solids, vegetable water, and oil in much less time. This modern process makes the olive oil process continuous and decreases the risk of undesirable compounds forming in the oil due to oxidation from the air and/or the degradation due to enzymes present in the vegetable water. There are two types of centrifugation process i.e. the three-phase process and the two-phase process.

1.2.2.1. Three-phase process

In the three-phase process, the olive fruits are crushed to form a paste. The paste is then stirred at 27 °C to improve the oil droplets aggregation. This step is called malaxation. The paste is then pumped to a large horizontal centrifuge called decanter, where water is added to facilitate the flow of the paste to the decanter and the separation of oil from the solid particles. The decanter has three outlets one for the olive oil, another for the olive mill wastewater, and a third outlet for the solids (pomace).

The three-phase process produces large amount of olive mill wastewater (OMWW) containing flavors, antioxidants and polyphenols washed off from the olive oil. Due to the complex composition of the OMWW, managing such waste product became a challenge (Aragon and Karagouni, 2000).

1.2.2.2. Two-phase process

In order to reduce the large quantity of OMWW produced from the three-phase process, the two-phase process was introduced to the olive oil industry in the late 90s. Similar to the three-phase process, the two-phase process uses large horizontal centrifuge (decanter) to separate the oil from the solids and vegetable juices. By contrast, the two-phase process does not require the addition of water to the olive paste. Consequently, the OMWW quantities produced from such process are very low, but the solid waste (pomace) is wet and hard to process.

The oil production from the two-phase process is less efficient than the three-phase one because there is no added water to enhance the separation of the oil from the paste in the decanter. However, the olive oil produced from the two-phase process has more polyphenol and overall flavor compared to the three-phase process oil (Vossen, 2007), which explains why Spain (the major olive oil producer in the world) adopted the two-phase process despite its lower efficiency compared to the three-phase process (Kotronarou and Méndez, 2003).

Table 1 represents the material and energy balance for each of the three processes by which olive oil is being produced around the world. The traditional cold press process consumes less energy and requires less complicated equipment, but it has lower productivity (batch process), labor-intensive, and there is high contamination risk of the oil (oxidation and enzymatic degradation).

The three-phase process is a continuous process with much higher productivity than the traditional cold press process, however, the former produces large quantity of OMWW (100 to 120 wt.% of the olive mass) and requires around two times the energy required by the traditional process. The two-phase process produces almost no OMWW, however it is less efficient than the three-phase process, and the waste product is a semisolid residue (wet pomace) that is hard to deal with.

Table 1

Comparison of the olive oil manufacturing processes (Aragon and Karagouni, 2000)

PRODUCTION PROCESS	INPUT	AMOUNT OF INPUT	OUTPUT	AMOUNT OF OUTPUT
Traditional pressing process	Olives	1000 kg	oil	200 kg
	Washing water	0.1 — 0.12 m ³	solid waste (c. 25 % water + 6 % oil)	400 kg
	Energy	40 — 63 kWh	waste water (c. 88 % water)	600 kg
Three-phase decanter	Olives	1000 kg	oil	c. 200 kg
	Washing water	0.1— 0.12 m ³	solid waste (c. 50 % water + 4 % oil)	c. 500 — 600 kg
	Fresh water for decanter	0.5 —1 m ³	waste water (c. 94 % water + 1 % oil)	c. 1000- 1200 kg
	Water to polish the impure oil	c. 10 kg		
	Energy	90 —117 kWh		
Two-phase decanter	Olives	1000 kg	oil	200 kg
	Washing water	0.1 — 0.12 m ³	solid waste (c. 60 % water + 3 % oil)	800 — 950 kg
	Energy	< 90 - 117 kWh		

c.: calculated value.

1.3. Worldwide generation of olive mill wastewater

From 2008 to 2013, an average of 2,821.4 kilotons/year of olive oil were produced around the world. Around 98 % of that olive oil was produced by Mediterranean countries especially Spain which contributed by 43% of the world olive oil production (“International olive council,” 1959).

These statistics highlight not only the importance of olive oil industry in the Mediterranean basin, but also the abundance of its resulting waste products. The waste product of the olive mill industry consists of solid residue (pomace) and wastewater (OMWW).

The volume of OMWW produced depends on the extraction process. While the traditional press process produces 0.4-0.6 m³ of OMW/ton of olives, the continuous three-phase process produce more diluted wastewater (average of 1 m³ of OMWW/ton of olives) (Ministry of the Environment, 2000) because of the considerable amount of warm water used to wash the paste before extraction of the olive oil. In order to reduce the OMWW produced from the three phase process, the two-phase process was established. In this process, much less water is used in the decanter to separate the oil from the pomace. On average 0.05-0.06 m³ of OMWW/ton of olives is produced from the two-phase process.

OMWW is an aqueous effluent containing olive skin (Vitolo et al., 1999) characterized by an offensive smell and high organic matter content including high molecular weight phenolic compounds and long-chain fatty acids (Gonzalez et al., 1990). These compounds are highly toxic to micro-organisms and plants, which makes the OMWW a serious threat to the environment if not managed properly.

1.4. Olive mill industry waste product handling

As for the handling of the waste products of the olive oil industry i.e. olive pomace and olive mill wastewater, several techniques are adopted. The olive pomace (the solid waste of olive oil industry) generated by the traditional press process and the three-phase process

is called virgin pomace and it contains residual oil (6% and 4%, respectively). Therefore, it is processed in the olive pomace industry to extract the oil using hexanes as solvent.

After extraction of the residual oil from the virgin pomace, the defatted olive pomace is dried and used for energy recovery, landfilled, or used for agricultural application such as land fertilizer (Caputo et al., 2003), and/or as animal feed compliment (Nasopoulou and Zabetakis, 2013). Another interesting application of the olive pomace is the production of ethanol and recovery of high value phenols (Ballesteros et al., 2002). As for the two-phase olive pomace, and due to its high moisture content (Table 1 and 2), it is not profitable to process it in the pomace industry. It was suggested that composting would be the best option to handle such waste product (Azbar et al., 2004).

Table 2

Example of material balance of the olive mill industry waste product (Toscano and Montemurro, 2012)

Milling technology	H ₂ O added (%)	Pomace (kg/100 kg olive)	Pomace moisture (%)	Waste waters (kg/100 kg olive)
3 phase continuous	50	55-57	48-54	80-110
Traditional	0-10	30-35	25-30	56-58
2 phase	0-10	75-80	60-70	10

The olive mill wastewater is the liquid waste product of the olive oil industry. During the processing of the olive fruits, the OMWW generated is 1.8 and 1.7 times higher than the olive pomace produced using the traditional cold press and the three-phase process, respectively. The OMWW consists of 88% and 95% water for the traditional and the three-

phase process, respectively.

Unlike the olive pomace, the olive mill wastewater is much more difficult to manage due to:

- Its high water content ranging from 88 to 94% of the OMWW (Table 1), which rules out the possibility of energy recovery application.
- Its high chemical oxygen demand to biological oxygen demand ratio ranging from 2.5 to 5, which makes the direct biological treatment of OMW impossible because of the low efficiency of the process (Aragon and Karagouni, 2000).
- The presence of recalcitrant organic compounds (water soluble phenols and polyphenols) washed off from the olive paste, which makes the agricultural application of the OMWW as land fertilizer a risky task due to the phytotoxic effect of these organic compounds (McElhatton and do Amaral, 2011).

1.5. Management and handling of the olive mill wastewater

The OMWW consists of olive juice, added water, fine olive pulp, and unrecoverable oil (McElhatton and do Amaral, 2011). Depending on the variety of the olive fruit and the extraction process, the characteristics of the OMWW can vary.

1.5.1. Composition and characteristics of the OMWW

Typically, the OMWW consists of 88-94% water, 4-16% organic compounds (oils, proteins, polysaccharides polyalcohols organic acids and phenolic compounds), and 0.4-2.5% mineral salts (mainly potassium and sodium salts) (McElhatton and do Amaral, 2011).

The high organic matter concentration and the presence of polyphenols make the OMWW a natural resource and a threat to the environment at the same time. While the high organics load and the polyphenols are considered a threat to the environment (high COD/BOD and phytotoxicity), scientist have managed to find way to valorize the OMWW by recycling the water in the waste product and using the solid residue as a fertilizer or for the production of antioxidants. When dried, the solid residue (sludge) can be used for biogas production (anaerobic digestion) or as fuel for energy production (combustion) (Azbar et al., 2004).

1.5.2. Direct application of the OMWW

In order to solve the environmental threat of the OMWW, several attempts to revalorize such waste product were conducted. The direct application of the OMWW as agricultural land fertilizer have failed because of the phytotoxic effect of the water-soluble phenols and polyphenols. Another attempt of using the dried OMWW as animal feed had also failed because of its high concentration of phenolic compound and sodium (Hamdi, 1993), which caused diarrhea for the ruminants.

However, the use of *Aspergillus* sp and *Geotricum candidum* for single cell protein production from OMWW was successful and resulted in a highly digestible biomass with a protein content of 30% (Hamdi, 1993).

1.5.3. Processing of the OMWW

The processing techniques used to treat the OMWW can be classified into three categories; physical treatment, chemical treatment, and biological treatment. The physical

treatment range from the simple separation of the solid particulates from the bulk wastewater (evaporation, settling, centrifugation, filtration and floatation) to the more advanced membrane separation of macromolecules and colloids from the filtered wastewater.

The chemical treatment includes coagulation/floatation and chemical oxidation used to remove the COD, and adsorption and Ion-exchange techniques that selectively remove undesirable compounds in the OMWW such as coloring substances, long-chain fatty acids, phenols, polyphenols, etc. As for the biological treatment it includes the anaerobic and aerobic digestion (McElhatton and do Amaral, 2011).

While the aerobic digestion of the OMWW produces stable sludge and require high oxygen intake, the anaerobic treatment produces valuable biogas and less sludge. However, the phenolic compounds have an adverse effect on both aerobic (Olori et al., 1990; Ragazzi and Veronese, 1973) and anaerobic microorganisms (Beccari et al., 1998; Boari et al., 1984; Hamdi, 1991a, 1991b). Long-chain fatty acids were also proven to irreversibly inhibit the anaerobic microorganisms (Angelidaki and Ahring, 1992). Therefore pretreatment of the OMWW is necessary in order to increase the efficiency of the biological treatment.

1.6. Recovery/production of high-added-value products from the OMWW

Some of the organic compounds in the OMWW (water-soluble phenols, polyphenols, and long-chain fatty acids) are considered inhibitory and toxic to microorganisms. However, when properly recovered/converted, these compound are valuable.

Polyphenols are natural antioxidants that can be used to improve the nutritional properties and preservation of food. Around 98% of the polyphenols in olive fruit are

washed-off in the OMWW (Rodis et al., 2002). The extraction of polyphenols can be done using organic solvents such as ethyl acetate resulting in 90% phenols recovery (Khoufi et al., 2008), or using membrane filtration. Both techniques require the pre-separation of the solids from the wastewater to improve upon the recovery of polyphenols. Pectins are another valuable class of compounds that can be used as gelling agents, emulsifiers and stabilizers in the food industry (McElhatton and do Amaral, 2011). Coimbra and co-workers reported that arabinose rich pectic polysaccharides were the major components of the cell wall material prepared from olive pulp (Coimbra et al., 1994).

Enzyme production on OMWW was reported by several authors (D'Annibale et al., 2006a, 2006b; Fenice et al., 2003; Petruccioli et al., 1988; Scioli and Vollaro, 1997). These enzymes include lipase, lignin-oxidizing enzymes, and pectic enzymes.

The production of lipase over undiluted OMWW using 12 different fungal strains was investigated by D'Annibal and co-workers (D'Annibale et al., 2006a, 2006b). They reported that all 12 fungus strains, used in their study, were able to grow in the OMWW and produce lipase, with *C. cylindracea* being the most promising.

Lignin-oxidizing enzymes (lacasse, lignin peroxidase, and manganese-dependent peroxidase) are of industrial interest because they result in the delignification of lignocellulosic biomass resulting in greater exposure of the substrate (carbohydrate) to the fermentation microorganisms. Such enzymes can be used for ethanol production (Elander and Hsu, 1995), paper products industry (Widsten and Kandelbauer, 2008), and the decolorization of industrial wastewater (Rodríguez Pérez et al., 2008).

Pectinase is another useful enzyme that can be produced using pretreated OMWW (Petruccioli et al., 1988). Pectinase has the ability of breaking down structural polymers (pectins) of plant cells. Moreover, Petruccioli and co-workers reported that the addition of purified pectinase to the olive paste during the malaxation phase can increase the olive oil yield by 10% (Petruccioli et al., 1988).

There are several bioproducts that can be produced from the OMWW. Biofuels can be obtained through the thermochemical conversion (pyrolysis) of concentrated OMWW to produce liquid fuels (Petarca et al., 1997) or the biochemical conversion of pretreated OMWW to produce ethanol (Massadeh and Modallal, 2008; Oliveira, 1974).

The OMWW has been used for the production of biopolymers such as polyhydroxyalkanoates (PHAs) (Gonzalez-Lopez et al., 1996; Massadeh and Modallal, 2008; Pozo et al., 2002), pullulan (Israilides, 1994), xanthan (Lopez and Ramos-Cormenzana, 1996; López et al., 2001).

Mercader and co-workers investigated the production of biosurfactant (rhamnolipid) over the OMWW using aerobic bacteria and they reported the suitability of the diluted OMWW for the production of rhamnolipids. They also reported that the COD of the OMWW was reduced by 50% within 72 hours (Mercader et al., 1993).

1.7. Pyrolysis: a potential thermochemical process for the valorization of OMWW

1.7.1. Pyrolysis

Pyrolysis is the thermochemical breakdown of the organic fraction of biomass in the limited presence or total absence of oxidizing agents. The products of the pyrolysis reaction consist of three simpler compounds i.e. bio-char, bio-oil, and non-condensable gases.

Depending on the heating rate of the biomass and the residence time of the organic vapors, pyrolysis can be classified as slow, intermediate or fast (Table 3).

While low temperature and long residence time favor the production of char, moderate temperature (~500 °C) and short residence time (~1s) result in maximizing the liquid yield (up to 75%). The liquid product of pyrolysis (bio-oil) is considered as a source of high value chemicals and energy carrier (Czernik and Bridgwater, 2004). It has higher energy density compared to the original feedstock and is easier to transport (Aglevor et al., 1995). It is a complex mixture of organic compounds and water.

The water in the bio-oil consists of pyrolytic water (dehydration reaction) and moisture in the biomass (Bridgwater, 2012). The organic fraction of the bio-oil contains a wide variety of oxygenated hydrocarbons such as alcohols, aldehydes, phenols, acids, ketones, ethers, sugars, and aromatics in addition to alkenes (Vamvuka, 2011).

The fast pyrolysis process is designed to maximizing the liquid product yield by carefully controlling the reaction temperature (~500 °C), very high heating rate of the finely ground biomass (< 3 mm) to insure a very high heat transfer, minimizing the residence time of the pyrolysis vapors in the reactor to avoid secondary reactions, rapid separation of the char from the pyrolysis vapors to minimize their cracking, and finally insure the quenching of the vapors to obtain the bio-oil (Bridgwater, 2012).

Table 3

Typical product yields (dry wood basis) obtained by different modes of pyrolysis of wood (modified from (Bridgwater, 2000))

Mode	Conditions	wt.%		
		Liquid	Char	Gas
Slow-Torrefaction	~290 °C, solids residence time ~30 mins	-	82	18
Slow-Carbonization	~400 °C, long vapour residence time hrs -> days	30	35	35
Intermediate	~500 °C, hot vapour residence time ~10-30 s	50	25	25
Fast	~500 °C, short hot vapour residence time ~1 s	75	12	13

1.7.2. Fast pyrolysis

Fast pyrolysis is a very promising thermochemical process that converts feedstock to a liquid fuel product called bio-oil along with biochar and non-condensable gases. Although fast pyrolysis can produce high bio-oil yield that can reach up to 75% (Onay and Koçkar, 2006), the quality of this bio-oil such as its high water content, acidity and low heating value restricts its application (Czernik and Bridgwater, 2004).

Olive mill wastewater sludge (OMWS), is the solid residue that remains in the evaporation ponds when the water evaporates from the OMWW with time. This dry organic matter can be a potential feedstock for bio-fuel production. In fact, pyrolysis of OMWS give a bio-oil characterized by a high heating value, high pH and low moisture and sugar contents. The feasibility was first proved by Dr. Kamel Halouani and Dr. Foster Agblevor, who produced such bio-oil from OMWS. However, the viscosity and stability of the produced bio-oil makes it less competitive with petroleum crude.

1.8. Applications of the fast pyrolysis bio-oil

The production of valuable chemicals from the pyrolysis whole bio-oil was adopted for many centuries, until the discovery of cheaper alternative feedstock derived from coal, crude oil or natural gas (Czernik and Bridgwater, 2004). However, wood fast pyrolysis bio-oil contains hundreds of valuable organic compounds, when recovered at high purity.

Unfortunately, the recovery of those valuable chemicals is neither practical nor cost effective because of the complexity of the bio-oil, thus the technical difficulty of selective separation of specific compounds. Therefore, easier and cheaper technologies that aims for the production of useful chemicals from the whole bio-oil were developed. Some examples of such technologies were reported in the literature.

The production of biodegradable fertilizer with slow-release nitrogen from the whole pyrolysis bio-oil was reported by (Bridgwater, 2000; Radlein et al., 1997). They took advantage of the high content of carbonyl groups in the bio-oil by reacting it with urea, ammonia or other $-NH_2$ containing materials, which resulted in the formation of various amide and imide bonds, allowing up to 10% nitrogen incorporation in the organic matrix (bio-oil). Another application of the whole bio-oil, is the production of organic compounds that can capture undesirable sulfur oxides and nitrogen oxides generated from coal combustion. These compounds can be obtained by reacting lime with the carboxylic acids and phenols present in the bio-oil. A concrete example of such application is the patented BioLime produced by Dynamautive Corporation.

Wood preservation can be achieved by impregnating the wood with bio-oil (Freel and Graham, 2002). This preservation effect is due to the terpenoid and phenolic compounds that act as fungicides and insecticides (Kasper et al., 1983). The bio-oil consists of two phases i.e. water soluble phase and water insoluble phase.

While the former has been used to produce meat browning agents (Kasper et al., 1983) and environmentally friendly road de-icers (Oehr et al., 1993), the latter, consisting of lignin degradation oligomers, brings lower cost and toxicity when used as a substitute for phenols in phenol-formaldehyde resins (Giroux et al., 2001; Himmelblau, 1991).

There are numerous valuable chemicals in the bio-oil. Levoglucosan (LG) is produced from the pyrolysis of cellulose and can be hydrolyzed to produce glucose which is a valuable feedstock for the production of bio-ethanol (Bennett et al., 2009). There are several methods for the purification of LG from the bio-oil (Howard et al., 1993; Moens, 1994; Scott et al., 1995).

Levoglucosenone (LGO) is produced from the combined depolymerization and dehydration reactions during the pyrolysis of cellulose or biomass. Due to its unique structure (a highly activated keto-group, an enone system, and an acetal center), LGO has been used in the synthesis of organic compounds such as tetrodotoxin, thiosugars, and ras activated inhibitors (Momba, 2010). LGO can be recovered through distillation of bio-oil (Marshall, 2008). Hydroxyacetaldehyde, the most abundant product formed due to the ring scission of holocellulose (Shimada et al., 2008) is another valuable compound that can be used as ingredient in cosmetic industry or as meat-browning agent (Underwood and Graham, 1991).

1.9. Application of bio-oil for energy/power generation

The liquid (bio-oil) from fast pyrolysis has a variety of applications. It can be used as fuel for boilers to generate heat (Czernik and Bridgwater, 2004), as the main compound (72%) in a fuel blend for a single-cylinder Lister Petter diesel engine (Suppes et al., 1996), as fuel (preheated bio-oil) in a 0.45 L Ricardo single-cylinder direct injection diesel engine (Shihadeh, 1998), on small scale combined heat and power production (Bandi and Baumgart, 2001), or used to make emulsions of bio-oil in diesel fuel (Chiaramonti et al., 2003). However, it was reported that using an emulsion of diesel and pyrolysis bio-oil resulted in the formation of deposits and erosion of the injectors of their 6.25 kW single-cylinder engine.

Chiaramonti and co-workers confirmed the risk of using emulsion of diesel and pyrolysis bio-oil on diesel operating engines. They tested four different engines and the damages caused by the combustion of the emulsion (significant damage of the fuel pump and injectors) were greater than those caused by the combustion of the bio-oil alone (Chiaramonti et al., 2003). Another application of the bio-oil as energy source is to use it as fuel on properly modified turbines for power generation. The first tests on gas turbines using pyrolysis bio-oil were conducted in the early 1980s by Kasper and co-workers (Kasper et al., 1983). They used slow pyrolysis bio-oil from forest and agricultural residues (resembling typical fast pyrolysis bio-oil) on a J69-T-29 gas turbine combustor rig. The reported combustion efficiency in the rig was 95%. However, and in addition to slag buildup in the exhaust of the turbine, the CO emissions were higher whereas the CH and NO_x were within the limits compared to petroleum fuel.

Strenziok and co-workers were able to operate a small commercial gas turbine using dual fuel mode (bio-oil and diesel) at 73% of the full power. They reported the formation of deposits in the combustion chamber and on the turbine blades. They also reported higher CO and CH emissions, and lower NO_x emissions from the dual fuel runs compared to the diesel fuel runs (Strenziok et al., 2001).

For its application as fuel. Upgrading the fast pyrolysis bio-oils by minimizing these oxygenated compounds is an essential process before using them as fuel. Rejection of oxygen from the fast pyrolysis bio-oil can be achieved by two type of processes i.e. hydrotreating and catalytic cracking. The former uses hydrogen under high pressure and oxygen is rejected as water, whereas the latter uses solid cracking catalyst under atmospheric pressure without hydrogen supply (Pütün et al., 2006).

The product distribution as well as the bio-oil quality obtained from the catalytic cracking of feedstock is significantly dependent on the characteristic of the catalyst used (Bridgwater, 1996; Horne and Williams, 1996; Vitolo et al., 1999).

One of the most common synthetic catalysts used in the catalytic cracking process is HZSM-5. This catalyst is acidic, shape-selective and highly active. It converts hydrocarbons and oxygenated hydrocarbons into aromatic products similar to gasoline components (Mathews et al., 1985). HZSM-5 converts the oxygenated components (aldehydes, ketones, and carboxylic acids) into less reactive deoxygenated products. As a result, the bio-oil produced from the catalytic cracking over HZSM-5 is stable and has lower viscosity (Williams and Nugranad, 2000). In order to reduce the overall cost of the upgraded bio-oil production, low-cost materials have being investigated as alternative

catalysts. A good example is the use of natural limestone or dolomite as tar cracking catalysts (Nokkosmäki et al., 1998).

Red mud, a mixture of Fe_2O_3 , Al_2O_3 , SiO_2 , TiO_2 , CaO , and Na_2O is the waste by-product of the Bayer process for the refining of bauxite ore into pure Al_2O_3 , the first step in the production of aluminum metal. Red mud is produced as an aqueous slurry on a very large scale ($>70 \times 10^6$ ton/year) and is highly alkaline (pH 14) (Karimi et al., 2010a).

Reduced red mud was used as a catalyst for upgrading the bio-oil from Hemp-seed pyrolysis which was carried under hydrogen pressure of 800 psi and at a temperature of 350°C . The upgraded bio-oil contained fewer oxygenated compounds but more saturated hydrocarbons. The viscosity of the upgraded bio-oil was improved (Karimi et al., 2010a). Red mud in its virgin or reduced form was also reported as an effective catalyst able to reduce the acidity of the pyrolysis bio-oils (Karimi et al., 2010b).

Preliminary work has proven that red mud is able to crack hydrocarbons (cracking of virgin olive oil over red mud at 450°C). Farther, Yathavan and Agblevor used red mud in the fractional catalytic pyrolysis of pinyon-juniper, and they reported that red mud rejects oxygen in the pyrolysis vapors as water and CO_2 (rather than CO), which increased the overall carbon efficiency of the process compared to HZSM-5 experiment (Yathavan and Agblevor, 2012). Another interesting feature of red mud is its catalytic activity which is dependent on the external surface area. When using red mud in a fluidized bed reactor, Yathavan and Agblevor noticed that red mud maintained its activity for around 3 hours. That was due to the constant attrition of the particles in the fluid bed, which considerably reduced the coke formation on the surface of the catalyst (Yathavan and Agblevor, 2012).

1.10. Problem statement

Both OMWS and red mud are waste materials that are difficult to deal with because they are environmental pollutants. OMWS has bad smell, phytotoxic effect in plants (high mineral salt content, low pH, and phenols), and negatively affect the properties of soil (immobilization of available nitrogen, increased salinity) when directly applied as fertilizer.

Red mud is a waste by-product of the Bayer process. It is an environmental pollutant because of its high alkalinity. In fact, lands where red mud is stored (holding ponds) become sterile and draining effluent from red mud ponds increases the alkalinity of the groundwater. Therefore, the disposal of the waste materials present a challenge that needs to be addressed carefully.

1.11. Research hypothesis

Fractional catalytic pyrolysis (FCP) of lignocellulosic biomass produces biocrude oil that is stable and has high calorific value (30 MJ/kg) (Agblevor et al., 2010).

Red mud consists of a mixture of oxides such as Fe_2O_3 , Al_2O_3 , SiO_2 , TiO_2 , CaO , and Na_2O . Lu and co-workers reported the catalytic pyrolysis of hybrid poplar over several nano-oxides (MgO , CaO , TiO_2 , Fe_2O_3 , NiO and ZnO) in a pyroprobe at 500 °C. While Fe_2O_3 resulted in the formation of hydrocarbons, CaO reduced significantly the acid content of the catalytic bio-oil. As for TiO_2 and the three remaining oxides, they reduced the anhydrosugars in the bio-oil (Lu et al., 2010). Therefore, it was hypothesized that red mud would be a potential catalyst for the upgrading of the OMWS fast pyrolysis bio-oil.

Furthermore, the red mud is believed to produce catalytic pyrolysis oil with comparable properties to those of the HZM-5 catalytic pyrolysis oil.

1.12. Research goals and objectives

The ultimate goal of this research is to produce a cheap, renewable liquid fuel from the catalytic pyrolysis of an agricultural waste (OMWS) using an industrial by-product (red mud). To achieve this goal, the catalytic pyrolysis of the OMWS over red mud will be conducted and the performance of this catalyst will be compared to that of HZSM-5. Further, the catalytic pyrolysis of the OMWS hexanes soluble fraction and the solid residue after extraction will be conducted in order to reveal the contribution of each fraction in the composition of the pyrolysis bio-oil and gas product.

The research objectives and results are organized and presented as follows:

1. Characterization of the OMWS.
2. Catalytic pyrolysis of OMWS over red mud and HZSM-5.
3. Catalytic pyrolysis of the OMWS fractions.

1.13. References

- Agblevor, F., Beis, S., Mante, O., Abdoulmoumine, N., 2010. Fractional catalytic pyrolysis of hybrid poplar wood. *Ind. Eng. Chem. Res.* 49, 3533–3538. doi:10.1021/ie901629r
- Agblevor, F., Besler, S., Wiseloge, A., 1995. Fast pyrolysis of stored biomass feedstocks. *Energy & Fuels* 9, 635–640. doi:10.1021/ef00052a010
- Angelidaki, I., Ahring, B.K., 1992. Effects of free long-chain fatty acids on thermophilic anaerobic digestion. *Appl. Microbiol. Biotechnol.* 37, 808–812. doi:10.1007/BF00174850

- Aragon, J., Karagouni, A., 2000. Improvements of treatments and validation of the liquid-solid waste from the two-phase olive oil extraction.
- Azbar, N., Bayram, A., Filibeli, A., Muezzinoglu, A., Sengul, F., Ozer, A., 2004. A review of waste management options in olive oil production. *Crit. Rev. Environ. Sci. Technol.* doi:10.1080/10643380490279932
- Ballesteros, I., Oliva, J.M., Negro, M.J., Manzanares, P., Ballesteros, M., 2002. Ethanol production from olive oil extraction residue pretreated with hot water. *Appl. Biochem. Biotechnol.* 98-100, 717–732. doi:10.1385/ABAB:98-100:1-9:717
- Bandi, A., Baumgart, F., 2001. Stirling engine with flax burner fuelled with fast pyrolysis liquid, in: Bridgwater, A. V. (Ed.), *Progress in Thermochemical Biomass Conversion*. Wiley-Blackwell, pp. 1459–1467. doi:10.1002/9780470694954.ch120
- Beccari, M., Majone, M., Torrisi, L., 1998. Two-reactor system with partial phase separation for anaerobic treatment of olive oil mill effluents. *Water Sci. Technol.* 38, 53–60. doi:10.1016/S0273-1223(98)00497-1
- Bennett, N.M., Helle, S.S., Duff, S.J.B., 2009. Extraction and hydrolysis of levoglucosan from pyrolysis oil. *Bioresour. Technol.* 100, 6059–6063. doi:10.1016/j.biortech.2009.06.067
- Boari, G., Brunetti, A., Passino, R., Rozzi, A., 1984. Anaerobic digestion of olive oil mill wastewaters. *Agric. Wastes* 10, 161–175. doi:10.1016/0141-4607(84)90057-X
- Bridgwater, A.V., 1996. Production of high grade fuels and chemicals from catalytic pyrolysis of biomass. *Catal. Today* 29, 285–295. doi:10.1016/0920-5861(95)00294-4
- Bridgwater, A. V., 2012. Review of fast pyrolysis of biomass and product upgrading. *Biomass and Bioenergy* 38, 68–94. doi:10.1016/j.biombioe.2011.01.048
- Bridgwater, A. V., 2000. Slow release fertilizers by pyrolytic recycling of agricultural wastes. *PyNe Newsl.* 9.
- Caputo, A.C., Scacchia, F., Pelagagge, P.M., 2003. Disposal of by-products in olive oil industry: Waste-to-energy solutions. *Appl. Therm. Eng.* 23, 197–214. doi:10.1016/S1359-4311(02)00173-4

- Chiaromonti, D., Bonini, M., Fratini, E., Tondi, G., Gartner, K., Bridgwater, A. V., Grimm, H.P., Soldaini, I., Webster, A., Baglioni, P., 2003. Development of emulsions from biomass pyrolysis liquid and diesel and their use in engines - Part 1: Emulsion production. *Biomass and Bioenergy* 25, 85–99. doi:10.1016/S0961-9534(02)00183-6
- Coimbra, M.A., Waldron, K.W., Selvendran, R.R., 1994. Isolation and characterisation of cell wall polymers from olive pulp (*Olea europaea* L.). *Carbohydr. Res.* 252, 245–262. doi:10.1016/0008-6215(94)84136-5
- Czernik, S., Bridgwater, A.V., 2004. Overview of applications of biomass fast pyrolysis oil. *Energy & Fuels* 18, 590–598. doi:Doi 10.1021/Ef034067u
- D'Annibale, A., Brozzoli, V., Crognale, S., Gallo, A.M., Federici, F., Petruccioli, M., 2006a. Optimisation by response surface methodology of fungal lipase production on olive mill wastewater. *J. Chem. Technol. Biotechnol.* 81, 1586–1593. doi:10.1002/jctb.1554
- D'Annibale, A., Sermanni, G.G., Federici, F., Petruccioli, M., 2006b. Olive-mill wastewaters: a promising substrate for microbial lipase production. *Bioresour. Technol.* 97, 1828–1833. doi:10.1016/j.biortech.2005.09.001
- Elander, R.T., Hsu, T., 1995. Processing and economic impacts of biomass delignification for ethanol production. *Appl. Biochem. Biotechnol.* 51-52, 463–478. doi:10.1007/BF02933448
- Fenice, M., Giovannozzi Sermanni, G., Federici, F., D'Annibale, A., 2003. Submerged and solid-state production of laccase and Mn-peroxidase by *Panus tigrinus* on olive mill wastewater-based media. *J. Biotechnol.* 100, 77–85. doi:10.1016/S0168-1656(02)00241-9
- Freel, B., Graham, R.G., 2002. Bio-oil preservatives. U.S. Patent No. 6,485,841 B1.
- Giroux, R., Freel, B., Graham, R., 2001. Natural resin formulations. U.S. Patent No. 6,326,461 B1.
- Gonzalez, M.D., Moreno, E., Quevedo-Sarmiento, J., Ramos-Cormenzana, A., 1990. Studies on antibacterial activity of waste waters from olive oil mills (alpechin): Inhibitory activity of phenolic and fatty acids. *Chemosphere* 20, 423–432. doi:10.1016/0045-6535(90)90073-3

- Gonzalez-Lopez, J., Pozo, C., Martinez-Toledo, M.V., Rodelas, B., Salmeron, V., 1996. Production of polyhydroxyalkanoates by *Azotobacter chroococcum* H23 in wastewater from olive oil mills (alpechin). *Int. Biodeterior. Biodegradation* 38, 271–276. doi:10.1016/S0964-8305(96)00060-1
- Hamdi, M., 1993. Future prospects and constraints of olive mill wastewaters use and treatment: A review. *Bioprocess Eng.* 8, 209–214. doi:10.1007/BF00369831
- Hamdi, M., 1991a. Effects of agitation and pretreatment on the batch anaerobic digestion of olive mill wastewater. *Bioresour. Technol.* 36, 173–178. doi:10.1016/0960-8524(91)90176-K
- Hamdi, M., 1991b. Nouvelle conception d'un procédé de dépollution biologique des margines, effluents liquides de l'extraction de l'huile d'olive. Provence University, Marseille, France.
- Herbs-Treat and Taste [WWW Document], 2010. URL <http://www.herbs-treatandtaste.blogspot.com/2011/01/olive-tree-medicinal-benefits-of-olive.html>
- Himmelblau, A., 1991. Method and apparatus for producing water-soluble resin and resin product made by that method. U.S. Patent No. 5,034,498 A.
- Horne, A., Williams, P.T., 1996. Influence of temperature on the products from the flash pyrolysis of biomass. *Fuel* 75, 1051–1059. doi:10.1016/0016-2361(96)00081-6
- Howard, J., Longley, C., Morrison, A., Fung, D., 1993. Process for isolating levoglucosan from pyrolysis liquids. CA Patent No. 2,084,906 A1.
- International olive council [WWW Document], 1959. URL www.internationaloliveoil.org/estaticos/view/76-the-olive-tree
- Israilides, C., 1994. Characterization of pullulans produced from agro-industrial wastes. *Carbohydr. Polym.* 25, 203–209. doi:10.1016/0144-8617(94)90205-4
- Karimi, E., Briens, C., Berruti, F., Moloodi, S., Tzanetakis, T., Thomson, M.J., Schlaf, M., 2010a. Red mud as a catalyst for the upgrading of hemp-seed pyrolysis bio-oil. *Energy and Fuels* 24, 6586–6600. doi:10.1021/ef101154d
- Karimi, E., Gomez, A., Kycia, S.W., Schlaf, M., 2010b. Thermal decomposition of acetic and formic acid catalyzed by red mud - Implications for the potential use of red mud as a pyrolysis bio-oil upgrading catalyst, in: *Energy and Fuels*. pp. 2747–2757. doi:10.1021/ef1000375

- Kasper, J.M., Jasas, G.B., Trauth, R.L., 1983. Use of pyrolysis-derived fuel in a gas turbine engine. New York.
- Khoufi, S., Aloui, F., Sayadi, S., 2008. Extraction of antioxidants from olive mill wastewater and electro-coagulation of exhausted fraction to reduce its toxicity on anaerobic digestion. *J. Hazard. Mater.* 151, 531–539. doi:10.1016/j.jhazmat.2007.06.017
- Kotronarou, N., Méndez, M., 2003. IMPEL olive oil project.
- López, M.J., Moreno, J., Ramos-Cormenzana, A., 2001. The effect of olive mill wastewaters variability on xanthan production. *J. Appl. Microbiol.* 90, 829–835. doi:10.1046/j.1365-2672.2001.01326.x
- Lopez, M.J., Ramos-Cormenzana, A., 1996. Xanthan production from olive-mill wastewaters. *Int. Biodeterior. Biodegradation* 38, 263–270. doi:10.1016/S0964-8305(96)00059-5
- Lu, Q., Zhang, Z.F., Dong, C.Q., Zhu, X.F., 2010. Catalytic upgrading of biomass fast pyrolysis vapors with nano metal oxides: an analytical Py-GC/MS study. *Energies* 3, 1805–1820. doi:10.3390/en3111805
- Marshall, J.A., 2008. An improved preparation of levoglucosenone from cellulose. Iowa State University, Ames.
- Massadeh, M.I., Modallal, N., 2008. Ethanol production from olive mill wastewater (OMW) pretreated with *Pleurotus sajor-caju*. *Energy and Fuels* 22, 150–154. doi:10.1021/ef7004145
- Mathews, J.F., Tepylo, M.G., Eager, R.L., Pepper, J.M., 1985. Upgrading of aspen poplar wood oil over HZSM-5 zeolite catalyst. *Can. J. Chem. Eng.* 63, 686–689.
- McElhatton, A., do Amaral, P., 2011. Novel technologies in food science: their Impacts on Products, Consumer Trends, and the Environment. Springer-Verlag, New York.
- Mercade, M.E., Manresa, M.A., Robert, M., Espuny, M.J., De Andres, C., Guinea, J., 1993. Olive oil mill effluent (OOME). New substrate for biosurfactant production. *Bioresour. Technol.* 43, 1–6. doi:10.1016/0960-8524(93)90074-L
- Ministry of the Environment, 2000. Pollution prevention in olive oil production. Barcelona, Spain.
- Moens, L., 1994. Isolation of levoglucosan from pyrolysis oil derived from cellulose. U.S. Patent No. 5,371,212 A.

- Momba, M.N.B. (Ed.), 2010. Biomass. Sciyo, Rijeka, Croatia.
- Nasopoulou, C., Zabetakis, I., 2013. Agricultural and Aquacultural Potential of Olive Pomace A Review. *J. Agric. Sci.* 5, 116–127. doi:10.5539/jas.v5n7p116
- Nokkosmäki, M., Krause, a. O., Leppämäki, E., Kuoppala, E., 1998. A novel test method for catalysts in the treatment of biomass pyrolysis oil. *Catal. Today* 45, 405–409. doi:10.1016/S0920-5861(98)00276-4
- Oehr, K.H., Scott, D.S., Czernik, S., 1993. Method of producing calcium salts from biomass. U.S. Patent No. 5,264,623 A.
- Oliveira, J.S., 1974. Effluents from olive oil extracting plants subsidies for the study of the obtention of sealable products with simultaneous elimination of BOD, in: *International Congress of Agro-Food Industries*. Athens, Greece.
- Olori, L., de Fulvio, S., Morgia, P., 1990. Acque di vegetazione. Le problematiche ambientali e gli aspetti igienico. *Inquinamento* 1, 40–46.
- Onay, O., Koçkar, O.M., 2006. Pyrolysis of rapeseed in a free fall reactor for production of bio-oil. *Fuel* 85, 1921–1928. doi:10.1016/j.fuel.2006.03.009
- Petarca, L., Vitolo, S., Bresci, B., 1997. Pyrolysis of concentrated olive mill vegetation waters, in: *Proceeding International Conference on Biomass Gasification and Pyrolysis*. pp. 374–381.
- Petruccioli, M., Servili, M., Montedoro, G.F., Federici, F., 1988. Development of a recycle procedure for the utilization of vegetation waters in the olive oil extraction process. *Biotechnol. Lett.* 10, 55–60.
- Pozo, C., Martinez-Toledo, M. V, Rodelas, B., Gonzalez-Lopez, J., 2002. Effects of culture conditions on the production of polyhydroxyalkanoates by *Azotobacter chroococcum* H23 in media containing a high concentration of alpechin (wastewater from olive oil mills) as primary carbon source. *J. Biotechnol.* 97, 125–131.
- Pütün, E., Uzun, B.B., Pütün, A.E., 2006. Fixed-bed catalytic pyrolysis of cotton-seed cake: Effects of pyrolysis temperature, natural zeolite content and sweeping gas flow rate. *Bioresour. Technol.* 97, 701–710. doi:10.1016/j.biortech.2005.04.005
- Radlein, D.S.A.G., Piskorz, J.K., Majerski, P.A., 1997. Method of producing slow-release nitrogenous organic fertilizer from biomass. U.S. Patent No. 5,676,727 A.
- Ragazzi, E., Veronese, G., 1973. Research on the phenolic components of olive oils. *Riv. Ital. Sost. Grasse* 50, 443–452.

- Rodis, P.S., Karathanos, V.T., Mantzavinou, A., 2002. Partitioning of olive oil antioxidants between oil and water phases. *J. Agric. Food Chem.* 50, 596–601. doi:10.1021/jf010864j
- Rodríguez Pérez, S., García Oduardo, N., Bermúdez Savón, R.C., Fernández Boizán, M., Augur, C., 2008. Decolourisation of mushroom farm wastewater by *Pleurotus ostreatus*. *Biodegradation* 19, 519–526. doi:10.1007/s10532-007-9157-z
- Scioli, C., Vollaro, L., 1997. The use of *Yarrowia lipolytica* to reduce pollution in olive mill wastewaters. *Water Res.* 31, 2520–2524. doi:10.1016/S0043-1354(97)00083-3
- Scott, D.S., Piskorz, J., Radlein, D., Majerski, P., 1995. Process for the production of anhydrosugars from lignin and cellulose containing biomass by pyrolysis. U.S. Patent No. 5,395,455 A.
- Shihadeh, A.L., 1998. Rural electrification from local resources: Biomass pyrolysis oil combustion in a direct injection diesel engine. Massachusetts Institute of Technology.
- Shimada, N., Kawamoto, H., Saka, S., 2008. Different action of alkali/alkaline earth metal chlorides on cellulose pyrolysis. *J. Anal. Appl. Pyrolysis* 81, 80–87. doi:10.1016/j.jaap.2007.09.005
- Strenziok, R., Hansen, U., Künstner, H., 2001. Combustion of bio oil in a gas turbine, in: Bridgwater, A. V. (Ed.), *Progress in Thermochemical Biomass Conversion*. Wiley-Blackwell, Hoboken, New Jersey, p. 1744.
- Suppes, G.J., Natarajan, V.P., Chen, Z., 1996. Autoignition of select oxygenate fuels in a simulated diesel engine environment, in: *AIChE National Meeting*. New Orleans.
- Toscano, P., Montemurro, F., 2012. Olive Mill By-Products Management, in: Muzzalupo, I. (Ed.), *Olive Germplasm - The Olive Cultivation, Table Olive and Olive Oil Industry in Italy*. pp. 173–200.
- Underwood, G., Graham, R.G., 1991. Method of using fast pyrolysis liquids as liquid smoke. U.S. Patent No. 4,994,297 A.
- Vamvuka, D., 2011. Bio-oil, solid and gaseous biofuels from biomass pyrolysis processes-An overview. *Int. J. Energy Res.* doi:10.1002/er.1804
- Vitolo, S., Petarca, L., Bresci, B., 1999. Treatment of olive oil industry wastes. *Bioresour. Technol.* 67, 129–137. doi:10.1016/S0960-8524(98)00110-2.

- Vossen, P., 2007. Olive oil: history, production, and characteristics of the world's classic oils. *HortScience* 42, 1093–1100.
- Widsten, P., Kandelbauer, A., 2008. Laccase applications in the forest products industry: a review. *Enzyme Microb. Technol.* doi:10.1016/j.enzmictec.2007.12.003
- Williams, P.T., Nugranad, N., 2000. Comparison of products from the pyrolysis and catalytic pyrolysis of rice husks. *Energy* 25, 493–513. doi:10.1016/S0360-5442(00)00009-8
- Yathavan, B.K., Agblevor, F., 2012. Catalytic conversion of pinyon-juniper into upgraded biooils, in: *AIChE 2012 - 2012 AIChE Annual Meeting, Conference Proceedings*.

CHAPTER 2

CHARACTERIZATION OF THE OLIVE MILL WASTEWATER SLUDGE

Abstract

Olive mill wastewater sludge (OMWS) is the solid residue that remains in the evaporation ponds after evaporation of the majority of water in the Olive mill wastewater (OMW). OMWS is a major environmental pollutant in the olive oil producing regions. It has a bad smell, phytotoxic effect on plants, and can cause sterility of the land where it is stored. In order to determine the structural and elemental composition of the OMWS, this study focuses on its characterization. The analyses carried out included proximate and ultimate analysis, as well as compositional analysis. The ash content of the OMWS was 15.73 wt.% (dry basis), the volatile organic matter and fixed carbon were 60.1 wt.% and 24.17 wt.%, respectively. The carbon and hydrogen contents were 57.3 wt.% and 8 wt.%, respectively. The sulfur content was lower than the detection limit of the instrument. The nitrogen and oxygen contents were 2.3 wt.% and 23.9 wt.%. The OMWS had high energy content i.e. 30 MJ/kg and close to neutral pH (6.39) as a slurry. The non-structural materials accounted for 74.35 wt.% of the OMWS. The hexanes soluble fraction (HSF) had the highest yield of 41.16 wt.%, followed by 19.81 wt.% for the ethanol soluble fraction (ESF), and 13.38 wt.% for the water soluble fraction (WSF).

The GC/MS data showed an abundance of free fatty acids (oleic acid and palmitic acid) in the HSF, and glycerin and di-ketone in the ESF. The saponification value (SAP) of the HSF was 64.41 mg KOH/g of HSF), the saponifiables accounted for 6.16 wt. % to the OMWS.

The high ash content in the OMWS will result in a high char/coke yield. The nitrogen content of the OMWS will reduce the quality of the bio-oil.

2.1. Introduction

In order to reduce our dependence on fossil fuels (petroleum, coal, and natural gas) and mitigate the environmental impact of processing those fuels, a renewable and sustainable alternative is needed. Biomass is any organic matter that can be converted into energy. It covers plants, agricultural residues, and industrial organic waste products. Even though biomass is one of the main energy resources available, it is the only source of renewable fuels (liquid, solid, and gaseous) (Bridgwater et al., 1999). In order to evaluate any biomass as potential source of biofuels, it is necessary to characterize it. The physical-chemical characterization of biomass will enable the prediction of its behavior during combustion, gasification and pyrolysis (Kazagic and Smajevic, 2007). The OMW consists mainly of water and a total suspended solid concentration of 44.26 (g/L). It also contains sugars (3.4 g/L), protein (3.2 g/L), lipids (5.6 g/L), and polyphenols (4.99 g/L) (Kazagic and Smajevic, 2007).

The OMWS is the solid residue that remains in the evaporation ponds after evaporation of water in the OMW under atmospheric condition. Thus the distribution of the different compounds in the OMWS should be different from the OMW.

It is hypothesized that the lipid fraction in the OMWS will result in the production of hydrocarbon rich liquid fuel. In fact, pyrolysis and catalytic pyrolysis of lipids (vegetable oils, animal fats, Triglycerides, Fatty acid methyl esters and free fatty acids) has been investigated for long time.

It was reported that the liquid obtained from the pyrolysis of vegetable oils is rich in hydrocarbons and could be used as feedstock to produce petrochemicals and petroleum based distillates (Graboski and McCormick, 1998). In order to evaluate the OMWS as a potential biofuel source, it is necessary to determine its chemical and physical properties especially the lipids content and composition. The goal of this chapter is to characterize the OMWS and evaluate its potential as a biofuel feedstock.

2.2. Materials and methods

2.2.1. Materials

OMWS samples were collected as solid chunks from a 1-2 years old evaporation ponds in the region of Agareb in the Sfax governorate, Tunisia. The samples were ground as received to pass a 2 mm screen using a Wiley mill (model 4) (Thomas Wiley Scientific, Swedesboro, NJ, USA).

2.2.2. Methods

The OMWS was characterized for moisture, ash, ultimate, proximate, and extractives content.

2.2.5. Moisture

The moisture content of the OMWS samples was measured using an IR 60 infrared moisture analyzer (Denver Instruments, Bohemia, NY, USA) according to ASTM E1756-08. One to 1.5 g of the sample was spread on an aluminum pan placed on the instrument balance.

The moisture was determined gravimetrically by heating the sample from room temperature to 105 °C, then cooling down to room temperature. The moisture content of the sample was shown as mass percent of moisture.

2.2.4. Ash

The ash content of the OMWS was determined according to the standard procedure ASTM E1755-01 (2007). 1-2 g of the OMWS was loaded into a crucible and placed in a Lindburg Blue M box furnace model BF51842 (Thermo Scientific, Waltham, MA, USA) heated from room temperature to 250 °C at 10 °C/min, then held for 30 minutes. Afterward, the temperature was increased to 575 °C and held for 3 hours. The samples were cooled in a desiccator then weighed. The samples were put back into the furnace at 575 °C for 1 hour, then cooled and weighed.

This step was repeated three times and yet the mass differences was higher than 0.3 mg, therefore the samples were left in the oven for 12 hours, cooled and weighed, then put back in the oven at 575 °C for 1 hour, then cooled and weighed. Finally the weight difference was within 0.3 mg.

The ash content of the sample was calculated on dry basis using the Eq. (1). The average value of triplicates was recorded as the ash content of the OMWS.

$$\text{Ash (wt. \%)} = [(M_{ac} - M_{ct}) / (M_{sc} - M_{ct})] \times 100 \quad (1)$$

where

Ash (wt. %) = the mass percent of ash of the OMWS on dry basis.

M_{ac} = the mass of the ash and the crucible in grams.

M_{ct} = the mass of the crucible in grams.

M_{sc} = the mass of the OMWS sample in grams.

2.2.5. Volatile organic matter and fixed carbon

The proximate analysis of the OMWS was conducted using a TA instrument thermogravimetric analyzer TGA Q500 (TA instruments, New Castle, DE, USA). Approximately 40 mg of sample was loaded to a platinum pan. The sample was heated under 100 ml/min of nitrogen gas. The temperature was increased from room temperature until the weight loss curve indicated a stable mass. The final temperature was 596 °C. The

mass loss consisted of moisture and volatile matter. The solid residue consisted of fixed carbon and ash.

2.2.6. Ultimate analysis

The elemental analysis of the OMWS was conducted using a Flash 2000 CHNS-O analyzer (Thermo Scientific Inc, Waltham, MA, USA). 2-3 mg of sample was loaded to a tarred tin cup then placed manually into the loading chamber. The sample was combusted at 950 °C in a quartz tubular reactor and the gases produced were analyzed by GC equipped with a thermal conductivity detector (TCD). The average values of triplicates were reported as the organic elemental composition of the OMWS on dry basis. The oxygen content was determined by difference according to Eq. (2).

$$O \text{ (wt. \%, dry basis)} = 100 - C - H - N - S - O_{\text{water}} \quad (2)$$

where

O: oxygen content of the bio-oil, on dry basis.

C: carbon content of the bio-oil, on dry basis.

H: hydrogen content of the bio-oil, on dry basis.

N: nitrogen content of the bio-oil, on dry basis.

S: sulfur content of the bio-oil, on dry basis.

O_{water}: oxygen content of the water in bio-oil.

2.2.7. Higher heating value

The higher heating value (HHV) of the OMWS was measured using IKA C200 basic bomb calorimeter (IKA Works Inc, Wilmington, NC, USA). 0.5 g of sample was loaded to a quartz crucible and combusted in a type 2 stainless steel vessel.

During the combustion of the sample, the heat produced was detected and the energy content of the sample was shown as Mega Jules per kilogram (MJ/kg). The average of the triplicates was reported as the HHV of the OMWS on dry basis.

2.2.8. pH

The pH of OMWS slurry was measured using a pH meter (Mettler Toledo AG, Switzerland) equipped with an InLab® Expert Pro Electrode. Fourteen grams of OMWS was added to 200 ml of de-ionized water and stirred manually. The pH measurements were done multiple times to ensure reproducibility.

2.2.9. Sequential extraction

The sequential extraction of the OMWS was conducted using a Soxhlet extractor. The solvents used were hexanes, 95vol% ethanol, and de-ionized water.

Approximately 20 g of ground OMWS were loaded into the extraction thimbles. 250-300 ml of solvent were added to the round bottom flask and the apparatus was assembled. The cycles were set to 12-15 cycle/min for a total extraction time of 24 hours.

Using a rotary evaporator, the solvent was recovered and the extracted material was left in the vacuum over for 24 hours at 40 °C and 3 mmHg vacuum.

The extracted fractions were placed under continuous flow of nitrogen gas until stable mass. The results (triplicates) were reported as mass percent (dry basis).

2.2.10. Hexanes extraction of the OMWS

The effect of extraction method of the OMWS on the yield of the HSF was investigated by comparing two extraction methods i.e. Soxhlet extraction and the boiling extraction, which is simpler than the former method. Both experiments were conducted for 24 hours and the yields of the HSF were compared. During the boiling extraction 1 to 3 ratio of OMWS and hexanes (Hexanes, mixture of isomers, Sigma Aldrich, St. Louis, MO, USA) were loaded to 1 L Erlenmayer flask. The flask and its content were refluxed for 24 hours. The slurry was continuously stirred using a PTFE magnetic bar.

After extraction, the slurry was filtered. The permeate (HSF) was placed on a rotary evaporator until most of the solvent was collected. After evaporation of the solvent, the recovered HSF was placed in the vacuum oven for 24 hours. The smell of hexanes was still present in the vacuum oven, therefore the round bottom flasks containing the HSF were placed under nitrogen gas flow until the total mass stabilized. The retentate (SR) was placed on a pan in the fume hood overnight.

This solid residue can be described as defatted OMWS. The SR collected was a gray blend of coarse and very fine powder.

2.2.11. Optimal extraction time

The effect of the extraction time of the OMWS on the HSF yield was investigated using the boiling extraction method. Fifteen grams of the OMWS and 50 g of hexanes were

loaded to a 100 mL Erlenmeyer flask and extracted for 1h, 2h, 4h, 6h, 8h, 10h, 12h, and 14h.

The slurry was then filtered and the solvent was recovered from the filtrate (HSF + hexanes) using a rotary evaporator. The solid residue after filtration (SR) was dried in the fume hood overnight.

2.2.12. Elemental composition of the HSF and the SR

The elemental composition analysis of the HSF and the SR was determined using a Thermo Scientific Flash 2000 organic elemental analyzer (ThermoFisher Scientific, Cambridge, UK). The sample size used was 2-4mg and the oxygen content of the oils was determined by difference.

2.2.13. Gas chromatography/mass spectroscopy

The gas chromatography/mass spectroscopy (GC/MS) analyses were done at the Chemical Engineering Department of Kangwon National University (Gangwon-do, Republic of Korea). The instrument used was an Agilent 7890A equipped with a 5975C VL Mass selective detector and a HP-5MS 5% Phenyl Methyl Silox column (length 30m - Diameter 0.25 mm - film 0.25 micrometer). Helium was used as the carrier gas at 1 mL/min. The hexanes soluble fraction was dissolved in hexanes.

The 95vol% soluble fraction was dissolved in methanol. 0.2 ml of the sample was added to 10 ml of solvent and the mixture was filtered using a PTFE filter membrane (pore diameter = 0.5 micrometer).

The injected sample volume was 1 μL . The split ratio was 50:1. The HSF was held at 40 $^{\circ}\text{C}$ for 5 minutes then ramp to 250 $^{\circ}\text{C}$ at 15 $^{\circ}\text{C}/\text{min}$ and hold for 5 minutes, then ramp to 300 $^{\circ}\text{C}$ at 20 $^{\circ}\text{C}/\text{min}$ and hold for 5 minutes. The ESF sample was held at 40 $^{\circ}\text{C}$ for 5 minutes, then the temperature was increased to 280 $^{\circ}\text{C}$ at 10 $^{\circ}\text{C}/\text{min}$ and held for 10 minutes.

2.2.14. Saponification value

The saponification value (SAP) of the hexanes soluble fraction (HSF) was determined according to ASTM D-1962-67 (Reapproved 1973). Approximately, 4 g of the HSF were transferred to a 200 mL Erlenmeyer flask. 25 ml of alcoholic KOH (40 g of KOH per liter of distilled ethanol) solution was added to the sample and to an empty 200 mL Erlenmeyer flask (blank).

A reflux condenser was placed on each flask and the assemblies were heated in a water bath. The reflux was carried for 1 hour and the bath temperature was set to 80 $^{\circ}\text{C}$.

After cooling both flasks to room temperature, phenolphthalein was added to both flasks and titration was conducted using 0.5 N of H_2SO_4 until reaching the equivalence point. The saponification value of the HSF was calculated using Eq. (3).

$$\text{Saponification value} = [(B - A) \times N \times 56.1]/C \quad (3)$$

where

A = volume of H_2SO_4 used to titrate the sample, in milliliters.

B = volume of H_2SO_4 used to titrate the blank, in milliliters.

N = normality of the H_2SO_4 .

C = mass of sample used, in grams.

56.1g/mol = molar mass of KOH.

2.3. Results and discussion

2.3.1. Proximate analysis of the OMWS

The proximate analysis of the OMWS is reported in Table 4. The TGA was used to estimate the volatile matter and fixed carbon contents of the biomass (Fig. 1). The purpose of the TGA analysis of biomass was to have a rough estimate of the pyrolysis products distribution. The ash content of the OMWS was 15.73 wt.%, which is within the range reported in the literature (Gokce et al. 2009; Jarboui et al., 2010). The high ash content was attributed to the inorganic elements in the OMWS such as potassium, phosphorus and calcium. The intrinsic inorganic compounds (alkali and alkaline earth metals) in the ash were reported to have a catalytic effect in the vapor phase during the pyrolysis of biomass (Mohan et al., 2006; Pattiya et al., 2010; Yildiz et al., 2015).

It was reported that adding 0.002 wt.% of pine ash to the sand bed decreased the yield of surgras, phenols, and ketones and increased the yield of acids in the bio-oil. It was observed that the effect of ash, when used during the catalytic experiments (using a blend of spray dried heterogeneous HZSM-5 based catalyst and sand), was comparable with that of catalyst deactivation or/and selective catalyst losses (Yildiz et al., 2015). Therefore, it is necessary to separate the biochar from the catalyst before regeneration of the latter, in order to avoid the drawback of ash on the catalytic pyrolysis of the OMWS.

The volatile organic matter and the fixed carbon content were 60.1 wt.% and 24.17 wt.%. While the volatile organic matter can be converted to bio-oil and bio-gas during pyrolysis of the OMWS, the fixed carbon will remain in the bio-char product.

2.3.2. Ultimate analysis of the OMWS

The ultimate analysis of the OMWS is reported in Table 4. Carbon represented the major element (57.3 wt.%, dry basis) in the OMWS. The nitrogen contents was 2.33 wt.%. The sulfur was below the detection limit of the instrument. The high nitrogen content in the OMWS could potentially be incorporated in the pyrolysis oil, which will reduce the quality of the latter. The oxygen content of the OMWS was 23.85 wt. %. The oxygen content of the OMWS is relatively low compared to most lignocellulosic biomass because this is an industrial residue that contains some lipids. The HHV of the OMWS (30 MJ/kg) was higher than all reported values for olive mill waste products such as olive-oil residue (Uzun et al., 2007), fresh olive husk (Demirbas, 2008), olive bagasse (Encinar et al., 1996), olive kernel (Zabaniotou et al., 2000).

The high HHV value of the OMWS could be attributed to the residual oil in the OMW. The olive oil, like any other vegetable oil, has a high heating value (39-40 MJ/kg) (Zabaniotou et al., 2000). The HHV of the OMWS indicated a significant energy content in the biomass, thus making it a potential source of biofuels. The OMWS slurry had a slightly acidic pH (6.39). The pH of the OMWS slurry was higher than that of the OMW reported in the literature (Al-Malah et al., 2000; Azbar et al., 2004; Eroğlu et al., 2004), probably because of the calcium hydroxide spread over the OMW evaporation ponds as mosquito treatment (Jarboui et al., 2010).

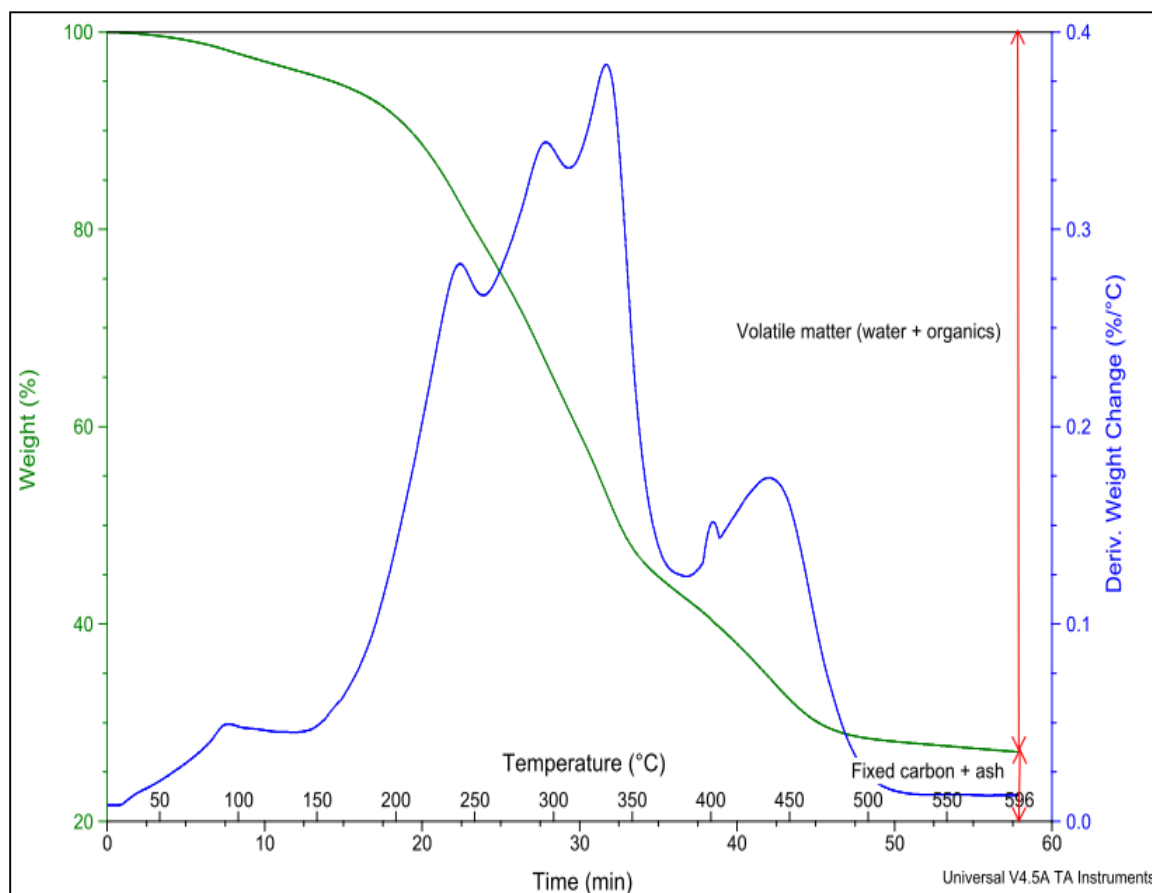


Fig. 1: Thermogravimetric analysis (TGA) and differential thermal analysis (DTA) of OMWS under nitrogen gas (L/min).

2.3.3. Solvent extraction of the OMWS

The compositional analysis of the OMWS using the sequential exhaustive solvent extraction is shown in Fig. 2. The yield of the hexanes soluble fraction was 41.16 wt.%, whereas the yields of the 95vol% ethanol and de-ionized water soluble fractions were 19.81 wt. % and 13.38 wt. %, respectively. Hexane is capable of extracting simple and complex lipids. Ethanol dissolves waxes and extractives. De-ionized water dissolves inorganic materials, non-structural sugars, and nitrogenous compounds.

At room temperature, the HSF was a green gel-like material that became free flowing when held in the palm of a hand for 15 minutes. The ESF was a brown gel-like material. It took 30 minutes for the ESF to become free flowing, when held in the palm of a hand. After water extraction, the rotary evaporator was not a good equipment to separate the solvent from the soluble solute, therefore, the content of the round bottom flask was placed in a vacuum oven until all the water evaporated. A black solid residue coated the inner surface of the glass container.

Table 4
Proximate and ultimate analysis of the OMWS

Properties	Units of measurement	Values
Moisture	wt. % (dry basis)	7.8
Volatile organics ^a		60.1
Fixed carbon ^a		24.17
Ash		15.73±0.39
Carbon		57.3±0.36
Hydrogen		8.0±0.06
Nitrogen		2.3±0.11
Sulfur		Bdl ^b
Oxygen ^c		23.9±0.53
HHV		MJ/kg (dry basis)
pH (slurry)	-	6.39±0.01

a: calculated from TGA curve, b: below detection limit, c: calculated by difference.

The OMWS consisted of 74.35 wt. % (dry basis) non-structural compounds. The OMWS is a mixture of olive skin, pulp, pits, leaves, and small branches. Each of these fractions contributes unique compounds that results in the complexity of the OMWS.

Sequential extraction (Soxhlet) was conducted for freeze dried OMW sample, using hexanes, methanol, and water. The extracted fractions yields (dry bases) were 13 wt.%, 8.6 wt.%, and 5 wt.%, respectively. The lower yields could be due to the shorter extraction time (30 min) and/or the source of the sample (Obied et al., 2005).

The HSF and the ESF are of big importance for the biofuel application of the OMWS. These two fractions are believed to contain significant amount of lipids and hydrocarbons. The potential of fats and oils as an alternative source of liquid fuel has been emphasized in the literature (Graboski and McCormick, 1998; Karaosmanoglu, 1999), therefore, it is important to identify the composition of these two fractions.

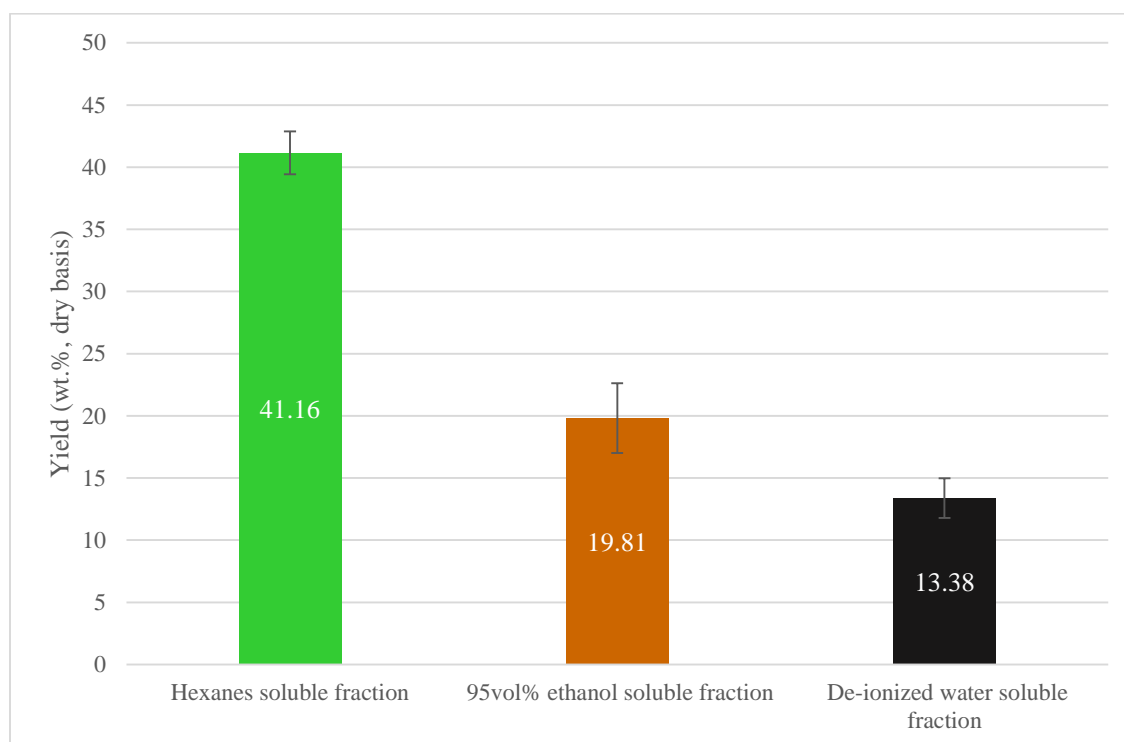


Fig. 2: Yields of various OMWS extractives

The effect of the extraction time of the OMWS on the HSF yield is shown in Fig. 3. As the extraction time increased from 1 hour to 24 hour, the HSF yield varied between 36 wt. % and 38 wt. %. Interestingly, there was no significant difference between the HSF yield obtained after 1 hour extraction and the yield from any longer extraction time (up to 24 hours).

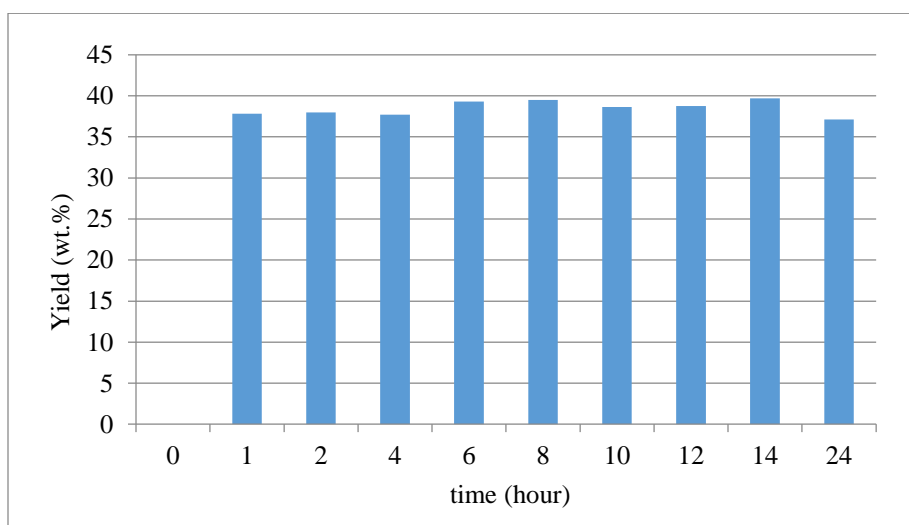


Fig. 3: Yield of HSF as a function of extraction time

The ^{13}C NMR spectra of the HSF from 1 hour extraction and 24 hour extraction are shown in Fig. 4. The spectra look very similar except for the signal intensity of the aliphatic compound at 27.3 ppm, which was slightly higher for the HSF from the boiling extraction. This signal was attributed to the allylic carbons (C8 and C11) in oleic acid (Sacchi et al., 1997).

Such difference could be due to a slight difference in the composition of the original OMWS. Therefore, it was concluded that the extraction method of the OMWS does not affect the carbon distribution within the HSF.

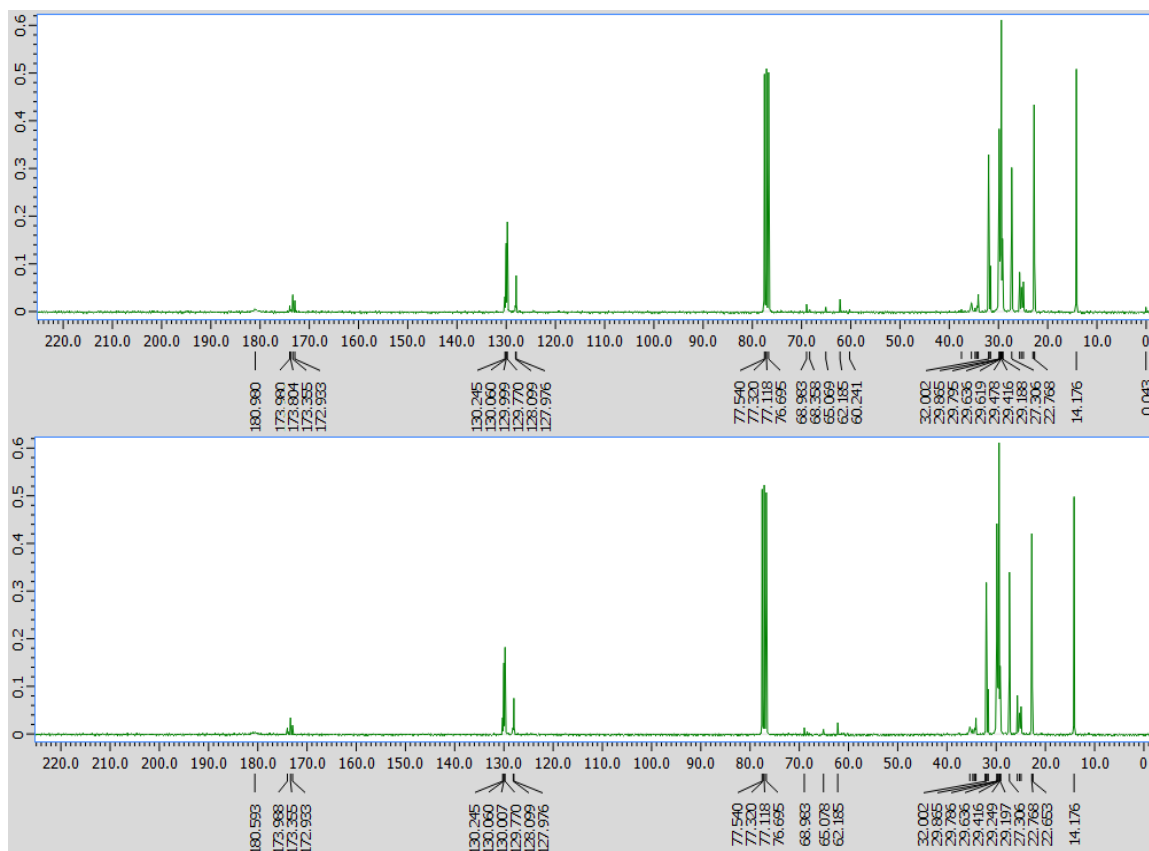


Fig. 4: ^{13}C NMR spectra of the HSF fraction extracted from the OMWS for one hour using (a) Soxhlet extraction and (b) boiling extraction.

The elemental composition of the HSF and the SR is shown in Table 5. The HSF contains consisted mainly of carbon (75.08 wt. %) and hydrogen (11.064 wt. %). The oxygen content was 8.78 wt. % and lower than the carbon and hydrogen contents. This was an expected result since the HSF consists mainly of fatty acids, which consists mainly of

carbon and hydrogen. The sulphur content was below the detection limit of the instrument, whereas the nitrogen content was 0.11 wt. %. The ash content of the HSF was 4.39 wt. %.

The considerably low content of nitrogen and sulphur, and the high content of carbon and hydrogen in the HSF made it a potential feedstock for the production of bio-fuels. The energy content of the HSF was 37.5 MJ/kg.

The SR contained carbon (47.36 wt. %), hydrogen (5.13 wt. %), and oxygen (22.19 wt. %). The nitrogen and sulphur accounted for 3.34 wt. % and 0.38 wt. %, respectively. The high nitrogen content of the SR will affect the quality of the bio-oil. The ash content of the SR (21.6 wt. %) was 4.9 times higher than that of the HSF. The energy content of the SR was 16.4 MJ/kg, which was 56.27 % lower than that of the HSF.

Table 5
Elemental composition of the HSF and the SR

	value (wt. %, dry basis)	
	HSF	SR
C	75.08±0.71	47.36±0.75
H	11.64±0.11	5.13±0.14
N	0.11±0.01	3.34±0.01
S	bdl	0.38±0.05
O and or Cl*	8.78±0.81	22.19±0.81
ash	4.39±0.1	21.6±0.06
HHV (MJ/kg)	37.5±0.11	16.4±0.67

*: calculated by difference, bdl: below detection limit.

The ^{13}C NMR spectra of the HSF and the extra virgin olive oil (EVOO) are shown in Fig. 5. They were integrated (Table 6) for semi-quantitative comparison. The EVOO had more intense signals around the glycerol backbone region (60-70 ppm) and the carbonyl carbon area (172-174 ppm) compared to the HSF. The EVOO is known to contain mainly triglycerides and small quantities of free fatty acids (“The olive oil source,” 1998). The signals at 127-131 ppm in the EVOO spectrum corresponded to C-12 and C-10 in linoleyl and C-9 and C-10 in oleyl moieties in triglycerides (Sacchi et al., 1997). The integration of both ^{13}C NMR spectra showed that the HSF and the EVOO had similar content of linear aliphatics and olefins. Compared to the the EVOO, the HSF had significantly lower triglycerides content.

Table 6
 ^{13}C NMR integration for the HSF and EVOO

	HSF	EVOO
Saturated aliphatics (0-50 ppm)	86.29	82.18
Aliphatic chains with heteroatoms (O and/or N) and methoxy group (50-110 ppm)	0.95	4.8
Olefins and aromatics (110-160 ppm)	11.22	10.01
esters, carboxylic acids (160-180)	1.53	3.01

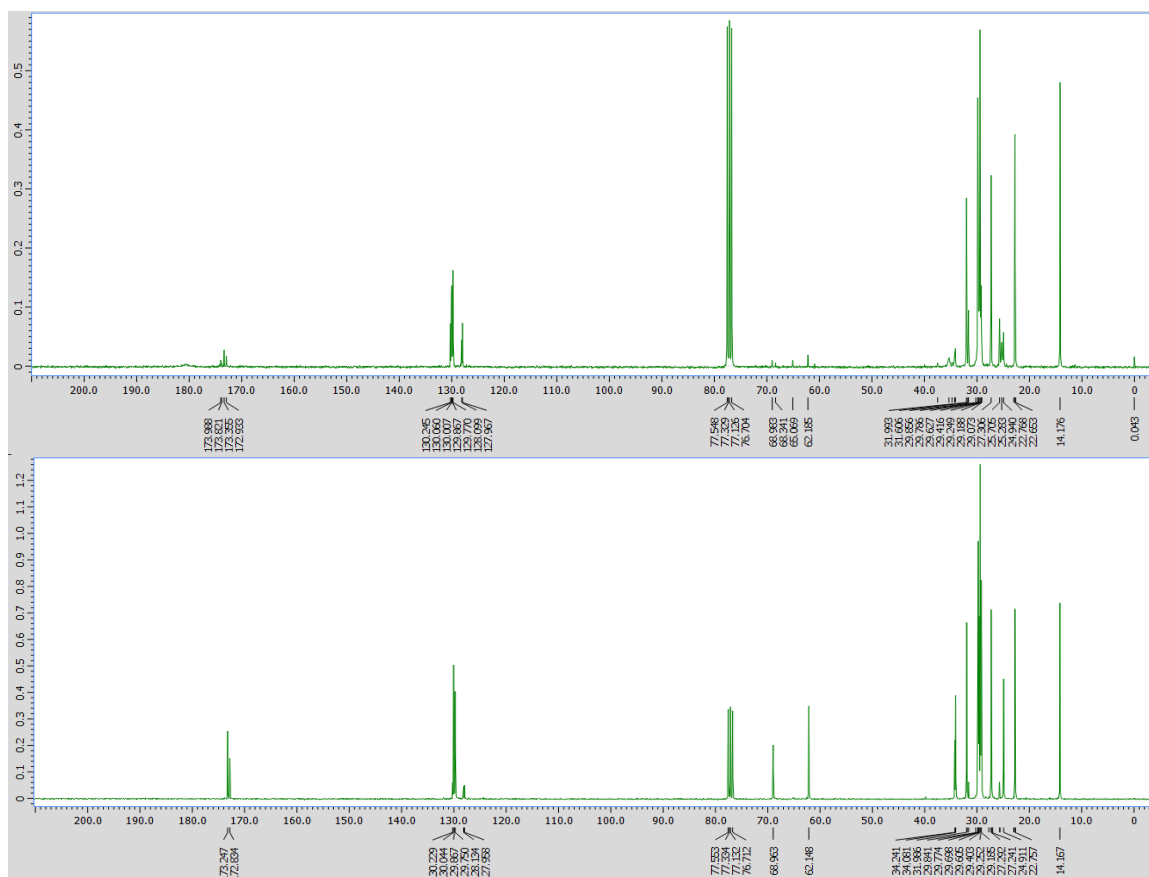


Fig. 5: ^{13}C NMR of the (a) HSF and (b) the extra virgin olive oil.

2.3.4. GC/MS analysis of the HSF and the ESF

The GC/MS data for the HSF and the ESF are sited in Fig. 6 and Table 7 as well as Fig. 7 and Table 8, respectively. The volatile fraction of the HSF consisted mainly of oleic and palmitic acid, which are also the major fatty acids in the OMW (Nasopoulou and Zabetakis, 2013). Minor compounds included ketones and esters in addition to 2,3-dihydro-N-hydroxy-4-methoxy-3,3-dimethyl-Indole-2-one. The volatile fraction of the ESF consisted mainly of glycerin and 2-Methyl-1,3-cyclohexanedione (di-ketone). Other compounds

were also present in the ESF such as Pyrimidine 1-acetylhexahydro-2,3-dimethyl- (9CI), 2-Methylcyclopentyl propylphosphonofluoridate, and tyrosol.

Compared to the ESF, the HSF contained more aliphatic compounds. Thermal cracking of vegetable oils was found to produce liquid products rich in hydrocarbons, however, oxygenated compounds such as carboxylic acids and ketones were also present in the liquid product (Alencar et al., 1983; Dandik et al., 1998; Fortes and Baugh, 1994; Lima et al., 2004). Therefore, research focus in the literature has shifted to catalytic cracking to reduce the oxygen content and improve upon the fuel properties of the liquid product.

Surprisingly, the GC/MS data of the HSF (Fig. 6 and Table 7) didn't include any triglycerides. This is because the GC/MS column cannot resolve raw triglycerides, they need to be converted to fatty acid methyl esters (FAME) before analysis. The transesterification of the Triglycerides in the HSF was not conducted. It is worth noting that in the GC/MS spectra of the HSF and the ESF, the baseline exhibited a spike after 24 minutes. This could be explained by the fact that a fraction of the sample was not volatile, thus did not elute off the column.

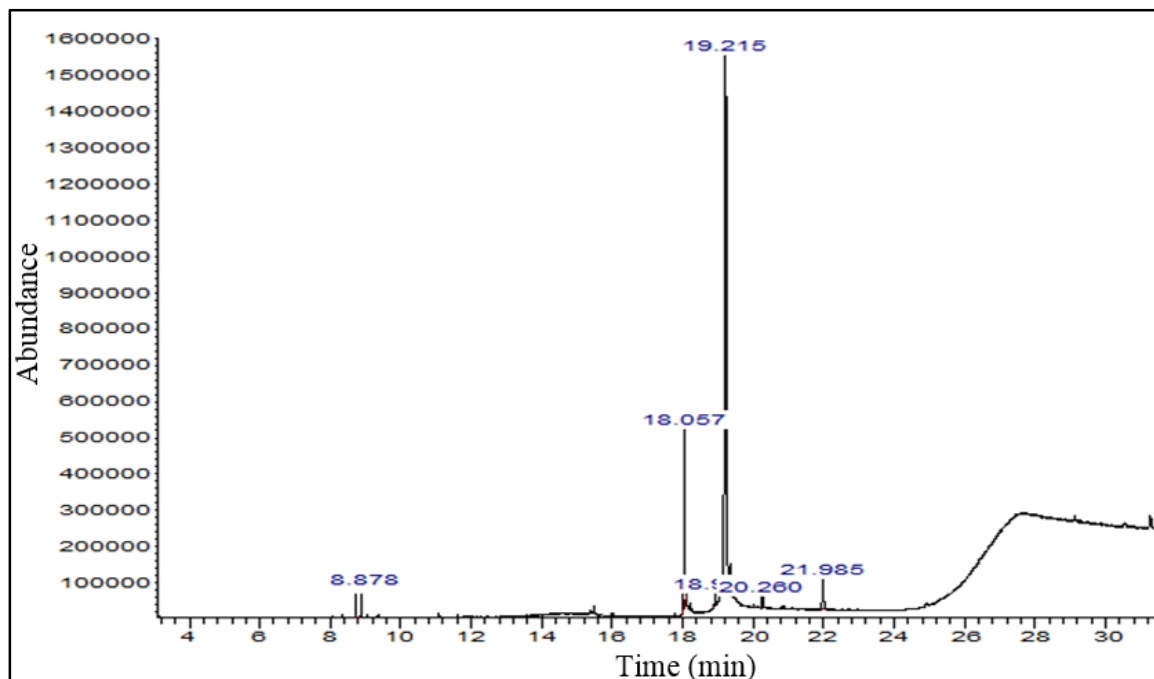
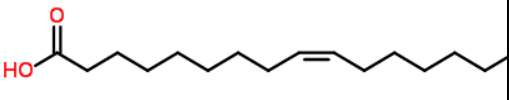
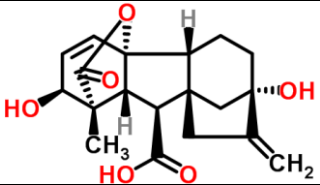
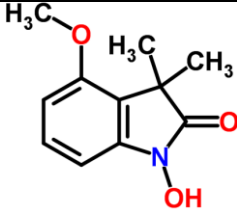


Fig. 6: Chromatogram from the GC/MS analysis of the hexanes soluble fraction of the OMWS

Table 7

Composition of the hexanes soluble fraction determined by GC/MS

Order	Compound	2D chemical structure	% Area
1	2-Nonanone	<chem>CCCCCCCC(=O)C</chem>	1.55
2	4-Methylpentyl Methoxyacetate	<chem>COCC(=O)OCCCC(C)C</chem>	1.81
3	Palmitic acid	<chem>CCCCCCCCCCCCCCCC(=O)O</chem>	15.05
4	Methyl Oleate	<chem>CCCCCCCC=CCCCCCCC(=O)OC</chem>	0.81

5	Oleic acid		76.36
6	Gibberellic acid		0.83
7	2,3-dihydro-N-hydroxy-4-methoxy-3,3-dimethyl-Indole-2-one		3.58

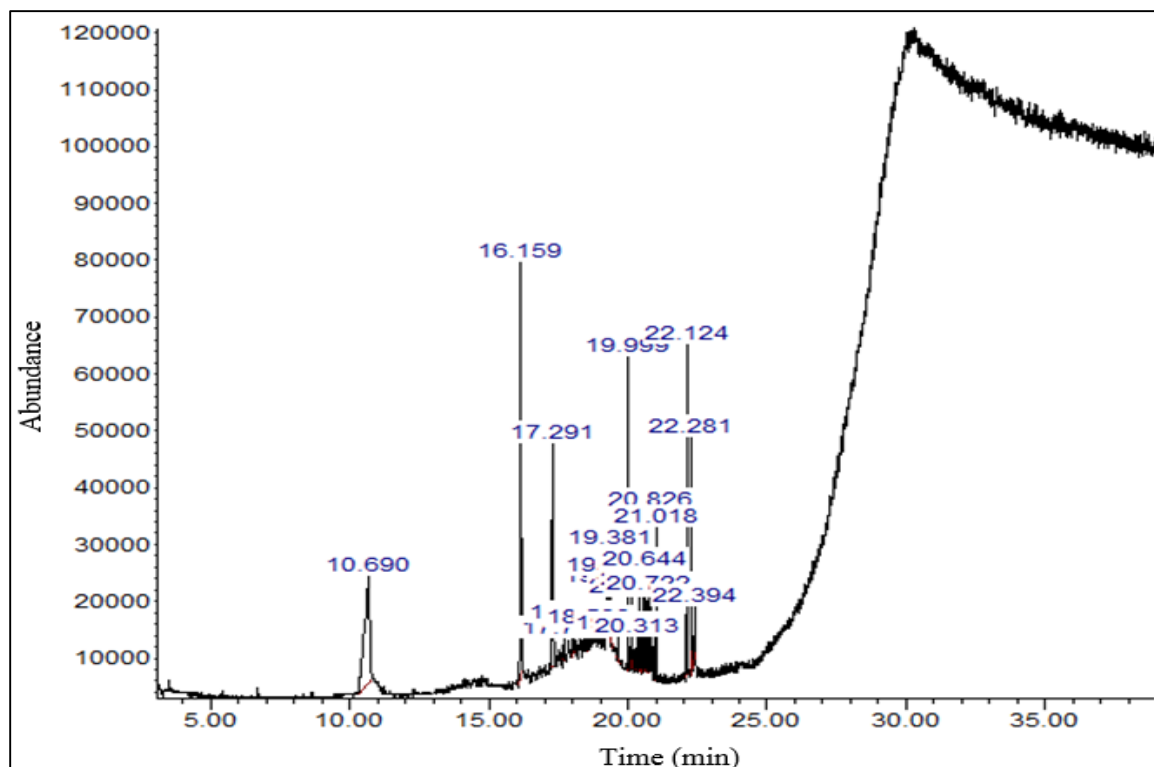
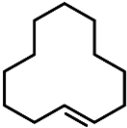
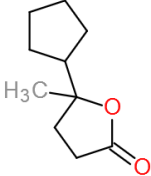
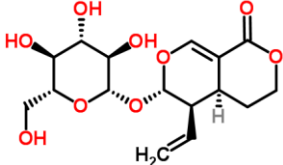
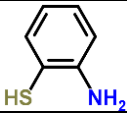
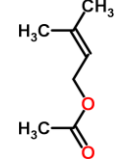
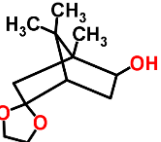
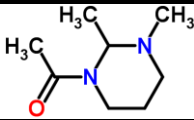
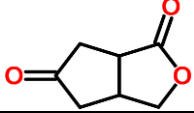
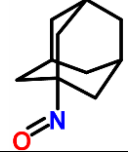


Fig. 7: Chromatogram from the GC/MS analysis of the 95 vol% ethanol soluble fraction of the OMWS

Table 8

Composition of the 95 vol% ethanol soluble fraction determined by GC/MS

Order	Compound	2D chemical structure	% Area
1	Glycerin		23.01
2	2-Methyl-1,3-cyclohexanedione		16.27
3	4-hydroxy-Benzeneethanol		7.5
4	bis (trimethylsilyl) ester Propanephosphonic acid		2.27
5	3-[p-Methoxyphenyl]-5-methylrhodanine		0.78
6	Stearyl iodide		1.32
7	Octadecyl ether		1.96
8	2-Methylbutyl heptanoate		2.29
9	1H-Indole, 2-(1,1-dimethyl-2-propenyl)-6-(3-methyl-2-butenyl)-		0.89
10	2-Methylcyclopentyl propylphosphonofluoridate		7.62
11	Methyl pentyl acetylene		1.42
12	n-Butanal		0.8

13	trans-Cyclododecene		2.22
14	2(3H)-Furanone, 5-cyclopentylidihydro-5-methyl-(CAS)		3.01
15	Sweroside		2.01
16	2-amino- (CAS) Benzenethiol		2.34
17	Prenyl acetate		4.51
18	5,5-ethylenedioxy-2-Bornanol		4.5
19	1-Acetyl-2,3-dimethylhexahydropyrimidine		8.43
20	3-Oxabicyclo[3.3.0]octane-2,7-dione		5.64
21	1-Nitrosoadamantane		1.21

2.3.5. Saponification value of the HSF

The SAP of the HSF was 64.41 mg KOH/g of sample (Table 9), which was lower than that of the extra virgin olive oil reported in the literature (181-192 mg KOH/g of sample) (Méndez and Falqué, 2007). The saponifiable compounds are those containing an ester group such as triglycerides, waxes, glycolipids, phospholipids, and sphingolipids. These compounds accounted for 14.97 wt.% of the HSF. The non-saponifiable fraction of the HSF may contain long-chain alcohols, sterols, and hydrocarbons.

Table 9
Saponification value and saponifiables yield (wt.%) of the hexanes soluble fraction

	HSF
Saponification value (mg KOH/g of sample)	64.41 ± 0.915
Saponifiables (wt.%)	14.97 ± 0.733

2.4. Conclusions

The OMWS was characterized and evaluated as potential feedstock for fast pyrolysis. The OMWS had high energy content, which will result in more valuable pyrolysis products from an energy perspective. The high ash content of the biomass will increase the biochar yield at the expenses of the volatile matter yields. The high nitrogen content will negatively affect the quality of the pyrolysis oil, whereas the very low sulfur content of the OMWS is beneficial. The high yield of the HSF is believed to be the major factor behind the high energy content of the OMWS.

2.5. References

- Alencar, J.W., Alves, P.B., Craveiro, a a, 1983. Pyrolysis of tropical vegetable oils. *J. Agric. Food Chem.* 31, 1268–1270. doi:10.1021/jf00120a031
- Al-Malah, K., Azzam, M.O.J., Abu-Lail, N.I., 2000. Olive mills effluent (OME) wastewater post-treatment using activated clay. *Sep. Purif. Technol.* 20, 225–234. doi:10.1016/S1383-5866(00)00114-3
- Azbar, N., Bayram, A., Filibeli, A., Muezzinoglu, A., Sengul, F., Ozer, A., 2004. A review of waste management options in olive oil production. *Crit. Rev. Environ. Sci. Technol.* doi:10.1080/10643380490279932
- Bridgwater, A. V., Meier, D., Radlein, D., 1999. An overview of fast pyrolysis of biomass. *Org. Geochem.* 30, 1479–1493. doi:10.1016/S0146-6380(99)00120-5
- Dandik, L., Aksoy, H., Erdem-Senatarlar, a, 1998. Catalytic conversion of used oil to hydrocarbon fuels in a fractionating pyrolysis reactor. *Energy & Fuels* 1148–1152. doi:10.1021/ef980012u
- Demirbas, A., 2008. Relationships derived from physical properties of vegetable oil and biodiesel fuels. *Fuel* 87, 1743–1748. doi:10.1016/j.fuel.2007.08.007
- Encinar, J.M., Beltrán, F.J., Bernalte, A., Ramiro, A., González, J.F., 1996. Pyrolysis of two agricultural residues: Olive and grape bagasse. Influence of particle size and temperature. *Biomass and Bioenergy* 11, 397–409. doi:10.1016/S0961-9534(96)00029-3
- Eroğlu, E., Gündüz, U., Yücel, M., Türker, L., Eroğlu, I., 2004. Photobiological hydrogen production by using olive mill wastewater as a sole substrate source. *Int. J. Hydrogen Energy* 29, 163–171. doi:10.1016/S0360-3199(03)00110-1
- Fortes, I.C.P., Baugh, P.J., 1994. Study of calcium soap pyrolysates derived from Macauba fruit (*Acrocomia sclerocarpa* M.). Derivatization and analysis by GC/MS and CI-MS. *J. Anal. Appl. Pyrolysis* 29, 153–167. doi:10.1016/0165-2370(94)07942-0
- Gokce, C.E., Guneyusu, S., Aydin, S., Arayici, S., 2009. Comparison of activated carbon and pyrolyzed biomass for removal of humic acid from aqueous solution. *Open Environ. Pollut. Toxicol. J.* 1, 43–48. doi:10.2174/1876397900901010043
- Graboski, M.S., McCormick, R.L., 1998. Combustion of fat and vegetable oil derived fuels in diesel engines. *Prog. Energy Combust. Sci.* doi:10.1016/S0360-1285(97)00034-8

- Jarboui, R., Chtourou, M., Azri, C., Gharsallah, N., Ammar, E., 2010. Time-dependent evolution of olive mill wastewater sludge organic and inorganic components and resident microbiota in multi-pond evaporation system. *Bioresour. Technol.* 101, 5749–5758. doi:10.1016/j.biortech.2010.02.069
- Karaosmanoglu, F., 1999. Vegetable oil fuels: a review. *Energy Sources* 21, 221–231. doi:10.1080/00908319950014858
- Kazagic, A., Smajevic, I., 2007. Experimental investigation of ash behavior and emissions during combustion of Bosnian coal and biomass. *Energy* 32, 2006–2016. doi:10.1016/j.energy.2007.03.007
- Lima, D.G., Soares, V.C.D., Ribeiro, E.B., Carvalho, D.A., Cardoso, É.C. V, Rassi, F.C., Mundim, K.C., Rubim, J.C., Suarez, P.A.Z., 2004. Diesel-like fuel obtained by pyrolysis of vegetable oils. *J. Anal. Appl. Pyrolysis* 71, 987–996. doi:10.1016/j.jaap.2003.12.008
- Méndez, A.I., Falqué, E., 2007. Effect of storage time and container type on the quality of extra-virgin olive oil. *Food Control* 18, 521–529. doi:10.1016/j.foodcont.2005.12.012
- Mohan, D., Pittman, C.U., Steele, P.H., 2006. Pyrolysis of wood/biomass for bio-oil: a critical review. *Energy and Fuels*. doi:10.1021/ef0502397
- Nasopoulou, C., Zabetakis, I., 2013. Agricultural and aquacultural potential of olive pomace a review. *J. Agric. Sci.* 5, 116–127. doi:10.5539/jas.v5n7p116
- Obied, H.K., Allen, M.S., Bedgood, D.R., Prenzler, P.D., Robards, K., 2005. Investigation of Australian olive mill waste for recovery of biophenols. *J. Agric. Food Chem.* 53, 9911–9920. doi:10.1021/jf0518352
- Pattiya, A., Titiloye, J.O., Bridgwater, A. V., 2010. Evaluation of catalytic pyrolysis of cassava rhizome by principal component analysis. *Fuel* 89, 244–253. doi:10.1016/j.fuel.2009.07.003
- Sacchi, R., Addeo, F., Paolillo, L., 1997. ¹H and ¹³C NMR of virgin olive oil. An overview. *Magn. Reson. Chem.* 35, S133–S145. doi:10.1002/(SICI)1097-458X(199712)35:13<S133::AID-OMR213>3.0.CO;2-K
- The olive oil source [WWW Document], 1998. URL <http://www.oliveoilsource.com/page/chemical-characteristics>

- Uzun, B.B., Pütün, A.E., Pütün, E., 2007. Composition of products obtained via fast pyrolysis of olive-oil residue: Effect of pyrolysis temperature. *J. Anal. Appl. Pyrolysis* 79, 147–153. doi:10.1016/j.jaap.2006.12.005
- Yildiz, G., Ronsse, F., Venderbosch, R., Duren, R. Van, Kersten, S.R.A., Prins, W., 2015. Effect of biomass ash in catalytic fast pyrolysis of pine wood. *Appl. Catal. B Environ.* 168-169, 203–211. doi:10.1016/j.apcatb.2014.12.044
- Zabaniotou, A.A., Kalogiannis, G., Kappas, E., Karabelas, A.J., 2000. Olive residues (cuttings and kernels) rapid pyrolysis product yields and kinetics. *Biomass and Bioenergy* 18, 411–420. doi:10.1016/S0961-9534(00)00002-7

CHAPTER 3

CATALYTIC PYROLYSIS OF OLIVE MILL WASTEWATER SLUDGE

Abstract

As a promising technology for generating alternative fuels, catalytic fast pyrolysis of biomass produces bio-oils with better fuel properties (higher pH, lower viscosity, lower oxygen content) compared with fast pyrolysis. In this work, two catalysts (red mud and HZSM-5) were evaluated for the catalytic pyrolysis of OMWS. A mixture of Olive Mill Wastewater Sludge (80 wt.%) and wood biochar (20wt.%) was pyrolysed in a bench-scale fluidized bed reactor using the sand/catalyst at temperature ranging from 400 °C to 500 °C, a fluidizing velocity (3 L/min) equal to three times the minimum fluidization velocity (3 L/min), and a feeding rate of 100 g/h. Physical and chemical characterization of the produced bio-oils was conducted. It was found that the organic liquid yield obtained at different reaction temperatures (400° C, 450° C, and 500 °C) was higher for red mud compared to HZSM-5, and the bio-oil produced at 450° C using red mud had the best fuel properties (higher heating value of 40 MJ/kg, dynamic viscosity of 5.4 cP, and pH 7.3). ¹³C NMR spectra of the bio-oils produced at 400 °C and 450° C using red mud and HZSM-5 had high content of aliphatic and aromatic compounds. Both catalysts rejected oxygen mainly as water. The red mud favoured decarboxylation over decarbonylation, whereas the HZSM-5 favoured the latter over the former.

Consequently, the oxygen and/or chlorine content of the red mud catalysis oil was lower than that from the HZSM-5 catalysis.

3.1. Introduction

Nowadays, the principal sources of fuels are petroleum, coal, and natural gas. The use of these fuels results in the release of undesirable pollutants such as SO_x, NO_x, and CO₂. Stimulated by the need to solve environmental issues and the security of energy supplies, researchers have been focusing on the development of renewable technologies and alternative energy sources. Waste agricultural biomass such as olive mill waste sludge, is a renewable energy source that is virtually free.

Olive mill wastewater sludge (OMWS) is an aqueous effluent containing olive skin and pits,¹ characterized by an offensive smell and high organic matter content including more than 30 phenolic compounds and long-chain fatty acids. These compounds are highly toxic to micro-organisms and plants. Therefore, technologies that would dispose of such waste material are needed. Fast pyrolysis is a very promising thermochemical process that converts feedstock to a liquid fuel product called bio-oil. Although fast pyrolysis can produce high bio-oil yield that can reach up to 75 wt. %, ² the quality of this bio-oil such as its high water content, acidity and low heating value restricts its application.³ OMWS can be considered as potential feedstock for bio-fuel production. In fact, pyrolysis of this agro-industrial waste material give a bio-oil characterized by a high heating value, high pH and low moisture and sugar contents.

The feasibility was first proved by the innovative work of Dr. Kamel Halouani and Dr. Foster Agblevor, who produced such bio-oil from OMWS. However, the viscosity and stability of the produced bio-oil makes it less competitive with petroleum crude.

The undesirable properties of the fast pyrolysis bio-oil originate from its chemical composition which consists mostly of oxygenated organic compounds. Hydrotreating and catalytic cracking are the major processes used to upgrade the bio-oil by rejection of oxygen. The catalytic cracking process is conducted at atmospheric pressure and does not require hydrogen supply.

This chapter focuses on the catalytic pyrolysis of the Olive Mill Wastewater Sludge (OMWS) using HZSM-5 and red mud in order to reduce the oxygenates in the bio-oils, resulting in an improved stability and lower viscosity of these bio-oils. Physical and chemical characterization of the catalytic bio-oils was conducted.

3.2. Experimental

3.2.1. Feedstock

Olive Mill Wastewater Sludge (OMWS) was collected from a Tunisian disposal site (Agareb 3030, Sfax, Tunisia). The sludge was collected from evaporation ponds containing aged OMWS (1-2 years). The feedstock was ground in a Wiley mill model 4 (Thomas Wiley Scientific, Swedesboro, NJ, USA) to pass a 2-mm screen.

The ash content of the OMWS was determined according to ASTM E1755. Consequently, the volatiles content was determined on dry weight basis.

3.2.2. Catalysts

The Red mud was obtained as slurry. After drying at room temperature for two days, it was ground using a mortar and pestle and sieved to obtain the desired particle size (125-180 μ m). The zeolite was supplied by BASF (BASF Catalyst LLC, Iselin, NJ, USA). The particle size of both red mud and ZSM-5 catalysts used in the catalytic pyrolysis experiments was 125-180 μ m.

The red mud was used as received, whereas the ZSM-5 was calcined at 550 $^{\circ}$ C for 5 hours in a Thermo Scientific laboratory-muffle-furnace. After activation, the ZSM5 was converted to HZSM-5.

The surface area measurement for the red mud was conducted on a Quantachrome BET surface analyzer (Quantachrome Instruments, Boyton Beach, FL). Approximately, 0.15-0.2 g of the sample was degassed for 3 hours at 300 $^{\circ}$ C under helium/nitrogen gas mixture (10% nitrogen and 90% helium).

The XRF analysis of the fresh red mud was conducted by the Analytics Laboratory in the Geology department at Utah State University (Logan, UT, USA). The HZSM-5 used in this work was from the same batch used by Yathavan and Agblevor (2013), therefore, its characterization can be found in their research paper.

3.2.3. Pyrolysis of olive mill wastewater sludge

In order to facilitate the flow of OMWS from the feeder into the reactor, mixtures of OMWS and biochar obtained from pyrolysis of wood at temperature ≥ 500 $^{\circ}$ C were prepared in a blender, and the proper OMWS/biochar ratio was determined. A mixture of

80 wt.% OMWS and 20 wt.% biochar was adopted and was fed to the bubbling fluidized bed reactor at 100 g/h.

Fast pyrolysis experiments were carried out using a bench-scale fluidized bed reactor located in the USTAR Bioinnovation Center building 620 at Utah State University, Logan, UT. The pyrolysis unit comprised of a K-Tron volumetric feeder, a 50 mm in diameter and 500 mm long bubbling fluidized bed reactor equipped with a 100 μm porous metal gas distributor.

The reactor was externally heated with a three-zone electric furnace (Thermcraft, Winston-Salem, North Carolina) and was connected, in series, with a hot gas filter, two condensers chilled with ethylenglycol/water mixture, an electrostatic precipitator, a coalescing filter and a Varian 490-Micro gas chromatograph (Agilent Technologies, Inc., Santa Clara, CA, USA).

About 100 g of silica sand or catalyst were used as the fluidizing medium. When using silica sand (250-425 μm) as the fluidizing medium, a total of 18.3 L/min of nitrogen gas was used to fluidize the bed and entrain the feedstock into the reactor. For both red mud and HZSM-5, a total of 8 L/min of nitrogen was used.

Using a screw feeder, the feedstock was conveyed from the hopper to an entrainment zone where nitrogen gas was used (5 L/min for both catalytic and non-catalytic experiments) to entrain the feed through a jacketed air-cooled feeder tube into the fluidized bed.

During pyrolysis, the mixture of vapors, gases and some of the biochar that exited from the reactor were separated by the hot gas filter maintained at 400° C to avoid the condensation of vapors going through it. The biochar particles were stopped by the hot gas filter, while the biochar-free vapors and non-condensable gases passed through two condensers connected in series. These first and second condenser was maintained at 10-13 °C and 4-6 °C, respectively, using an 18-liter Haake A82 Temperature Bath/Recirculator (Haake, Karlsruhe, Germany). The cooling liquid was 50/50 ethylene glycol and water. The aerosols and non-condensable gases that escaped from the condensers passed through an electrostatic precipitator (ESP) maintained at 20-30 kilovolts.

The aerosol particles which have similar charge as the ESP rod are repulsed to the plastic wall of the ESP body. The aerosols which escaped the ESP were trapped in a F72C Series oil removing coalescing filter (NORGREN, Littleton, Colorado, U.S.A.).

The clean non-condensable gases that came out of the coalescing filter passed through a totalizer which measured the total amount (Liters) of gases that went through the system. A sample of the non-condensable gases that came out of the coalescing filter was injected (every 10 minutes) into the Varian 490- micro gas chromatograph.

The liquid (organics/water) and solid (char/coke) product yields were determined gravimetrically by weighing the reactor, hot-gas-filter, water chilled condensers, and the ESP before and after each experiment. The pyrolysis experiments lasted for 2 hours each.

3.2.4. Gas analysis

A Varian 490 micro GC (Agilent Technologies, Inc. Santa Clara, CA USA) was used to identify and quantify the non-condensable gases generated from the pyrolysis of the OMWS. During pyrolysis, 1 μ L of the gases was automatically injected into the micro GC and analyzed online every 10 min. The micro GC was equipped with two channels where the first one was equipped with a 10 m Molsieve (MS) 5 Å column, and the second channel had a 10 m porous polymer column (PPU). Each module had a thermal conductivity detector. The MS column was used to analyze hydrogen, methane and carbon monoxide. Carbon dioxide and C₁–C₅ gases were analyzed by the PPU column.

3.2.5. Bio-oils characterization

The pyrolysis liquids collected from the water chilled condensers and from the ESP were analysed for their moisture content. The moisture of the bio-oils was determined by volumetric Karl Fisher titration method. A Metrohm 701KF Titrino (Brinkmann Instruments, Inc., NY, USA) and a 703 titration stand using Hydranal[®] composite 5 reagent. The bio-oils collected in the ESP were used for further analysis since they had very low (<1 wt.%) water content. The pH of the oils was measured using a Mettler Toledo SevenEasy pH meter and probe (Mettler-Toledo GmbH, Switzerland). The pH values were taken after 7-10 min of stabilization of the mechanically stirred oil.

The dynamic viscosity of bio-oils was measured at 40° C using a Brookfield DV-II+ Pro viscometer (Brookfield Engineering Laboratories, Middleboro, MA, USA). The

calorific value was determined using the IKA C2000 basic bomb calorimeter (IKA Works, Inc., NC, USA).

The organic elemental composition analysis of the catalytic bio-oil was determined using a Thermo Scientific Flash 2000 organic elemental analyzer (ThermoFisher Scientific, Cambridge, UK). The sample size was 2-4mg and the oxygen content of the oils was determined by difference.

The Fourier-transform infrared (FTIR) analysis was conducted for ESP oils over a range of 4000-650 $^{\circ}\text{Cm}^{-1}$ using a Nicolet Avatar IR spectrometer model 370 DTGS (Nicolet Instrument. Inc, Madison, WI, USA) equipped with a DTGS-KBr (potassium bromide) detector in multi-bounce horizontal attenuated total reflectance (HATR) mode. 0.03 to 0.04 g of oil was spread on the sample cell. For each sample, 128 scans and a resolution of 4 were used.

The ^{13}C NMR spectra of the ESP oils were obtained using a JOEL 300 MHz NMR spectrometer (JOEL Ltd, Tokyo, Japan) after 3000 scans. The pulse width was 14.75 μs and the acquisition time was 1.57 s with a 2 seconds relaxation delay. The ^{13}C NMR samples were prepared by dissolving approximately 0.1-0.2 g of bio-oil into 0.7 g of deuterated dimethylsulfoxide (DMSO- d_6) (Sigma Aldrich, St. Louis, MO, USA).

3.3. Results and discussion

3.3.1. Catalyst characterization

The properties of the red mud and HZSM-5 are shown in Table 10. At the same particle size, the surface area of the HZSM-5 was more than 3 times higher than that of the red mud. The pH of a red mud slurry was approximately 9.

The HZSM-5 is known to be an acidic catalyst.^{4,5} The red mud is a waste product from the Bayer process that refines bauxite to produce alumina, whereas the HZSM-5 is a patented synthetic catalyst. Therefore, the latter is much more expensive than the former.

Table 10. Properties of the red mud and the HZSM-5

	Red mud	HZSM-5*
B.E.T. surface area (m ² /g)	30	115
Particle size (µm)	125-180	125-180
Average composition (wt.%)	Fe ₂ O ₃ (54%), Al ₂ O ₃ (14%), SiO ₂ (9%), CaO (9%), TiO ₂ (6%), Na ₂ O (6%), P ₂ O ₅ (2%)	SiO ₂ /Al ₂ O ₃
Structure	Amorphous	Crystalline
pH	Alkaline	Acidic
Description	Waste byproduct of the Bayer process	Synthetic catalyst

*: adopted from Yathavan and Agblevor (2013).

3.3.2. Pyrolysis yields

3.3.2.1. Fast pyrolysis of the OMWS

The product yields distribution from the fast pyrolysis/catalytic pyrolysis of the OMWS-biochar blend at different reaction temperatures (400 °C, 450 °C, and 500 °C) are reported in Table 11. The biochar yield ranged from 24.5 to 31.8 wt.% and decreased with increasing reaction temperature. The gas yield ranged from 20.3 to 25.2 wt.% and increased with increasing reaction temperatures. The liquid product yields, which ranged from 39.4 to 44.9 wt.%, were higher than those of biochar and biogas, for all three temperatures. The reaction temperature of 450 °C gave the highest liquid yield (44.9 wt. %). The water yield

decreased as the reaction temperature increased. The maximum organics yield (30.6 wt. %) was obtained at 450 °C.

The decrease in the char/coke yield and increase in the gas yield with the increasing reaction temperature were in agreement with the literature.^{6,7,8} However, the maximum liquid yield achieved (44.9 wt. %, dry basis) as well as the best reaction temperature (450 °C) at which this yield was obtained, were different from those reported in the literature for the fast pyrolysis of most agricultural residues and biomass pyrolyzed using a fluidized bed reactor.^{9,10,11} The lower liquid yield could be due to the composition of the biomass and the hot vapors filter. In fact, the potassium in the biomass ash was reported to catalyze reactions that promote water and non-condensable gases formation, which will be competing with the pyrolysis reaction.^{12,13,14} Furthermore, the ash in biomass can lower the temperature at which the organics yield is maximized.¹⁵

The pyrolytic water could originate from condensation reactions and/or secondary cracking reactions. Another source of the pyrolytic water can be the ketonization reaction which converts two fatty acid molecules to a ketone, CO₂, and water.

Low reaction temperature (~ 400 °C) can result in a partial polymerization/condensation reactions of the species produced during the primary thermal decomposition of the OMWS. The result of such reactions is the formation of more biochar. As the reaction temperature increases (450 °C), the species produced from the primary thermal scission of the chemical bonds within the biomass, undergo further thermal cracking to form more volatile species. These volatile species are quenched to give rise to the bio-oil. The greater the volatiles release from the biomass, the lower the bio-char yield

will be. A further increase of the reaction temperature (500 °C) would result in a lower char yield and higher non-condensable gases. In fact, the higher the reaction temperature, the more energy is available to break chemical bonds in the biomass, to produce volatile matter, and within the volatile matter, to produce non-condensable gases.

3.3.2.2. Effect of catalyst on the pyrolysis products distribution

Based on the data from the fast pyrolysis of the OMWS (Table 11), it was concluded that 450 °C was the best reaction temperature for a maximum bio-oil yield. Therefore, the data from the fast pyrolysis of the OMWS at 450 °C was used as a baseline for the evaluation of the performance of HZSM-5 and red mud at the same reaction temperature.

The results of the catalytic pyrolysis are shown in Table 11. At 450 °C, the use of catalysts resulted in the decrease of the total liquid yield, whereas the gas product yield increased. While the organics yield decreased, the water content increased with the use of both catalysts. These trends were in agreement with the literature for both red mud and HZSM-5.^{16,17} The char/coke yield decreased slightly for the HZSM-5 catalyzed pyrolysis. The char/coke yield for the red mud catalyzed pyrolysis was higher than that obtained from the fast pyrolysis of the OMWS. It was speculated that during the red mud catalyzed pyrolysis, the hydrocarbons in the primary pyrolysis vapors could adsorb on the surface of the catalyst where they undergo homiletic cleavage. As a result of this reaction, radicals are formed. These radicals could react rapidly with each other to form coke. The catalytic pyrolysis of the OMWS resulted in a significant increase in the water yield. Cracking and dehydration reactions were reported to be the main reactions observed during zeolite catalyzed pyrolysis of biomass.^{18,19,20}

After adsorption of oxygenated compounds on the acidic sites of the zeolite, and depending on the pore size of the catalyst, decomposition and/or bimolecular monomer dehydration can occur.²⁰ As for the red mud catalyzed pyrolysis the water could be originating from the water-gas-shift reaction as well as the ketonization reaction. In fact, iron oxides are known to promote the water-gas-shift reaction as well as the ketonization reaction. Titanium oxide promotes ketonization reaction. Furthermore, the main activity of the non-activated alumina (Al_2O_3) as well as the silicon dioxide (SiO_2) is dehydration.²¹ During the red mud catalyzed pyrolysis, the organic fraction of the pyrolysis primary vapors was converted mainly into pyrolytic water and char/coke.

During the HZSM-5 catalyzed pyrolysis, the organic fraction was converted mostly into water. The catalytic pyrolysis gas product yield increased compared to the fast pyrolysis one. The red mud produced more gas than the HZSM-5.

3.3.2.3. Effect of reaction temperature on the performance of the catalysts

The effect of the pyrolysis reaction temperature was investigated by conducting catalytic pyrolysis of the OMWS at different temperatures (400, 450, and 500 °C). The data is presented in Table 11. For both catalysts, as the reaction temperature increased, the biochar yield decreased whereas the gas yield increased. As for the total liquids, it decreased with the increasing temperature.

For the red mud and HZSM-5 catalyzed pyrolysis, the biochar yield ranged from 24.5 to 37 wt. % and from 22.5 to 34.3 wt. %, the gas yield ranged from 23 to 31 wt.% and from 21.2 to 34.7 wt.%, the total liquid yield ranged from 36.8 to 43.9 wt. % and from 30.1 to 39.9 wt. %, respectively. The water yield ranged from 13.8 to 20.9 wt.% for the red mud

and from 17.7 to 19.9 wt. % for the HZSM-5. A maximum water yield was observed at 450 °C for both catalysts and was 20.9 wt. % for red mud and 19.9 wt.% for HZSM-5 catalyzed pyrolysis. The organic yield decreased with the increasing reaction temperature for both catalysts. It ranged from 21.8 to 25.3 wt. % for the red mud and from 12.2 to 22.2 wt. % for the HZSM-5 catalyzed pyrolysis.

3.3.3. Characterization of the pyrolysis oils

The bio-oil that was subject to the characterization study was collected from the ESP, where most of the organic fraction was. The properties of the ESP oil are presented in Table 12. All bio-oils from the fast pyrolysis and catalytic pyrolysis had pH close to neutral. The reaction temperature didn't have a significant effect on the pH of the bio-oil in the absence of catalyst. The bio-oil from the fast pyrolysis of the OMWS at 450 °C, had a pH of 6.4, which was the same as the pH of the OMWS slurry (pH 6.4). However, when catalyst was used at 450 °C, the pH of the bio-oil increased slightly and was 7.3 for the red mud catalyzed pyrolysis and 6.7 for the HZSM-5 catalyzed pyrolysis. The reaction temperature at which the bio-oil was produced influenced its pH. For the red mud catalyzed pyrolysis, the pH increased from 7.1 to 7.4 as the reaction temperature increased from 400 °C to 500 °C. A similar trend was observed for the pH of the bio-oils from HZSM-5 catalyzed experiments, however the pH values of the oils from HZSM-5 catalyzed pyrolysis were lower than those obtained for the red mud experiments.

The ESP oil from the fast pyrolysis of the OMWS at 450 °C had a gel-like texture at room temperature, however, it started flowing when held in the palm of a hand for a few minutes. The dynamic viscosity of this bio-oil was 42.92 c.P. As the fast pyrolysis reaction

temperature increased to 500 °C, the viscosity decreased to 28 c.P at 40 °C. At lower reaction temperature i.e. 400 °C, the fast pyrolysis oil looked similar to the one obtained at 450 °C and had roughly the same dynamic viscosity. For the catalytic pyrolysis experiments, the bio-oil collected was free flowing. The 450 °C red mud catalyzed pyrolysis bio-oil had a dynamic viscosity of 5.66 c.P, which was more than 7 times lower than that of the FP oil at the same reaction temperature. The bio-oil from the HZSM-5 experiment conducted at 450 °C had a dynamic viscosity of 7.06 c.P, which was 6 times lower than that of the FP bio-oil. The reaction temperature had a significant effect on the dynamic viscosity of the catalytic bio-oils.

At lower reaction temperature (400 °C), the viscosity of the red mud and HZM-5 oils were, respectively, 71 % and 21 % higher than those obtained at 450 °C. At higher reaction temperature (500 °C), the viscosity of the bio-oils from the red mud and HZM-5 catalyzed pyrolysis decreased by 15.5 % and 11.9 %, respectively, compared to the viscosity at 450 C. It was obvious that both catalysts reduced the viscosity of the bio-oil significantly. However, the red mud catalyzed pyrolysis produced less viscous bio-oil compared to FP and HZSM-5 catalyzed pyrolysis.

The energy content of the FP oil produced at 450 °C was 38.8 MJ/kg. When red mud and HZSM-5 were used at the same reaction temperature, the HHV of the produced bio-oils increased by 5.7 % and 2.1 %, respectively. The reaction temperature didn't have a significant effect on the HHV values for the fast pyrolysis and catalytic pyrolysis oils. Red mud catalyzed pyrolysis produced an oil with higher energy content compared to HZSM-5 and sand experiments.

Table 11. Product yields distribution for the catalytic/conventional pyrolysis of the OMWS

	Yields (wt. %, dry basis)											
	Sand			Fresh red mud			H-ZSM5					
	400 °C	450 °C	500 °C	400 °C	450 °C	500 °C	400 °C	450 °C	500 °C			
Char/coke	31.8±3.2	26±0.1	24.5±0.4	37±3.4	31.5±0.8	24.5±1.6	34.3±0.4	24.7±0.4	22.5±0.7			
Liquid	42.3±2.0	44.9±1.2	39.4±2.6	43.9±2.55	41.4±0.0	36.8±0.6	39.9±4.8	38±2.3	30.1±3.6			
Water	15.8±2.1	14.4±3.0	13.1±2.0	18.6±1.9	20.90±0.3	13.8±2.1	17.7±4.2	19.9±1.3	17.9±1.7			
Organics	26.5±0.1	30.6±1.8	26.3±0.6	25.3±0.5	20.49±0.2	21.8±1.5	22.2±0.6	18.2±0.9	12.2±1.9			
Gas	20.3±1.6	22.9±1.8	25.2±2.7	23±2.6	27.2±0.5	31±2.2	21.2±1.6	24.3±1.7	34.7±1.6			

Table 12. Properties of the ESP bio-oils for the catalytic/conventional pyrolysis of the OMWS

	Coarse sand			Fresh red mud			HZSM-5		
	400 °C	450 °C	500 °C	400 °C	450 °C	500 °C	400 °C	450 °C	500 °C
Reaction temperature (°C)									
Moisture (wt. %)	0.39	0.62	0.4	0.25	0.17	0.25	0.28	0.33	0.36
pH	6.5	6.4	6.4	7.1	7.3	7.4	6.4	6.7	7
Dynamic viscosity (cP) at 40 °C	42.87	42.92	28	9.68	5.66	4.78	8.54	7.06	6.22
HHV (MJ/kg)	38.7	38.8	39.4	40.4±1.2	41±0.9	41.3±0.2	39.1±0.7	39.6±1.1	38.4±0.0

The elemental composition of the conventional and catalytic pyrolysis oils produced at 450 °C is shown in Table 13. It can be clearly seen that the oxygen content of the catalytic oils decreased significantly compared to the conventional pyrolysis oil, which indicated that both catalysts promoted the deoxygenation of the pyrolysis primary vapors. The catalytic pyrolysis increased the carbon content of the bio-oil and decreased its oxygen and/or chlorine content. The nitrogen content of the red mud and the HZSM-5 catalytic oils were 2.13 wt. % and 3.55 wt. %, respectively. For all bio-oil samples (from catalytic and conventional pyrolysis), the sulfur content was below the detection limit of the instrument. The presence of nitrogen in the bio-oil could cause increased emission of NO_x during combustion. Farther the HHV value of the bio-oil is inversely proportional to its nitrogen content.

Table 13. Elemental composition of the ESP oils from the conventional/catalytic pyrolysis of the OMWS at 450 °C

	OMWS_sand	OMWS_FRM	OMWS_HZSM-5
C	77.15±0.14	83.54±0.12	81.75±0.26
H	11.78±0.06	11.45±0.01	10.64±0.09
N	2.75±0.03	2.13±0.06	3.55±0.06
S	bdl	bdl	Bdl
O and/or Cl*	8.32±0.23	2.88±0.04	3.94±0.38

*: calculated by difference, bdl: below the detection limit.

The FTIR spectrum of the 450° C non-catalytic bio-oil is shown in Figure 8a. The broad peak centered at 3200 °Cm⁻¹ could be due to N-H stretching in amides.²² The peak at 1708 cm⁻¹ was overlapping with another peak at 1660 cm⁻¹. While the latter indicated the presence of amides,²² the former could be due to carboxylic acids, ketones, aldehydes

and/or esters. The strong CH₂ and CH₃ stretching vibrations between 2850 °Cm⁻¹ and 2956 cm⁻¹ indicates the presence of aliphatic and aromatic hydrocarbons. The deformation vibrations between 1377 and 1456 cm⁻¹ support the presence of aliphatic hydrocarbons (alkanes).²³ The peak at 965 cm⁻¹ corresponds to the C-H stretching in trans-disubstituted olefins.

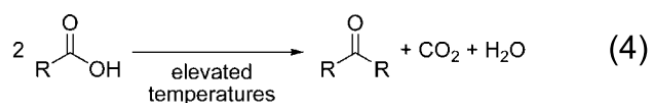
The FT-IR spectra of the catalytic bio-oils obtained at 450° C are shown in Figure 8b-c. It was clear that the use of both catalysts had significant effect on the chemical composition of the bio-oil. The two catalytic bio-oil spectra exhibited similarities. The strong CH₂ and CH₃ stretching vibrations between 2850 cm⁻¹ and 2956 cm⁻¹, indicating the presence of aliphatic and aromatic hydrocarbons, were more intense for both catalysts compared to the non-catalytic bio-oil spectrum. Additionally, the spectra of the catalytic bio-oils exhibited some peaks that were absent in the non-catalytic bio-oil spectrum.

Both catalytic bio-oils spectra had strong adsorption peaks at 698 and 750 °Cm⁻¹, which represent mono-substituted rings in aromatic compounds. Furthermore, the peak between 1605-1590 cm⁻¹ corresponding to the aromatic C=C bond was present in both catalytic bio-oil spectra.

It is worth noting that the signals corresponding to N-H stretch (3200 °Cm⁻¹), the amide II band in secondary acyclic amides (1552 cm⁻¹), and the C-N stretch of primary amides (1405 cm⁻¹) were absent in the catalytic bio-oils spectra.

The FT-IR spectra of the red mud and HZSM-5, also, exhibited some differences. The two peaks at 910 and 990 °Cm⁻¹ present in the red mud catalytic bio-oil spectrum corresponds to mono-substituted olefins. These two peaks were absent in the HZSM-5 oil

spectrum. The sharp C=O stretching peak at 1705 cm^{-1} in the HZSM-5 catalytic bio-oil shifted to 1713 cm^{-1} and was attenuated for the red mud catalytic bio-oil. This shift could be due to a change in the C=O environment. A possible explanation for this change is the ketonization of carboxylic acids (Equation 4). In fact, oxides such as Fe_2O_3 , CaO and TiO_2 , which are present in the red mud were reported to promote the formation of linear ketones.²⁴ The ketonization reaction would contribute to the deoxygenation of the pyrolysis primary vapors by rejecting oxygen as water and CO_2 .



It is worth noting the weak peak at 2225cm^{-1} (Figure 8-c) which was unique to the HZSM-5 catalytic bio-oil, and was attributed to the nitrile group ($\text{C}\equiv\text{N}$). It was believed that, due to its acidic nature, HZSM-5 catalyzed the dehydration of amides to give nitrile. In fact, the Brønsted acid site of the HZSM-5 would help protonating the hydroxyl group of the amide to give a water molecule and a nitrile.

The use of both catalysts brought a change to the chemical composition of the bio-oil. The differences in the FTIR spectra of the catalytic bio-oils indicated that red mud and HZSM-5 modify the pyrolysis vapors through different pathways. The FTIR gave a rough idea about the functional groups present in the bio-oils. In order to have more information about the chemical composition of the bio-oils, the NMR analysis was conducted.

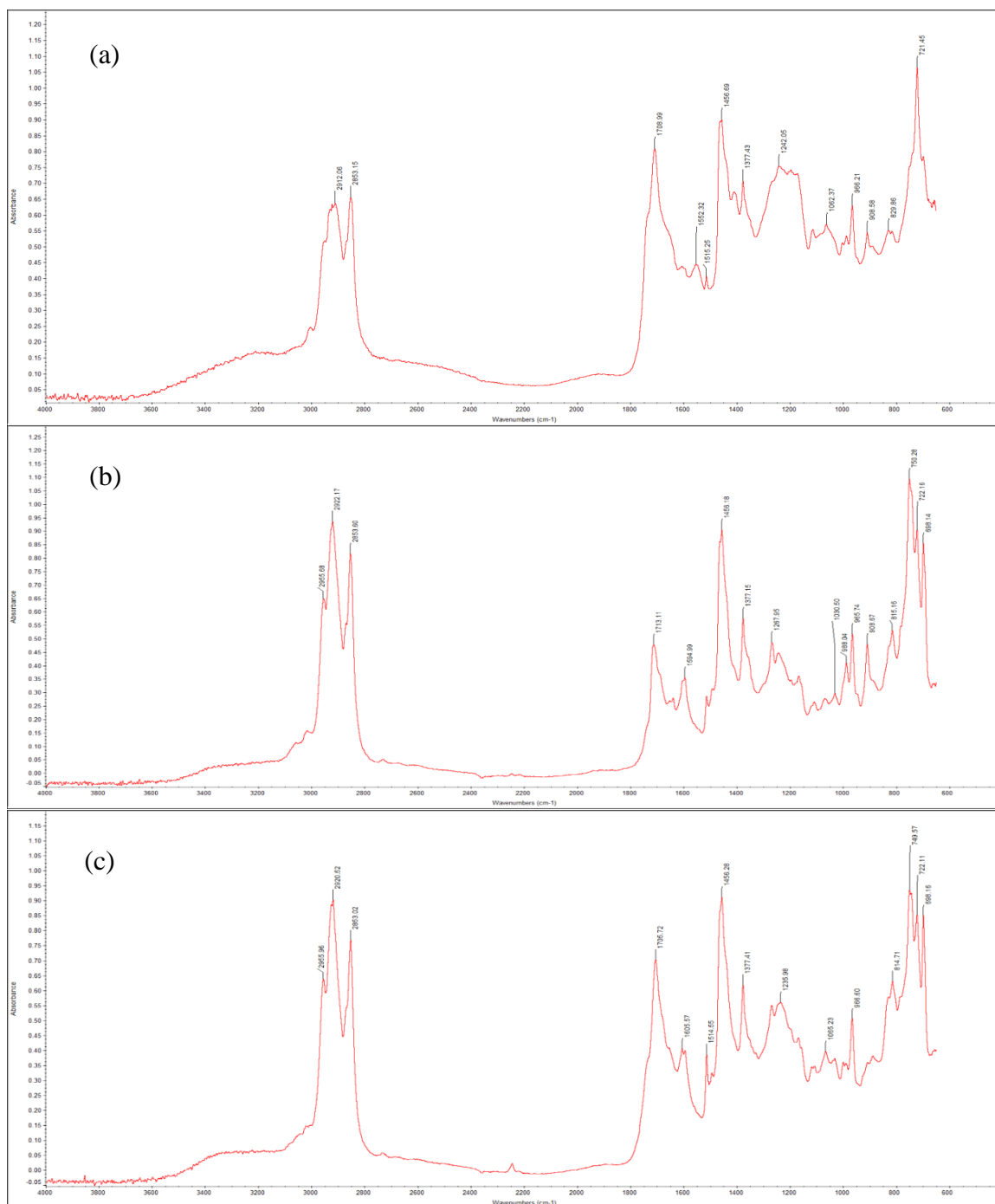


Figure 8. FT-IR spectra of the bio-oils from the (a) non-catalytic, (b) red mud catalyzed, and (c) HZSM-5 catalyzed pyrolysis of OMWS mixture at 450 °C.

The ^1H NMR spectra of the non-catalytic and catalytic bio-oils obtained at 450°C are shown in Figure 9a-c. In the non-catalytic bio-oil spectrum (Figure 9a), the aliphatic chain (0.5-3 ppm) were dominant, whereas the aromatic compounds signal (6.5-8.5 ppm) was weak. The peaks at 5.3, 1.9 and 2.65 ppm correspond to olefinic protons ($-\text{CH}=\text{CH}-$), α -methylene group to one double bond ($=\text{CH}-\text{CH}_2-$), and α -methylene group to two double bonds ($=\text{CH}-\text{CH}_2-\text{CH}=\text{}$), respectively. The sharp singlet at 3.15 ppm was attributed to methylene proton next to heteroatom (oxygen, nitrogen). Therefore, the bio-oil from non-catalytic of OMWS contained mainly aliphatic chains and olefins and low aromatic content. These results were in agreement with the FTIR data. It is worth noting the broad peak between 6.4 and 5.5 ppm corresponding to N-H proton, which indicate the presence of amide and possibly indole N-H groups and pyrole.^{22,25} The presence of amides is in agreement with the FTIR results.

For the catalytic bio-oils spectra, the 8.5-6.5 ppm region (aromatic compounds) was more intense compared to the non-catalytic bio-oil spectrum. The signals corresponding to the olefinic protons (5.3, 1.9 and 2.65 ppm) had reduced intensity compared to the non-catalytic bio-oil spectrum, which indicated that both catalysts cleaved some of the C=C double bonds. Interestingly, the peak at 5.3 ppm corresponding to ($-\text{CH}=\text{CH}-$) in olefins had higher intensity in the red mud bio-oil spectrum compared to the HZSM-5 one, which indicated that the HZSM-5 bio-oil contained less olefins compared to the red mud bio-oil, which was in agreement with the FTIR interpretation. The N-H signal between 6.4 and 5.5 ppm was absent in both catalytic bio-oils.

At lower pyrolysis reaction temperature (400 °C), the chemical composition of the non-catalytic oil was not significantly affected. The chemical composition of the catalytic bio-oils, however, was affected by the reaction temperature.

The ^1H NMR spectra of the catalytic bio-oils obtained at 400 °C are shown in Figure 10a-c. At lower reaction temperature, the fast pyrolysis oil contained more unsaturated compounds (2-2.2 ppm) and less aromatics (6.5-8.5 ppm). For both catalytic bio-oils, the aromatic signals decreased, whereas the aliphatic signals increased. It is also worth noting that unlike the red mud bio-oil, the HZSM-5 catalytic bio-oil spectrum did not have the signals corresponding to methylene groups attached to acid (2.34 ppm) and signals corresponding to methylene groups attached to an ester (2.31 ppm).

The ^1H NMR spectra of the conventional and catalytic pyrolysis oils obtained at 500 °C are shown in Figure 11a-c. At higher reaction temperature (500 °C), the N-H signal (6.4 and 5.5 ppm) and the methylene peak (3.15 ppm) were not present in the fast pyrolysis oil spectrum. The intensity of the signals at 5.3, 1.9 and 2.65 ppm corresponding to (-CH=CH-), α -methylene group to one double bond (=CH-CH₂-), and α -methylene group to two double bonds (=CH-CH₂-CH=), were lower at higher reaction temperature. As for the catalytic oils, the intensity of the signals at 5.3, 2.65, and 1.9 ppm decreased in the case of the red mud catalyzed pyrolysis, whereas the aromatics signal increased probably due to the cyclization of olefins to produce aromatics.

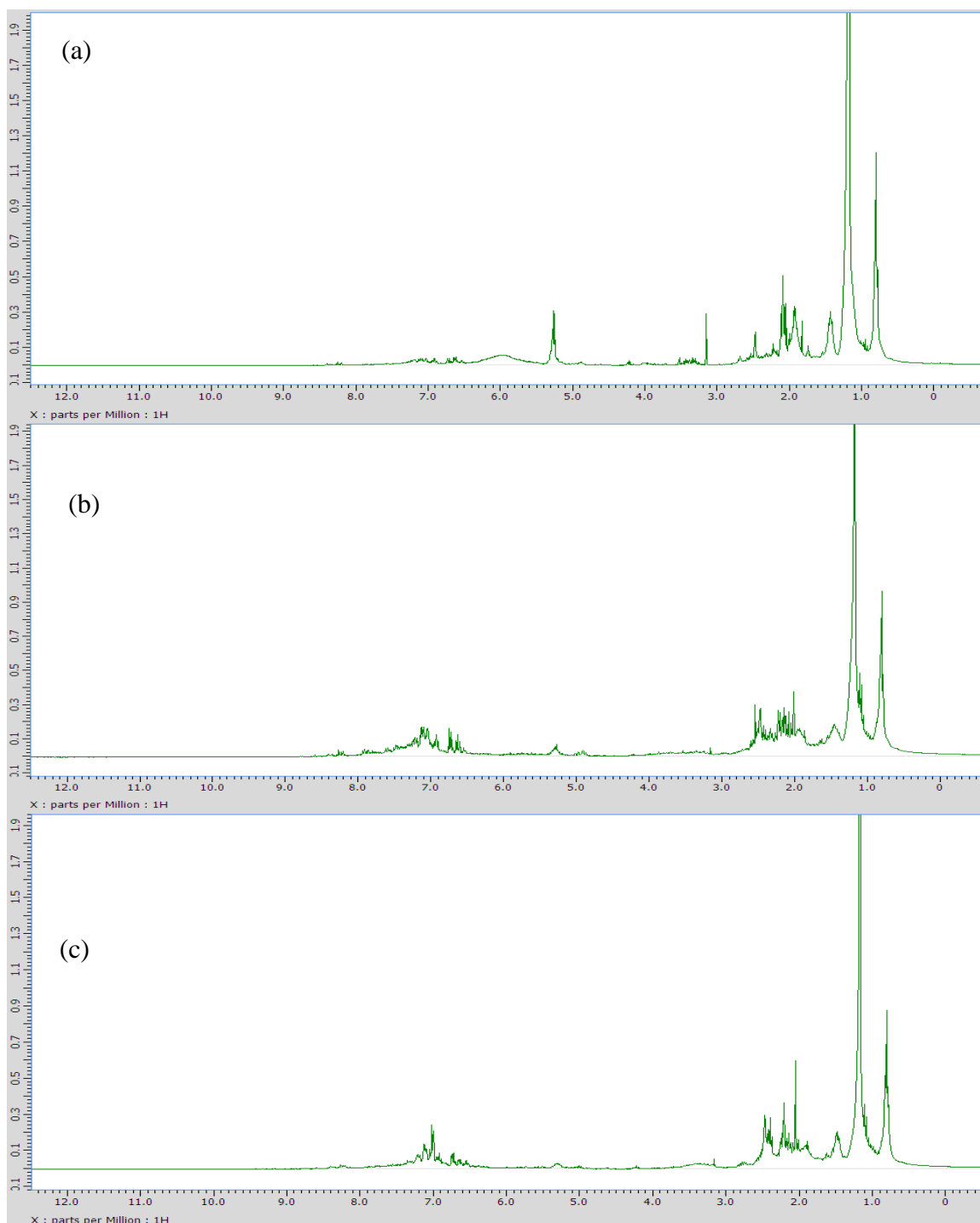


Figure 9. ^1H NMR spectra for the bio-oils from the (a) non-catalytic, (b) red mud catalyzed, and (c) HZSM-5 catalyzed pyrolysis of OMWS-wood biochar mixture at 450 $^{\circ}\text{C}$.

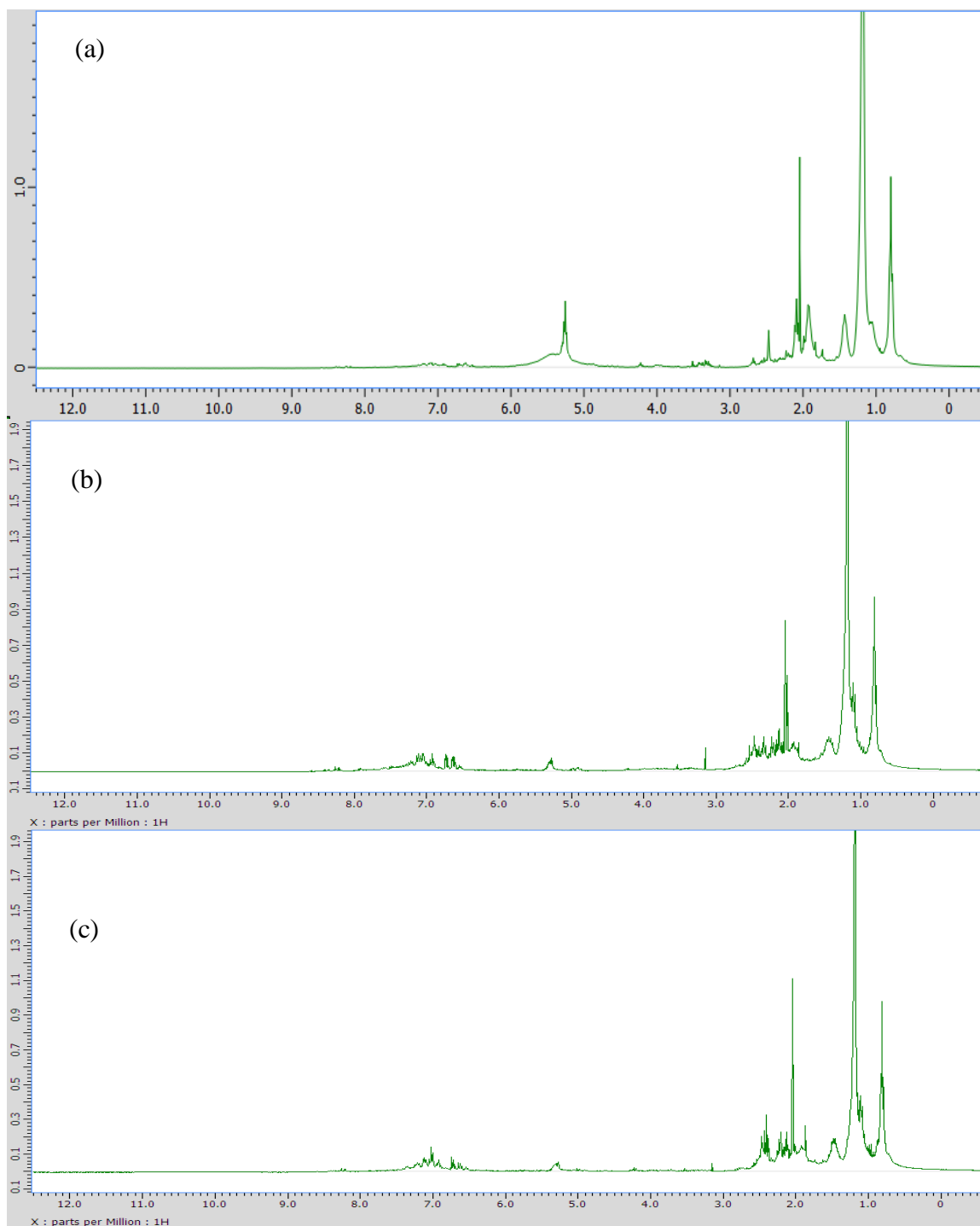


Figure 10. ^1H NMR spectra for the bio-oils from the (a) non-catalytic, (b) red mud catalyzed, and (c) HZSM-5 catalyzed pyrolysis of OMWS-wood biochar mixture at 400 $^{\circ}\text{C}$.

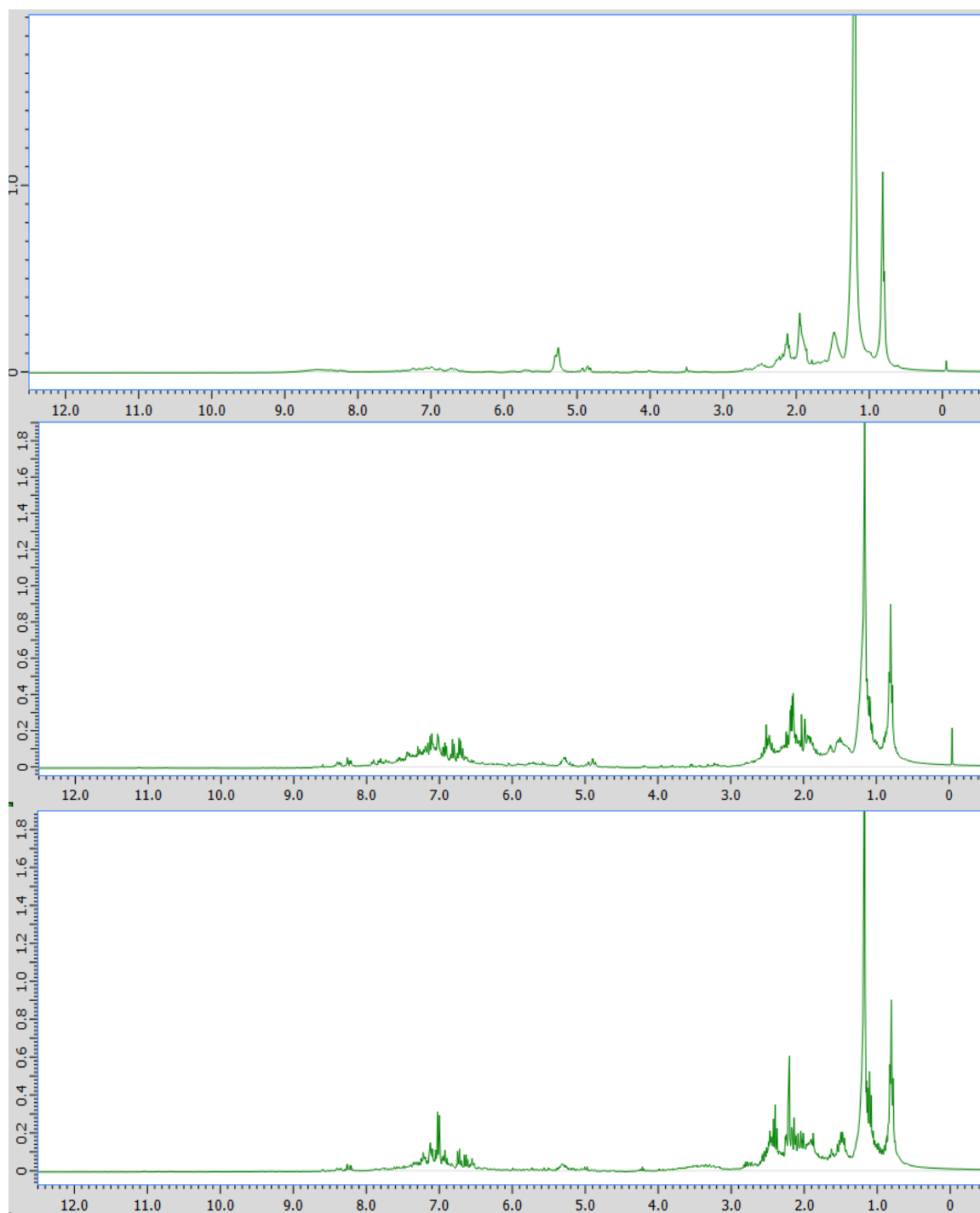


Figure 11. ^1H NMR spectra for the bio-oils from the (a) non-catalytic, (b) red mud catalyzed, and (c) HZSM-5 catalyzed pyrolysis of OMWS-wood biochar mixture at 500 $^{\circ}\text{C}$.

The ^{13}C NMR spectra of the non-catalytic and catalytic bio-oils obtained at 450°C are shown in Figure 12a-c. The intense peak at 40 ppm present in all spectra corresponded to the solvent DMSO-d_6 . ^{13}C NMR spectra can be divided into four regions i.e. carbon in saturated aliphatic chains (0-50ppm), aliphatic carbon substituted by oxygen and nitrogen and including the methoxyl groups of aromatic ethers (50 and 110 ppm), olefinic / or aromatic carbon (110 and 160 ppm), carboxylic carbon in ester, carboxylic acids or amide (160–180 ppm), carbonyl carbon in aldehydes and ketones (180-220 ppm).^{26,23} From the non-catalytic bio-oil spectrum (Figure 12a), it was clear that this bio-oil contained high content of aliphatic hydrocarbon. The aromatics signals (115-129 ppm and from 131-160 ppm) were weak. The intense peak at 130 ppm corresponds to vinyl carbons in olefins.²⁷ The weak peak at 174.8 ppm corresponded to amide carbonyl,²⁸ whereas the peak at 175 ppm was attributed to carbonyl carbon in ester and/or carboxylic acids, which was in agreement with the FTIR and ^1H NMR results. These observations indicated that the bio-oil produced from fast pyrolysis of OMWS was rich in aliphatic hydrocarbon chains and poorly aromatic.

The spectra of the catalytic bio-oils are shown in Figure 12b-c. For both spectra, most of the carbon resonance peaks were located in the aliphatic (0-55 ppm) and aromatic/olefinic (95-165 ppm) regions. The aliphatics region had more signals in the HZSM-5 bio-oil spectrum compared to the red mud one, whereas the spectrum of the latter contained more aromatics/olefins. The higher aliphatics content of HZSM-5 catalytic bio-oil was believed to be a consequence of fouling of the catalyst acid sites with time, which

resulted in less severe cracking of the pyrolysis organic vapors and consequently an increase in the dynamic viscosity of the catalytic bio-oil.

The loss of activity of HZSM-5 was due to the formation of coke in the pores and the surface of the catalyst with time. In fact, the cyclization of the small molecules in the pores of the HZSM-5 results in the formation of mono-aromatic compounds which accumulate to form coke precursors such as naphthalene and methylnaphthalene.²⁹ It is worth noting that peaks corresponding to oxygenated groups such as methoxyls (55-57 ppm), alcohols and sugars (55-95 ppm) were absent in both catalytic bio-oils spectra (Figure 12b, c). The low oxygenates content of both red mud and HZSM-5 catalytic bio-oils contributed to their high calorific values. Both catalytic bio-oils spectra contained a peak at 209 ppm that corresponds to ketones. In addition to that, the red mud catalytic bio-oil spectra contained a carbonyl carbon peak at 175 ppm. This peak was very weak in the HZSM-5 spectra. Considering the high pH of both catalytic bio-oils, the carbonyl peak (175 ppm) corresponded to an ester rather than a carboxylic acid.

The calorific value of the HZSM-5 catalyzed pyrolysis oil was lower than that of the red mud catalyzed pyrolysis oil. This could be explained by the fact that during catalytic pyrolysis of the OMWS, HZSM-5 promoted decarbonylation reaction (rejection of oxygen as CO), which means that for every oxygen atom rejected, one carbon atom is lost from the pyrolysis primary organic vapors. By contrast, red mud promoted decarboxylation reaction (rejection of oxygen as CO₂) over decarbonylation, which means that for every two oxygen atoms rejected, only one carbon atom is lost from the pyrolysis organic vapors. Therefore

the carbon concentration was expected to be higher for the red mud bio-oil compared to the HZSM-5 catalytic bio-oil.

The straight chain aliphatics in the pyrolysis primary vapors could enter the pores of the HZSM-5. Due to its acidic nature and intersecting three-dimensional channels system, HZSM-5 could convert these straight aliphatic chains into lighter products (olefins and paraffins).

Olefins with six carbon atoms or more could be converted to aromatic hydrocarbons through aromatization reaction,³⁰ whereas the olefins and paraffins with less than six carbon atoms are collected in the gas product. Due to its reduced surface area ($\sim 30 \text{ m}^2/\text{g}$) and pores volume as well as its reduced acidity (alkaline catalyst), red mud didn't promote significantly the formation of gaseous products ($\text{C}_2\text{-C}_5$), which can be seen in the gas product yields. Instead, it promoted the cracking of the long-chain hydrocarbons and the deoxygenation of the long-chain oxygenated hydrocarbons, which resulted in the formation of shorter chains of paraffins and olefins.

The $\text{C}_5\text{-C}_{10}$ olefins could have undergone further cyclization to form aromatic compounds via Diels-Alder reaction which generated hydrogen as a byproduct. Since red mud had a lower surface area and lower acidity than HZSM-5, it was believed that the red mud catalytic bio-oil contains more olefins than the HZSM-5 one, which was confirmed by the FTIR, ^1H NMR, and ^{13}C NMR spectra and can be a possible explanation of the higher calorific value of the former compared to the latter.

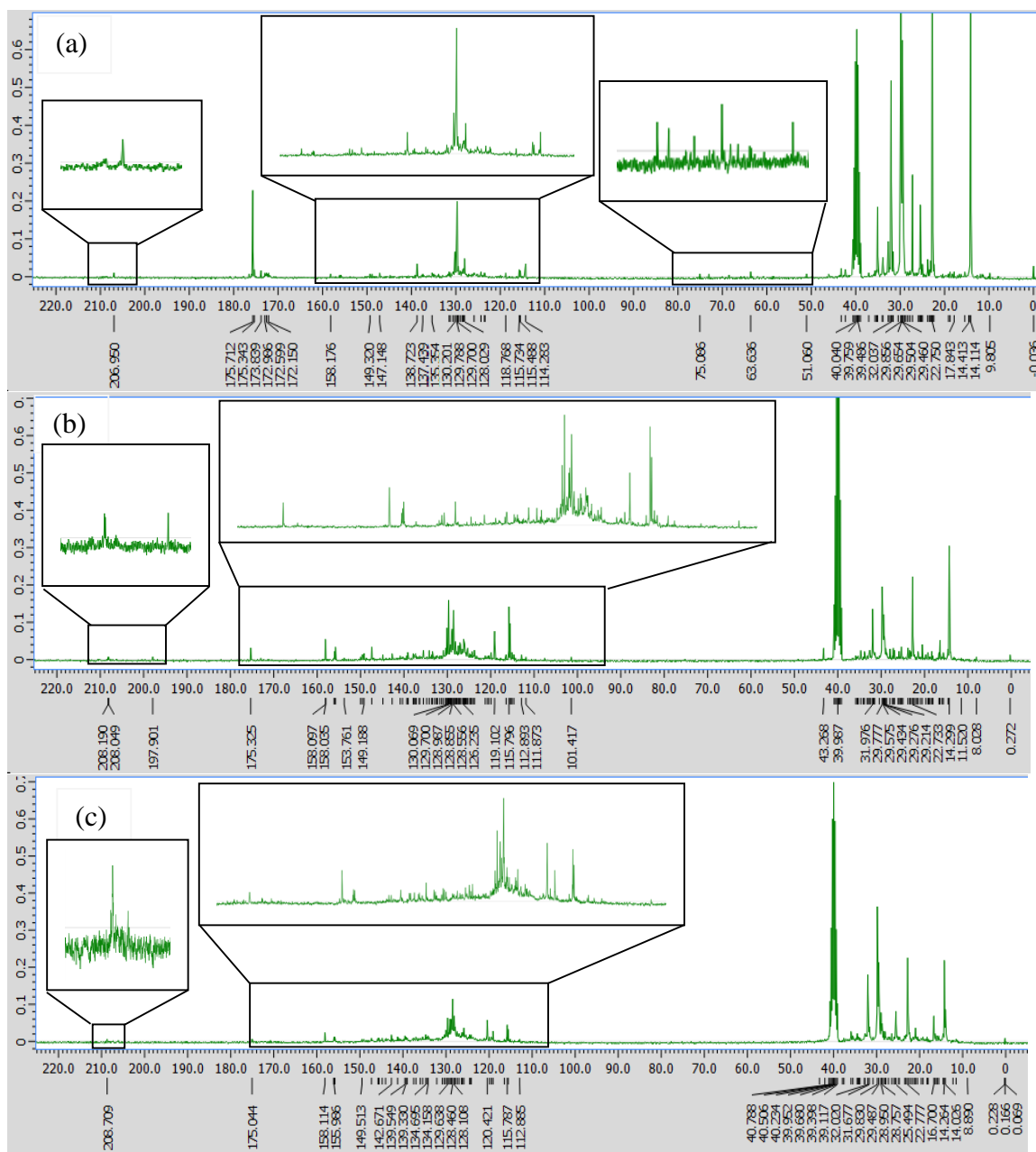
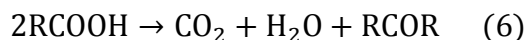


Figure 12. ^{13}C NMR spectra of the ESP oil from the catalytic pyrolysis at 450°C of the OMWS over (a) fresh red mud, (b) calcined red mud, and (c) regenerated red mud.

The ^{13}C NMR spectra of the conventional and catalytic oils obtained at 400 °C are shown in Figure 13. A decrease in the non-catalytic pyrolysis reaction temperature from 450° C to 400° C affected the bio-oil chemical composition, mainly in the aliphatic and carbonyl areas. The (-CH₂-) signal was higher and the carbonyl group signal was lower. These observations indicated that at lower reaction temperature, the cleavage of the long aliphatic chains is less efficient and the release of the fatty acids from the biomass particles is inhibited. For the catalytic pyrolysis oils, the carbonyl as well as the (-CH₂-) signals were stronger at lower reaction temperature (400 °C). Decreasing the reaction temperature led to less efficient cracking of the long chains of hydrocarbons (generated after thermal cracking of the lipids in OMWS) over both catalysts.

Farther, the formation of aromatics from olefins and from cyclization of paraffins is dependent on the reaction temperature. Therefore, decreasing the reaction temperature resulted in the production of less aromatic/olefinic bio-oils for both catalysts. It is worth noting the additional peak that appeared for both catalysts at 207 ppm. This peak corresponded to ketones that formed from the thermal decomposition of fatty acids (Equation 6).³¹ Apparently, both HZSM-5 and Red mud were not efficient in cracking those ketones at low temperature.



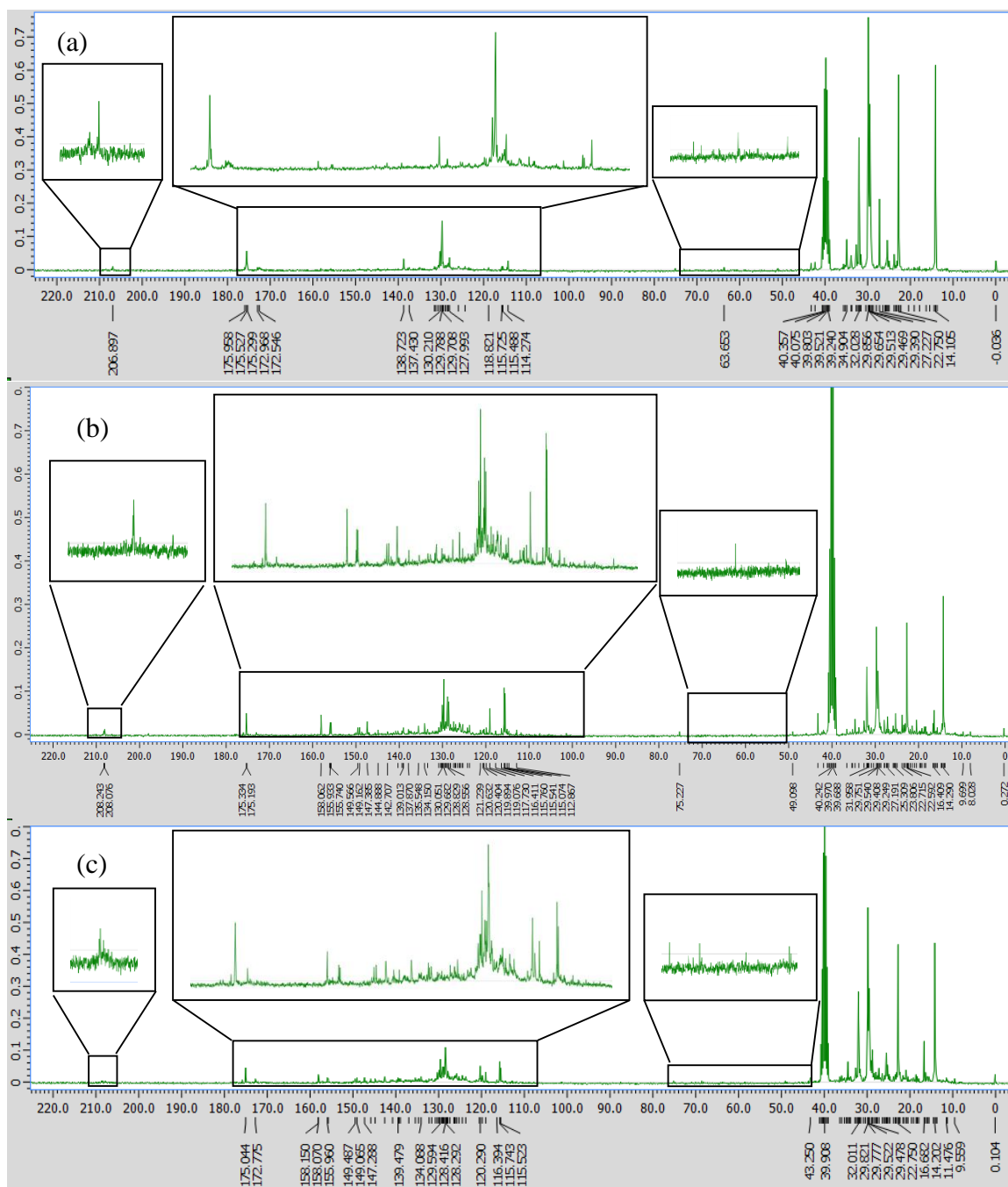


Figure 13. ^{13}C NMR spectra of the ESP oil from the catalytic pyrolysis at 400 °C of the OMWS over (a) fresh red mud, (b) calcined red mud, and (c) regenerated red mud.

The ^{13}C NMR spectra of the conventional/catalytic pyrolysis oils obtained at 500 °C are shown in Figure 14. An increase in the fast pyrolysis temperature from 450 to 500 °C resulted in the decrease of the carboxylic acid signal (~175 ppm) as well as the CH_3/CH_2 ratio. It appears that as the reaction temperature increased, less carboxylic acids survived the pyrolysis reaction.

3.3.4. Pyrolysis gas product composition

A Varian 490 micro GC (Agilent Technologies, Inc. Santa Clara, CA USA) was used in order to identify and quantify the non-condensable gases generated from the catalytic/non-catalytic pyrolysis of the OMWS. The gas product of the catalytic and non-catalytic pyrolysis at 450° C (Table 14) was a mixture of hydrogen, hydrocarbons and carbon oxides. For the fast pyrolysis experiment at 450 °C using silica sand, hydrogen (H_2) and carbon dioxide (CO_2) were the major gases and accounted for 76.2 mole % of the non-condensable gases produced during the reaction. The carbon monoxide (CO) accounted for 9.1 mole % and the $\text{C}_2\text{-C}_5$ hydrocarbons for 8.2 mole %. The methane (CH_4) concentration was 4.9 mole %. Other peaks were present in the chromatogram but were not identified and were referred to as “Other hydrocarbons” and they accounted for 1.3 mole % of the total gases. At lower reaction temperature (400 °C), the H_2 , CO , and CH_4 concentrations decreased, whereas the CO_2 concentration increased. As for the red mud catalyzed pyrolysis of the OMWS at 450 °C, the hydrogen yield accounted for 45.5 mole % of the total gases, CO_2 accounted for 38.2 mole %, and the CO accounted for 6 mole %. The gas product from the HZSM-5 experiment consisted of 55 mole % CO_2 , 17.4 mole % $\text{C}_2\text{-C}_4$ hydrocarbons, and 12.4 mole % CO .

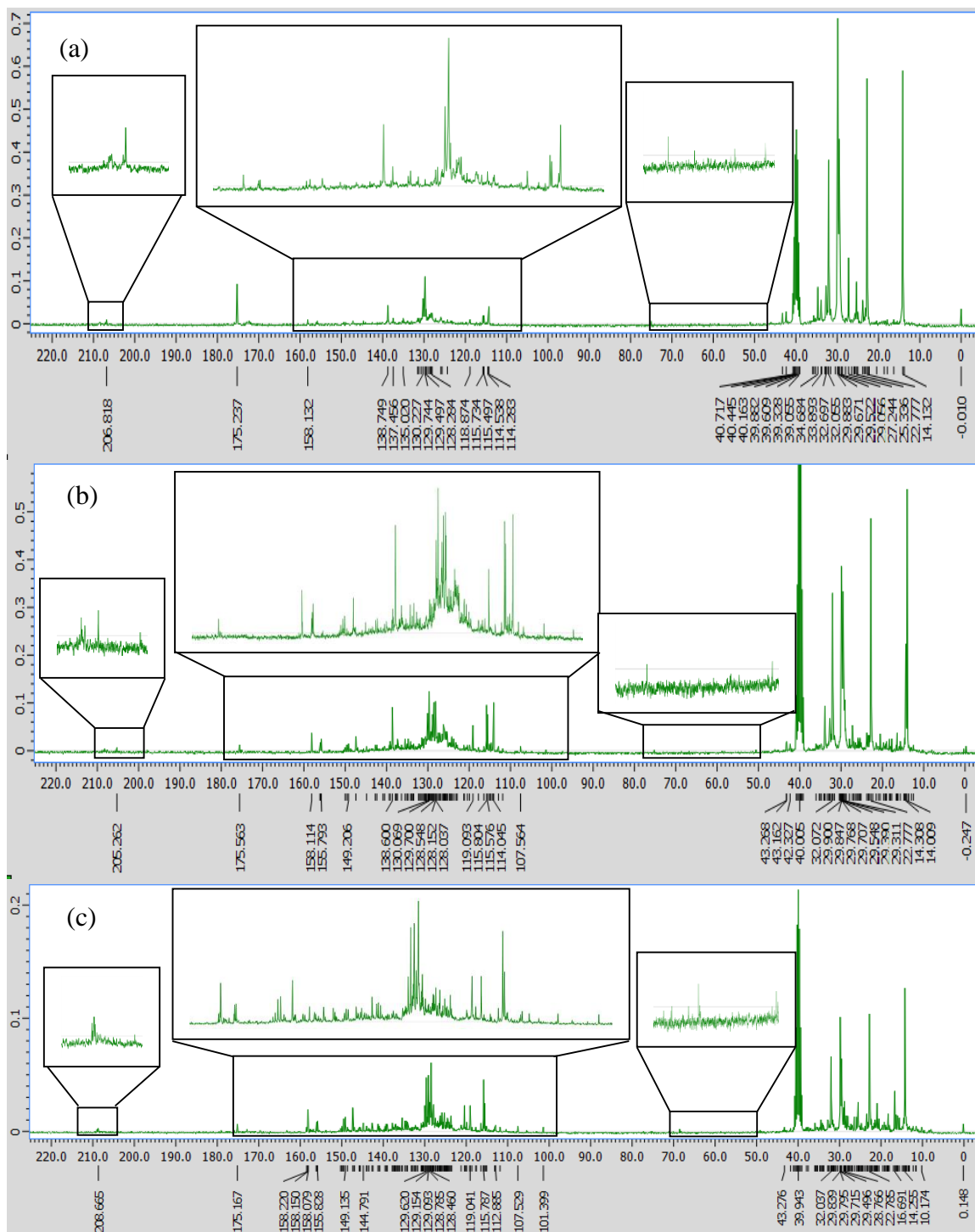


Figure 14. ^{13}C NMR spectra of the ESP oil from the catalytic pyrolysis at 500 °C of the OMWS over (a) fresh red mud, (b) calcined red mud, and (c) regenerated red mud.

Table 14. Gas product composition (mole % of total gases) from the conventional/catalytic pyrolysis of the OMWS over red mud and HZSM-5

	Yields (mole % of total gases)											
	Sand			Red mud			H-ZSM5					
	400 °C	450 °C	500 °C	400 °C	450 °C	500 °C	400 °C	450 °C	500 °C			
H ₂	8.7±0.69	15.2±3.82	18.8±2.35	31.7±0.74	45.5±0.16	44.8±0.4	3.2±0.69	6.0±0.39	11.4±1.61			
CO	6.6±0.27	9.1±1.79	7.3±0.72	6.3±0.29	6±0.12	8.8±1.1	9.5±0.06	12.4±0.13	15.2±1.35			
CO ₂	72.1±3.79	61±3.52	58.3±1.27	51.5±1.97	38.2±0.81	34.1±1.47	65.3±3.95	55.2±0.08	39.3±1.82			
CH ₄	3.8±1.15	4.9±0.37	5.5±0.66	3.0±0.54	4.4±1.2	5.4±0.06	2.2±0.18	4.6±0.19	4.7±0.05			
C ₂ -C ₅	8.2±1.94	8.23±1.63	9.2±1.20	5.8±0.42	5±0.04	6.7±0.005	16.5±3.87	17.4±0.52	25.2±2.40			
> C ₅	1.0±0.4	1.3±0.33	0.9±0.05	0.86±0.07	0.9±0.21	0.76±0.18	3.3±0.37	4.3±0.11	4.2±0.37			
CO/CO ₂	0.09	0.15	0.13	0.12	0.16	0.26	0.15	0.22	0.39			

In order to have a clearer idea of the overall yields of each gas component, the yields in weight percent relative to the OMWS mass pyrolyzed were calculated and are presented in Table 15. The gas phase was a mixture of hydrogen, hydrocarbons, and carbon oxides.

For the conventional pyrolysis experiment at 450 °C, carbon dioxide (CO₂) and C₂-C₅ hydrocarbons were the major gases. They respectively accounted for 74.5 % and 12.2 % of the total mass of gases.

The carbon monoxide accounted for 7.3 %, while hydrogen and methane accounted for 0.97 % and 2.42 %. Other peaks were present in the chromatogram but were not identified and were referred to as “Unknown” and they accounted for 2.68 % of the total mass of gases. At lower reaction temperature (400 °C), the H₂, CO, CO₂ and CH₄ concentrations decreased. When the reaction temperature increased (500 °C) the concentrations of these gases increased. The production of C₂-C₅ hydrocarbons during the fast pyrolysis at 450 °C could be due to the thermal decomposition of the lipids (41.1 wt.% of OMWS). It is well known that starting at 300° C, fatty acids and acrolein are produced from the gross pyrolysis of fats. A further increase of temperature (400-500 °C) would result in the formation of short chain hydrocarbons as a result of the cracking of these products.³²

When the red mud was used as catalyst at 450 °C, there was an increase in each gas compound yield. The hydrogen yield increased by 372.73 % and the C₂-C₅ yield increased by 5.78 %. The hydrogen producing reactions could be the dehydrogenation (Equation 4),³¹ and/or aromatic cyclization (Equation 5)³¹ of paraffins in the OMWS or the formation of aromatics from olefins by Diels-Alder reaction (Equation 6).³³ It is worth noting that, in

addition to hydrogen production, Equations 4-6 promotes the formation of gaseous and/or liquid hydrocarbons, which was in agreement with the increased C₂-C₅ yield.

The CO and CO₂ yields increased by 19.28 % and 16.06%, respectively, which indicated that the decarbonylation and decarboxylation reactions of the primary pyrolysis vapours was more effective over red mud than during thermal cracking.

The yields of all gases increased with the increasing reaction temperature from 400 °C to 500 °C, except for the CO₂ yield which had a maximum at 450 °C. Interestingly the pyrolytic water yield had a maximum at 450 °C as well. This observation indicated that the CO₂ yield and the pyrolytic water yield could be dependent on each other. It is well known that iron oxides are active catalysts for the water gas shift reaction (WGSR) at high temperature (350-450 °C). When oxides such as Al₂O₃ and TiO₂ are added to a matrix of Fe₂O₃, they promoted the WGSR.^{34,35} Therefore, the red mud could be promoting the WGSR. In order to prove this hypothesis, de-ionized water was fed into a bed of regenerated red mud that was fluidized using CO gas. Hydrogen and CO₂ were produced during the reaction. The reaction products distribution is shown in Table 16 and Table 17. After cooling down the reactor, the red mud collected was magnetic and had coke on it. The coke yield was 8.9 wt. %. The coke formation on the surface of the catalyst was probably due to the reaction of the CO with hydrogen to produce water and coke Equation 7. The water collected from the first condenser supports this hypothesis

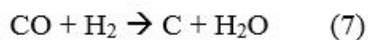
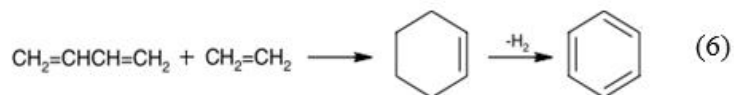
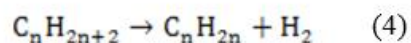
Table 15. Gas product composition (wt. %, dry basis) from the conventional/catalytic pyrolysis of the OMWS over red mud and HZSM-5

	Yields (wt,%, dry basis)											
	Sand				Red mud				H-ZSM5			
	400 °C	450 °C	500 °C	400 °C	450 °C	500 °C	400 °C	450 °C	500 °C	400 °C	450 °C	500 °C
H ₂	0.17±0.03	0.22±0.08	0.31±0.04	0.49±0.07	1.04±0.14	1.17±0.12	0.03±0.01	0.06±0.02	0.21±0.04			
CO	1.13±0.01	1.66±0.39	1.76±0.05	1.35±0.09	1.98±0.02	3.28±0.66	1.31±0.03	2.12±0.11	3.86±0.05			
CO ₂	14.94±1.1	16.94±0.75	18.67±2.13	17.94±2.1	19.66±0.06	19.58±0.9	14.22±0.6	13.92±0.1	15.59±1.7			
CH ₄	0.5±0.1	0.55±0.04	0.62±0.04	0.38±0.12	0.71±0.02	1.13±0.07	0.17±0.01	0.48±0.02	0.72±0.09			
C ₂ -C ₅	2.93±0.26	2.77±0.37	3.41±0.36	2.27±0.16	2.93±0.05	4.1±0.33	4.12±0.77	5.62±1.21	10.57±0.8			
Unknown	0.54±0.06	0.61±0.12	0.361±0.05	0.54±0.01	0.8±0.24	0.54±0.1	1.23±0.25	1.94±0.23	2.96±0.16			
CO/CO ₂	0.08±0.00	0.10±0.03	0.10±0.01	0.08±0.0	0.10±0.00	0.17±0.03	0.09±0.01	0.15±0.01	0.25±0.03			

Table 16. Products yield from the cracking of water over regenerated red mud under carbon monoxide atmosphere

	Weight (g)	Yield (wt. %)
coke	6	8.5
liquid	7	9.9
gas*	58	81.7
water fed	71	100

*: determined by difference.



The gas phase products distribution is shown in Table 17. It is worth noting the presence of methane and other gaseous hydrocarbons, which was an evidence supporting the Fisher-Tropsch reaction occurrence. The hydrogen and carbon dioxide production reached a steady state after 16 minutes, and the steady state was maintained for 2 hours.

Table 17. Gas product composition from the cracking of water over regenerated red mud under carbon monoxide atmosphere

	Value (vol. %)														
	0.5 min	16 min	31 min	46 min	63 min	76 min	91 min	106 min	122 min	136 min	151 min	166 min	181 min		
H ₂	0.160	10.88	9.840	12.92	11.52	10.59	8.020	9.500	8.580	10.410	7.650	3.070	4.220		
C ₂ H ₄	0.000	0.007	0.009	0.008	0.008	0.006	0.006	<0.001	0.007	0.006	0.004	0.001	0.001		
C ₂ H ₆	0.000	0.001	0.002	0.002	0.002	0.001	0.001	-	0.001	0.002	0.001	<0.001	<0.001		
CH ₄	0.000	0.048	0.046	0.049	0.037	0.034	0.021	0.013	0.016	0.022	0.018	0.285	0.010		
CO	88.22	62.51	70.21	69.30	68.95	72.24	76.20	76.74	76.88	75.25	79.31	88.59	86.34		
CO ₂	7.310	18.86	15.34	16.15	13.54	13.35	9.961	11.04	10.71	11.75	9.898	4.649	6.404		
C ₃ H ₆	0.000	0.001	0.002	0.002	0.002	0.003	0.002	0.001	0.002	0.002	0.002	<0.001	<0.001		

The FT-IR spectrum of the water collected from the first condenser is shown in Figure 15. The broad band observed at low wavenumber (662.2 cm^{-1}) corresponded to the collective normal mode called “librations” and involving many water molecules.

The signal at 1633.65 cm^{-1} corresponded to bending vibration of O-H. The weak and broad band at 2111.51 cm^{-1} was a combination of bending vibration and libration, whereas the broad band centered at 3318.66 cm^{-1} was due to the stretching vibration of O-H.³⁶

Interestingly, two weak bands were detected at around 2937.5 cm^{-1} and 3000 cm^{-1} . These bands corresponded to stretching vibrations of CH_2 and CH_3 groups and indicated the presence of hydrocarbons in the liquid product and confirming the occurrence of the Fisher-Tropsch reaction.

During the catalytic pyrolysis of the OMWS over the red mud, as the reaction temperature increased from 450 to $500\text{ }^\circ\text{C}$, the CO_2 yield decreased slightly, however, the hydrogen yield increased by 12.5% , this observation indicated that the water-gas-shift reaction was not the only responsible reaction for the high hydrogen yield. The use of HZSM-5 at $450\text{ }^\circ\text{C}$ resulted in a significant decrease (72.73%) in the hydrogen yield.

A possible reaction that could consume H_2 , would be the partial hydrocracking of coke molecules through dissociative adsorption of the H_2 on active sites of the catalyst (Bauer et al., 1996). Such phenomena would decrease the deactivation rate of the HZSM-5. Jong and co-workers (1998) confirmed the decrease of the coking rate on HZSM-5 in the presence of H_2 gas.

They also reported that there are two pathways of coke removal in the presence of H_2 i.e. hydrocracking removed the internal cokes, whereas the external coke was partially

cracked to less bulky polyaromatic compounds. With the use of HZSM-5, CO₂ yield decreased by 17.83 % compared to the fast pyrolysis. On the other hand, the CO yield increased by 27.71 % compared to the silica sand pyrolysis. It is worth noticing that the CO₂ production was more than 5 times higher than CO for the HZSM-5 catalyzed pyrolysis of the OMWS.

The dominance of CO₂ over CO in the gas product was observed by Benson during the catalytic pyrolysis of lipids over HZSM-5.²⁹ It was also reported that during the deoxygenation of lipids at high temperature, decarboxylation was the dominant reaction compared to decarbonylation.

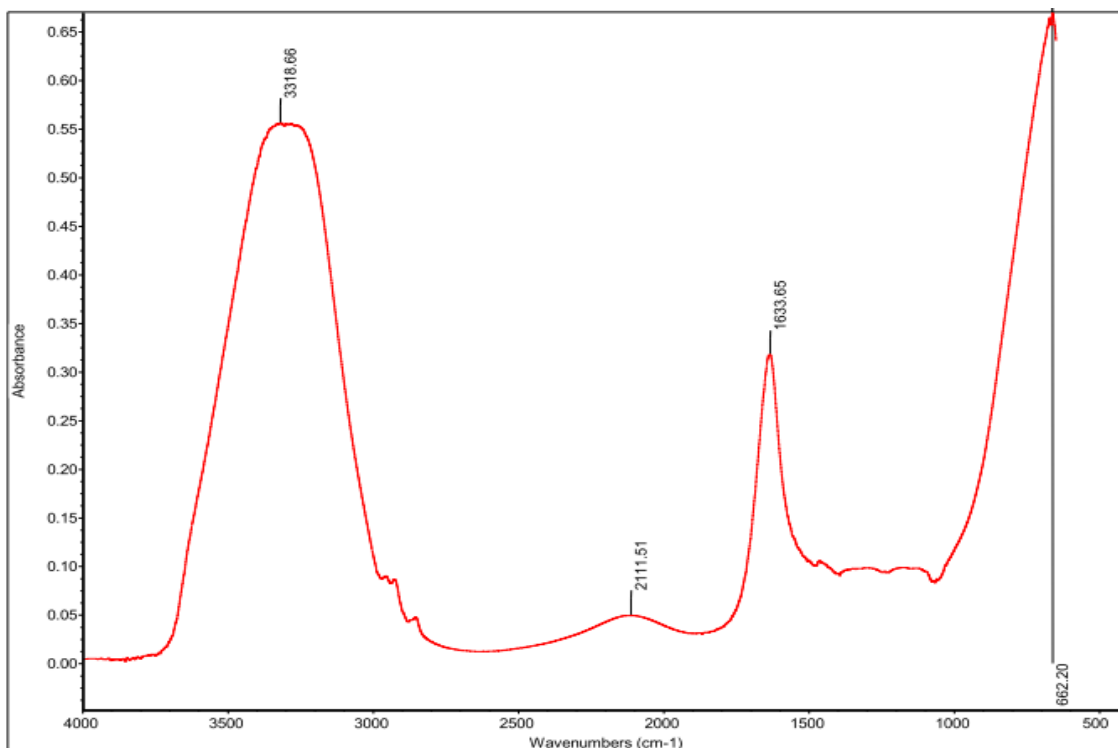


Figure 15. FTIR spectrum for the liquid in condenser one from the water-gas-shift reaction on regenerated red mud under CO atmosphere.

The CO/CO₂ ratio for the pyrolysis of the OMWS over sand, fresh red mud and HZSM-5 at 450 °C are presented in Figure 16. Since the CO₂ yield was higher than that of the CO for the non-catalytic and catalytic experiments, the CO/CO₂ ratio was less than 1 for all experiments. The CO/CO₂ ratio of the HZSM-5 catalyzed pyrolysis of the OMWS was around 0.26 during the first hour, then decreased as the time on stream increased. By the end of the experiment, the HZSM-5 lost some of its activity but still maintained a stable CO/CO₂ ratio of 0.2, which was higher than that of sand and red mud.

The slow deactivation rate of the HZSM-5 could be due to the partial hydrocracking and/or cracking of coke in the presence of hydrogen.³⁷ The red mud had a CO/CO₂ ratio around 0.17 in the first hour of the experiment, then the ratio decreased and stabilized around 0.15 for the rest of the experiment. It is worth noting that the CO/CO₂ ratio of the red mud and sand experiments were similar, however, the viscosity of the red mud bio-oil was much lower than that of the sand bio-oil. On the other hand, the CO/CO₂ ratio of the HZSM-5 experiment was always higher than that of the red mud, yet the bio-oil viscosity from the latter was lower than that from the former. In fact, the main deoxygenation route of the pyrolysis vapors over red mud at 450 °C was primarily through water formation, whereas the deoxygenation process over the HZSM-5 proceeded through dehydration and decarbonylation reactions.

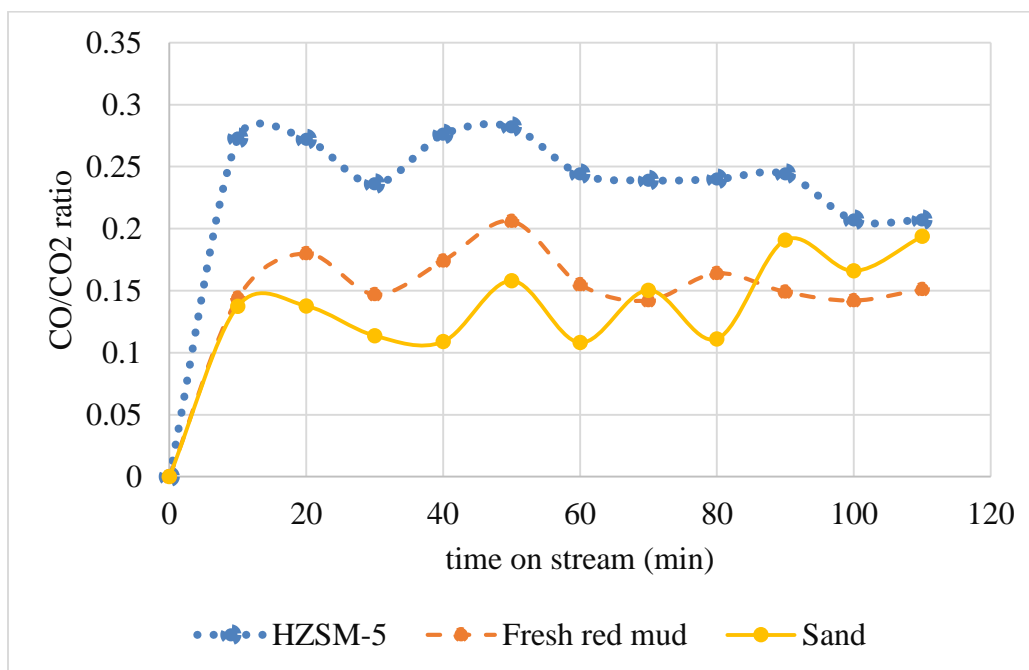


Figure 16. CO/CO₂ ratio for the conventional and catalytic pyrolysis of the OMWS at 450 °C

3.4. Conclusions

- The catalytic pyrolysis of the OMWS over red mud and HZSM-5 were demonstrated in a fluidized bed reactor. The best reaction temperature to maximize the liquid yield biooil was 450 °C. The organic phase collected from the ESP after catalytic pyrolysis of the OMWS had higher energy content and significantly lower viscosity compared to organic fraction obtained from the fast pyrolysis. The catalytic pyrolysis of the OMWS over red mud and HZSM-5 is a potential process for producing “Green diesel”.
- Based on the catalytic pyrolysis gas product and the ¹³C NMR data, it was concluded that the cracking chemistry of the red mud was different from that of the

HZSM-5. The red mud promoted dehydration and decarboxylation reaction over decarbonylation, whereas the HZSM-5 promoted dehydration and decarbonylation over decarboxylation.

- Red mud promoted the water gas shift reaction as well as the Fisher-Tropsch reaction. The former reaction was a major contributor to the significant hydrogen production during the catalytic pyrolysis of the OMWS over red mud, whereas the latter reaction occurred as a consequence of the hydrogen abundance and was catalyzed by the red mud.

3.5. References

- (1) Vitolo, S.; Petarca, L.; Bresci, B. *Bioresour. Technol.* **1999**, *67* (2), 129–137.
- (2) Onay, O.; Koçkar, O. M. *Fuel* **2006**, *85* (12-13), 1921–1928.
- (3) Czernik, S.; Bridgwater, A. V. *Energy & Fuels* **2004**, *18* (2), 590–598.
- (4) Ooi, Y. S.; Zakaria, R.; Mohamed, A. R.; Bhatia, S. *Catal. Commun.* **2004**, *5* (8), 441–445.
- (5) Twaiq, F. A. A.; Mohamad, A. R.; Bhatia, S. *Fuel Process. Technol.* **2004**, *85* (11), 1283–1300.
- (6) Bridgwater, A. V.; Meier, D.; Radlein, D. *Org. Geochem.* **1999**, *30* (12), 1479–1493.
- (7) Piskorz, J.; Majerski, P.; Radlein, D.; Scott, D. S.; Bridgwater, A. V. *J. Anal. Appl. Pyrolysis* **1998**, *46* (1), 15–29.
- (8) Wang, X.; Kersten, S. R. A.; Prins, W.; van Swaaij, W. P. M. *Ind. Eng. Chem. Res.* **2005**, *44* (23), 8786–8795.
- (9) Abdullah, N.; Gerhauser, H.; Sulaiman, F. *Fuel* **2010**, *89* (8), 2166–2169.
- (10) Azeez, A. M.; Meier, D.; Odermatt, J.; Willner, T. *Energy and Fuels* **2010**, *24* (3), 2078–2085.

- (11) Manurung, R.; Wever, D. A. Z.; Wildschut, J.; Venderbosch, R. H.; Hidayat, H.; van Dam, J. E. G.; Leijenhorst, E. J.; Broekhuis, A. A.; Heeres, H. J. *Food Bioprod. Process.* **2009**, *87* (3), 187–196.
- (12) Chiaramonti, D.; Oasmaa, A.; Solantausta, Y. *Renew. Sustain. Energy Rev.* **2007**, *11* (6), 1056–1086.
- (13) Fahmi, R.; Bridgwater, A. V.; Donnison, I.; Yates, N.; Jones, J. M. *Fuel* **2008**, *87* (7), 1230–1240.
- (14) Oasmaa, A.; Solantausta, Y.; Arpiainen, V.; Kuoppala, E.; Sipilä, K. *Energy and Fuels* **2010**, *24* (2), 1380–1388.
- (15) Butler, E.; Devlin, G.; Meier, D.; McDonnell, K. *Renew. Sustain. Energy Rev.* **2011**, *15* (8), 4171–4186.
- (16) Yathavan, B. K.; Agblevor, F. In *AIChE 2012 - 2012 AIChE Annual Meeting, Conference Proceedings*; 2012.
- (17) Zhang, H.; Xiao, R.; Huang, H.; Xiao, G. *Bioresour. Technol.* **2009**, *100* (3), 1428–1434.
- (18) Aho, A.; Kumar, N.; Eränen, K.; Salmi, T.; Hupa, M.; Murzin, D. Y. *Process Saf. Environ. Prot.* **2007**, *85* (5), 473–480.
- (19) Dickerson, T.; Soria, J. *Energies* **2013**, *6* (1), 514–538.
- (20) Mortensen, P. M.; Grunwaldt, J. D.; Jensen, P. A.; Knudsen, K. G.; Jensen, A. D. *Appl. Catal. A Gen.* **2011**, *407* (1-2), 1–19.
- (21) Campbell, I. M. *Biomass, Catalysis and Liquid Fuel*; Technomic Publishing Company (December 1983), 1983.
- (22) Mante, O. D.; Agblevor, F. A. *Waste Manag.* **2010**, *30* (12), 2537–2547.
- (23) Mante, O. D.; Agblevor, F. A.; Oyama, S. T.; McClung, R. *Bioresour. Technol.* **2012**, *111*, 482–490.
- (24) Lu, Q.; Zhang, Z. F.; Dong, C. Q.; Zhu, X. F. *Energies* **2010**, *3* (11), 1805–1820.
- (25) Silverstein, R. M.; Webster, F. X.; Kiemel, D. In *Organic Chemistry*; 2005; pp 1–550.

- (26) El Hajjouji, H.; Merlina, G.; Pinelli, E.; Winterton, P.; Revel, J. C.; Hafidi, M. *J. Hazard. Mater.* **2008**, *154* (1-3), 927–932.
- (27) Schaefer, J.; Stejskal, E. O. *J. Am. Oil Chem. Soc.* **1974**, *51* (5), 210–213.
- (28) Vane, C. H.; Drage, T. C.; Snape, C. E. *J. Agric. Food Chem.* **2003**, *51* (4), 947–956.
- (29) Benson, T. J. Elucidation of reaction pathways for catalytically cracked unsaturated lipids, Mississippi State University, 2008.
- (30) Adjaye, J. D.; Katikaneni, S. P. R.; Bakhshi, N. N. *Fuel Process. Technol.* **1996**, *48* (2), 115–143.
- (31) Chang, C. C.; Wan, S. W. *Ind. Eng. Chem.* **1947**, *39* (12), 1543–1548.
- (32) Crossley, A.; Heyes, T. D.; Hudson, B. J. F. *J. Am. Oil Chem. Soc.* **1962**, *39* (1), 9–14.
- (33) Schwab, A. W.; Dykstrab, G. J.; Selkeo, E.; Sorensonb, S. C.; Prydeo, E. H. *J. Am. Oil Chem. Soc.* **1988**, *65* (11), 1781–1786.
- (34) Bouarab, R.; Bennici, S.; Mirodatos, C.; Auroux, A. *J. Catal.* **2014**, *2014*, 1–6.
- (35) Popa, T.; Xu, G.-Q. G.; Barton, T. F.; Argyle, M. D. B. T.-H. temperature water gas shift catalysts with alumina. *Appl. Catal. A Gen.* **2010**, *379* (CAN 153:41058), 15–23.
- (36) Venyaminov, S. Y.; Prendergast, F. G. *Anal. Biochem.* **1997**, *248* (2), 234–245.
- (37) Jong, S. J.; Pradhan, A. R.; Wu, J. F.; Tsai, T. C.; Liu, S. B. *J. Catal.* **1998**, *174* (2), 210–218.

CHAPTER 4
CATALYTIC PYROLYSIS OF OLIVE MILL WASTEWATER SLUDGE
FRACTIONS

Abstract

The catalytic pyrolysis of the OMWS over red mud and HZSM-5 produced bio-oils with lower viscosity and lower oxygen content compared to the fast pyrolysis experiments. The ^{13}C NMR data revealed that the chemical composition of the bio-oil from the red mud experiments and from the HZSM-5 ones exhibited similarities as well as some differences. During the catalytic pyrolysis of the OMWS over the red mud, the CO/CO_2 ratio evolution was different from that obtained using HZSM-5, which indicated that the cracking chemistry of both catalysts were different. On the other hand the OMWS is a mixture of several compounds that contributes to the bio-oil composition. In this chapter, the contribution of the hexanes soluble fraction as well as the solid residue after extraction to the pyrolysis products distribution as well as the bio-oil quality was investigated. The red mud catalyzed pyrolysis of the HSF produced mainly organics (40.2 wt. %), whereas the HZSM-5 experiment produced mainly non-condensable gases (75.4 wt. %). The catalytic pyrolysis of the OMWS hexanes extraction solid residue (SR) over regenerated red mud and HZSM-5 produced mainly char/coke (40.6 wt. % and 41.7 wt. %, respectively).

The viscosity, pH, and HHV values for the oil obtained from the red mud catalyzed pyrolysis of the HSF were 3.2 cP, 5.4, and 44.8 MJ/kg, respectively. Whereas these values

were 5.9 cP, 4.7, and 41.2 MJ/kg, respectively, for the HZSM-5 catalyzed pyrolysis. The catalytic pyrolysis of the SR over regenerated red mud produced biooil with higher pH (7.8), higher dynamic viscosity (88.2 cP), and lower HHV (35.5 MJ/kg).

The HZSM-5 catalyzed pyrolysis of the SR produced bio-oil with pH, dynamic viscosity, and HHV of 7.1, 44.7 cP, and 36 MJ/kg, respectively. Both catalysts had higher activity during the HSF catalytic pyrolysis compared to the SR experiment.

4.1. Introduction

The production of bio-fuel from the olive mill waste has been addressed in the literature since 1989, when the pyrolysis of olive mill waste effluent and olive stones blend was conducted to valorize the olive stones and dispose of the olive mill wastewater. A dried solid-like mixture (6 % moisture) was pyrolysed in a vertical moving bed reactor. The pyrolysis vapors (oil and gas) were used to fulfill the energy demand of the drying process. The biochar collect was more valuable than the olive stones.¹ The fast/catalytic pyrolysis of oven dried olive mill waste effluent was also reported in the literature.^{2,3,4} However, the naturally dried olive mill wastewater sludge was not investigated. Due to the complexity of the OMWS, the investigation of the reaction mechanisms during its thermal decomposition (pyrolysis) and catalytic cracking (catalytic pyrolysis) is a difficult task. Therefore, it would be easier to study the pyrolysis of the OMWS fraction separately.

The HSF accounted for 41 wt. % of the OMWS and it consists mainly of simple and complex lipids. The thermal cracking of fatty acids would result in the production of

hydrocarbons, ketones, water and carbon dioxide.^{5,6} The ketones can undergo further thermal cracking to produce CO and hydrocarbons.

The catalytic cracking of fatty acids over zeolite and FCC catalyst has been reported in the literature. Benson conducted the catalytic cracking of oleic acid over HZSM-5 in a fixed bed reactor⁷. The liquid product was a mixture of olefins, paraffins, and aromatic compounds. Bielansky and co-workers⁸ used a conventional FCC zeolite catalyst to crack palmitic acid and oleic acid in a small scale fluid catalytic cracking pilot plant. They reported that (1) oleic acid produced the highest gasoline yield of 44 wt.% at 550 °C; (2) palmitic acid produced the highest gas yield of 43.9 wt.% at 550 °C; (3) the catalytic cracking of both fatty acids produced considerable amount of propene and ethane; (4) the oxygen in the fatty acids was converted mostly to water and carbon dioxide; (5) gasoline aromaticity increased with the reaction temperature; (6) The number of double bonds in the fatty acids, enhanced the formation of high boiling products.

As demonstrated in Chapter 3 of this thesis, the catalytic pyrolysis of the OMWS over red mud and HZSM-5 produced oils with low dynamic viscosities, close to neutral pH and high energy content. It was clear that both catalysts have different pathways through which the primary pyrolysis vapors were cracked. In an effort to and understand the cracking chemistry of the OMWS over HZSM-5 and red mud, the catalytic pyrolysis of the HSF and SR was conducted.

The goal of this chapter was to elucidate the contribution of each fraction to the pyrolysis products distribution, and to the composition of the bio-oil and pyrolysis gases.

4.2. Experimental

4.2.1. Materials

The hexanes soluble fraction (HSF) and the solid residue (SR) that were obtained from the extraction of the OMWS were used in these studies. Additionally, extra virgin olive oil (EVOO) was also investigated for comparison.

4.2.2. Catalytic pyrolysis of the OMWS fractions and extra virgin olive oil

The catalytic pyrolysis of the OMWS fractions as well as the extra virgin olive oil were conducted using a bench scale pyrolysis unit described in Chapter 3. In brief, the pyrolysis unit consists of a K-Tron volumetric feeder, a 500 mm long stainless steel bubbling fluidized bed reactor with an inner diameter of 50 mm. The reactor contains a 100 μm porous stainless steel gas distributor used to insure a uniform distribution of fluidizing gas. A three-zone electric furnace is used to heat the reactor. The HSF was a paste at room temperature and had a low melting point, therefore, it was fed into the reactor using a syringe pump. The glass syringe was kept warm by a heating tape, and this melted the HSF which was subsequently fed into the reactor. In the case of the SR, the sample was mixed with biochar to improve its flow properties and facilitate feeding it into the reactor. The separation of the pyrolysis vapors and the fine biochar particles is achieved by using a hot gas filter kept at 380-400 $^{\circ}\text{C}$ and placed downstream from the reactor. Two ethylglycol chilled (-8 C) stainless steel condensers were used to condense the pyrolysis vapors coming out of the hot gas filter.

The aerosols which escape the condensers are precipitated in the electrostatic precipitator, which consists of a PVC tube containing a metallic rod kept at 20-30 kilovolts.

The aerosols escaping the ESP were trapped in the coalescing filter and a glass wool packed filter flask. A small fraction of the gas stream was fed into the micro GC for analysis the miro-GC.

All experiments were conducted for two hours at 450 °C and using nitrogen gas at three times the minimum fluidization velocity. The HSF as well as the EVOO were fed at 38 g/h to the catalyst bed using a feeding tube. The solid residue (SR) after hexanes extraction was fed to the reactor at 62 g/h. The catalysts used were regenerated red mud (RRM) and HZSM-5.

4.2.3. Gas analysis

The non-condensable gases that were produced were analyzed using a Varian 490 micro GC equipped with 10 m Molsieve 5 Å column and a 10 m porous polymer column.

4.2.4. Bio-oil characterization

The pyrolysis liquids were analysed for moisture content using a volumetric Karl Fisher titration method. A Metrohm 701KF Titrino (Brinkmann Instruments, Inc., NY, USA) and a 703 titration stand using Hydranal[®] composite 5 reagent. Most of the organic fraction of the bio-oil was collected from the ESP, therefore this fraction was used for further characterization. The dynamic viscosity, kinetic viscosity and density of the pyrolysis oils were determined at 40 °C using a Stabinger SVM 3000 viscometer (Ashland, VA, USA). The pH of the bio-oils was measured using a Mettler Toledo SevenEasy pH meter and probe (Mettler-Toledo GmbH, Switzerland). The pH values were taken after 7-10 min of stabilization of the mechanically stirred oil. The energy content of the bio-oils was

determined using the IKA C2000 basic bomb calorimeter. The elemental composition of the bio-oils was determined using a Thermo Scientific Flash 2000 organic elemental analyzer. Two to three milligrams of sample were used for each bio-oil. The oxygen content of the bio-oils was determined by difference.

The ^{13}C NMR spectra of the ESP oils were obtained using a JOEL 300 MHz NMR spectrometer after 3000 scans. The pulse width was 14.75 μs and the acquisition time was 1.57 s with a 2 seconds relaxation delay. The ^{13}C NMR samples were prepared by dissolving the bio-oil in one of two NMR solvents i.e. dimethylsulfoxide- d_6 or chloroform- D .

Approximately 0.3-0.4 g of the SR pyrolysis oil and 0.3-0.4 g of deuterated dimethyl sulfoxide ($\text{DMSO-}\text{d}_6$) were loaded into a glass vial and mixed for 3 minutes using a Genie 2 vortex mixer (SCIENTIFIC INDUSTRIES, INC, Bohemia, NY, USA). The vial and its content were cooled down in a cold water bath, then 4-6 mg of tetramethylsilane (TMS) was added to the vial.

The TMS served as a reference for the NMR shifts and as a standard for the integration of the ^{13}C NMR spectra. 0.5-0.6 g of the NMR sample were loaded to a 5 mm in diameter NMR tube for analysis. The HSF bio-oils were dissolved in deuterated chloroform (CDCl_3). Approximately 0.2-0.3 g and 1.4-1.5 g of CDCl_3 were loaded into a glass vial. The mixture was shaken in a vortex shaker for about 3 minutes, then cooled in a cold water bath. About 0.5-0.6 g of the NMR sample were loaded to the NMR tube for analysis.

4.3. Results and discussion

4.3.1. Pyrolysis yields

The product yield distribution from the conventional and catalytic pyrolysis of the OMWS and its fractions at 450 °C is represented in Table 18. For the non-catalytic pyrolysis experiments, the organic liquid fraction from the HSF accounted for 49.9 wt. %, which was more than 3 times higher than that produced from the fast pyrolysis of the SR (15.7 wt. %). The char/coke yield from the HSF fast pyrolysis was 5.6 wt. % which was more than 6 times lower than the coke/char yield from the fast pyrolysis of the SR (38.5 wt. %). The high char/coke yield from the fast pyrolysis of the SR was attributed to its high ash content.⁹ The alkali metals (especially potassium) in biomass ash were reported to catalyse the formation of water and non-condensable gases during fast pyrolysis.^{9,10,11} The potassium content of OMW reported in the literature ranged from 0.17 to 3 g/L.^{12,13,14} Miranda and co-workers¹⁵ reported that K₂O accounted for 57.29 % of the total oxides in the ash of combusted concentrated olive mill wastewater.

As the water evaporates from the evaporation ponds, the concentration of the potassium in the OMWS increases. Since most of the ash in the OMWS remained in the SR (Table 5), the potassium in the latter would catalyse the water forming reactions.

The water content of the biooil produced from the thermal cracking of the HSF was 7 wt. %, whereas the water produced from the fast pyrolysis of the SR was 19.9 wt. %. The gas product from the fast pyrolysis of the HSF was 37.5 wt. %, compared to 25.9 wt. % for the SR. The catalytic experiments resulted in a significant change in the pyrolysis products

distribution. The regenerated red mud effect on the pyrolysis of the HSF was different from that of HZSM-5.

The pyrolysis of the HSF over the RRM resulted in a significant increase in the coke/char yield by 151.8 %, whereas the organics yield decreased by 19.4 % relative to the fast pyrolysis process. Interestingly, the gas yield did not increase significantly. The pyrolytic water yield increased by 30 %. The conversion of the organic phase to char/coke and water was favoured over its conversion into permanent gases. However, the increase of the coke/char yield and the decrease of the organics liquid yield was a proof that the cracking of the pyrolysis vapours occurred over the red mud. Furthermore, the significant increase of the pyrolytic water yield was a result of the deoxygenation of the pyrolysis vapours.

The red mud catalyzed pyrolysis of the EVOO gave 11.3 % lower coke/char yield, 10 % higher organics, and roughly the same gas yield compared to the HSF experiment conducted under the same conditions. The HSF contains polycyclic compounds such as the 2,3-dihydro-N-hydroxy-4-methoxy-3,3-dimethyl-Indole-2-one and the Gibberellic acid, which have stable cyclic structures that are more difficult to crack compared to triglycerides. Farther, these polycyclic compounds in the HSF have several hydroxyl and carbonyl groups, which are very reactive and can combine with each other to form more stable compounds i.e. coke/char. On the other hand, the ash in feedstock remains in the char/coke fraction during pyrolysis. The HSF has an ash content of 4.39 wt. % (dry basis), whereas the EVOO is ash free. The higher coke/char yield of the HSF catalyzed pyrolysis was at the expense of the organic and gas yields.

When HZSM-5 was used during the catalytic pyrolysis of the HSF, the main product of the reaction was non-condensable gases, which increased by 101.1 % relative to the fast pyrolysis process. The organics yield as well as the coke/char yield decreased by 78 % and 48.2 %, respectively. The water content of the biooil increased by 52.9 %. Apparently, the pyrolysis vapours underwent severe cracking once in contact with the HZSM-5 at 450 °C, which resulted in the formation of significant amount of gas. The coke yield from the HZSM-5 catalyzed pyrolysis of the HSF was significantly lower than that from the fast pyrolysis experiment, probably due to the occurrence of the partial in-situ hydrocracking of the coke on the HZSM-5.

The product yield distribution from the catalytic pyrolysis of the SR over the RRM and HZSM-5 exhibited some differences compared to its thermal cracking. When the regenerated red mud was used, the organics yield decreased by 60.2 %.

The coke/char yield increased by 5.5 %, whereas the water content of the bio-oil increased by 19.6 %. As for the HZSM-5 catalyzed pyrolysis of the SR, the organics yield decreased by 21.5 %. The coke/char increased by 8.1 %, and the water content of the biooil increased by 52.9 %.

It is worth noting that for each set of experiments (using sand, red mud, and HZSM-5) the yield for each product (biochar, bio-oil, and gas) from the conventional/catalytic pyrolysis of the OMWS fall between the values recorded for the conventional/catalytic pyrolysis of the HSF and the SR. The major product from the catalytic pyrolysis of the HSF depended on the catalyst used.

The use of the regenerated red mud resulted in the liquid product being the major product, whereas the use of the HZSM-5 produced mainly non-condensable gases. As for the catalytic pyrolysis of the SR, the major product was the char/coke, which could be explained by the high ash content of this feedstock.

4.3.2. Bio-oils characterization

The properties of the ESP oil from the conventional/catalytic pyrolysis of the OMWS fractions at 450 °C are presented in Table 19. The thermal cracking of the HSF produced an acidic oil (pH 4.7) with a dynamic viscosity of 7.8 cP, whereas the SR gave a slightly basic oil (pH 7.5) with a dynamic viscosity of 124.9 cP. The HHV of the oil from the fast pyrolysis of the HSF was 16.3 % higher than that of the SR.

The carbon and hydrogen contents of the HSF fast pyrolysis oil accounted for 95.13 % of the oil, whereas the oxygen and/or chlorine content was 4.87 wt. %. Interestingly, the nitrogen and sulphur contents were very low (below the detection limit of the instrument). As for the SR fast pyrolysis, the carbon and hydrogen accounted for 85.43 % of the oil.

The oxygen accounted for 8.74 wt. %. The nitrogen content was 5.74 wt. % and the sulphur accounted for 0.09 wt. %. The nitrogen in the biooil is a nuisance because it will lower the HHV of the fuel and produce NO_x during combustion.

The ESP oils from the catalytic pyrolysis of the HSF over HZSM-5 and regenerated red mud produced acidic oils with lower viscosities. The HZSM-5 catalyzed pyrolysis of the HSF produced an oil with similar pH to that produced from the non-catalyzed pyrolysis and 1.3 times less viscous than the fast pyrolysis oil. The regenerated red mud catalyzed

pyrolysis produced an oil that was less acidic (pH 5.4) and 2.4 times less viscous than the thermally cracked one.

The bio-oil from the red mud catalyzed pyrolysis of the HSF had higher pH, lower dynamic viscosity, and higher energy content compared to the bio-oil from the HZSM-5 experiment. Both catalytic pyrolysis oils had higher carbon content and lower oxygen content compared to the conventional pyrolysis oil.

The catalytic pyrolysis of the EVOO over RRM produced an oil with very similar properties compared to that from the RRM catalyzed pyrolysis of the HSF. However, the oxygen content of the latter was higher than that of the former, and that was due to the heavy oxygenated molecules in the HSF, which are more thermally stable compared to the triglycerides in the EVOO. Interestingly, the HZSM-5 catalyzed pyrolysis oil of the HSF had lower hydrogen content compared to the fast pyrolysis one.

The oils from the catalytic pyrolysis of the SR had similar pH, but lower viscosities compared to the fast pyrolysis oil. The HZSM-5 and regenerated red mud catalyzed pyrolysis produced oils that were, respectively, 64.2 % and 29.4 % less viscous than the fast pyrolysis oil. The HZSM-5 was more efficient than the regenerated red mud in cracking the SR pyrolysis vapours.

The elemental analysis of the SR catalytic oils revealed that the carbon content of the catalytic oils were similar to that of the fast pyrolysis one. The hydrogen content of the catalytic oils, however, were slightly lower than the latter. The oxygen and/or chlorine content of the oil from the HZSM-5 and the RRM catalyzed pyrolysis of the SR, were similar to that of the fast pyrolysis one.

Table 18. Product yield distribution from the conventional/catalytic pyrolysis of the OMWS fractions at 450 °C and using three times the minimum fluidization velocity

	Value (wt. %)											
	Sand				HZSM-5				Regenerated red mud			
	OMWS	HSF	SR	OMWS	HSF	SR	OMWS	HSF	SR	OMWS	HSF	EVOO
Char/coke	31.1	5.6	38.5	24.7	2.9	41.7	29.6	14.1	40.6	14.1	12.5	
Liquid	50.9	56.9	35.6	38.04	21.7	33.2	46.6	49.3	33.6	49.3	51.4	
Organics	37.8	49.9	15.7	18.2	11.0	12.4	26.7	40.2	10.4	40.2	44.2	
Water	13.1	7.0	19.9	19.9	10.7	20.8	19.9	9.1	23.2	9.1	7.2	
Gas*	18	37.5	25.9	37.25	75.4	25.1	23.8	36.6	25.8	36.6	36.1	

*: determined by difference

Table 19. Characteristics of the ESP bio-oils from the conventional/catalytic pyrolysis of the OMWS fractions at 450 °C and using three times the minimum fluidization velocity

	Sand			HZSM-5			RRM			EVOO
	OMWS	HSF	SR	OMWS	HSF	SR	OMWS	HSF	SR	
Moisture (wt. %)	0.577	0.053	0.631	0.33	0.066	0.612	0.198	0.085	2.45	-
pH	7.1	4.7	7.5	6.7	4.7	7.1	7.2	5.4	7.8	6.1
Dynamic viscosity (cP)	41.3	7.8	124.9	7.1	5.9	44.7	8.2	3.2	88.2	3.1
HHV (MJ/kg)	39.02	42.2±0.1	36.5±0.0	39.7±1.1	41.26	36.2±0.1	42.1	44.3±0.71	35.9	44.4±0.07
C H N S O and/or Cl*	78.1±0.5	82.8±0.0	76.3±0.2	81.8±0.3	86.2±0.0	76.7±0.1	81.1±0.4	85.5±0.6	76.69±0.01	86.1±0.02
	11.3±0.1	12.3±0.0	9.2±0.1	10.6±0.1	10.1±0.0	9.0±0.01	11.4±0.0	12±0.1	8.54±0.02	12.4±0.03
	1.9±0.0	bdl	5.7±0.1	3.55±0.1	bdl	5.7±0.03	2.1±0.2	bdl	5.89±0.06	bdl
	bdl	bdl	0.09±0.0	Bdl	bdl	0.07±0.0	bdl	bdl	0.08±0.01	bdl
	8.7±0.6	4.9±0.1	8.7±0.2	3.94±0.4	3.6±0.0	8.5±0.1	5.4±0.3	2.4±0.7	8.8±0.11	1.6±0.05

*: determined by difference, bdl: below detection limit of the instrument.

The ^1H NMR of the HSF are presented in Figure 17. The spectrum of the conventional pyrolysis oil exhibited dominance of aliphatic compounds (0.5-3 ppm) and olefins (4.5-6.5 ppm). The aromatic region (6.5-8.5 ppm) had few weak signals. The sharp singlet at 3.65 ppm was attributed to methoxy group, whereas the triplet centred at 9.75 ppm was characteristic of aldehydes.

The spectrum of the oil from red mud catalyzed pyrolysis of the HSF, had slightly less populated olefins region and significantly more populated aromatics region (6.5-8.5 ppm) compared to the non-catalytic oil. The quadruplet centred at 3.74 ppm could be due to the CH_2 protons adjacent to hydroxyl group. The intensity of aldehyde signal around 9.75 ppm has increased. The spectrum of the HZSM-5 bio-oil had more aromatics signals than the fast pyrolysis and the RRM oils. The olefins signals was significantly attenuated and the aldehyde signal was very close to the noise level of the spectrum, probably because they didn't survive the pyrolysis conditions.

The ^1H NMR spectra of the SR are presented in Figure 18. The thermal cracking of the SR resulted in an oil with a very complex composition. In addition to the aliphatics and aromatics, heteroatoms were abundant. The O-H signal of carboxylic acid signal (10.5-13 ppm) was present in the non-catalytic oil. The catalytic pyrolysis didn't bring significant change to the chemical composition of the bio-oil. The catalytic and conventional pyrolysis oils had weak signals between 10.5 and 11.3 ppm. These signals were attributed to carboxylic acids that have survived the pyrolysis conditions. Interestingly, there was no aldehyde signal in the RRM bio-oil, probably because if there were any aldehydes formed through hydroformylation of alkene, they would have been hydrogenated to alcohols.

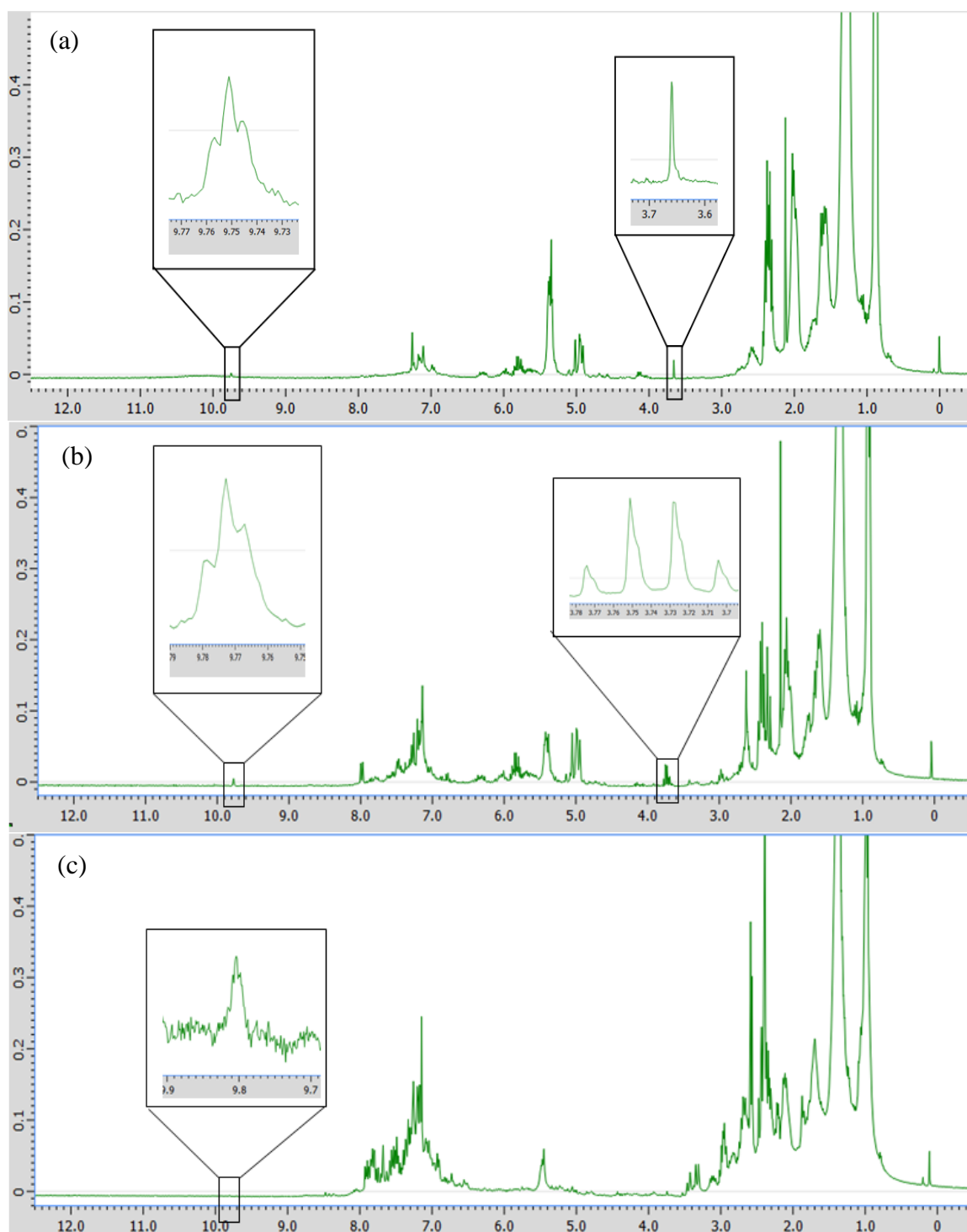


Figure 17. ^1H NMR spectra of the HSF ESP oil from the (a) fast pyrolysis, (b) catalytic pyrolysis over regenerated red mud, (c) and catalytic pyrolysis over HZSM-5

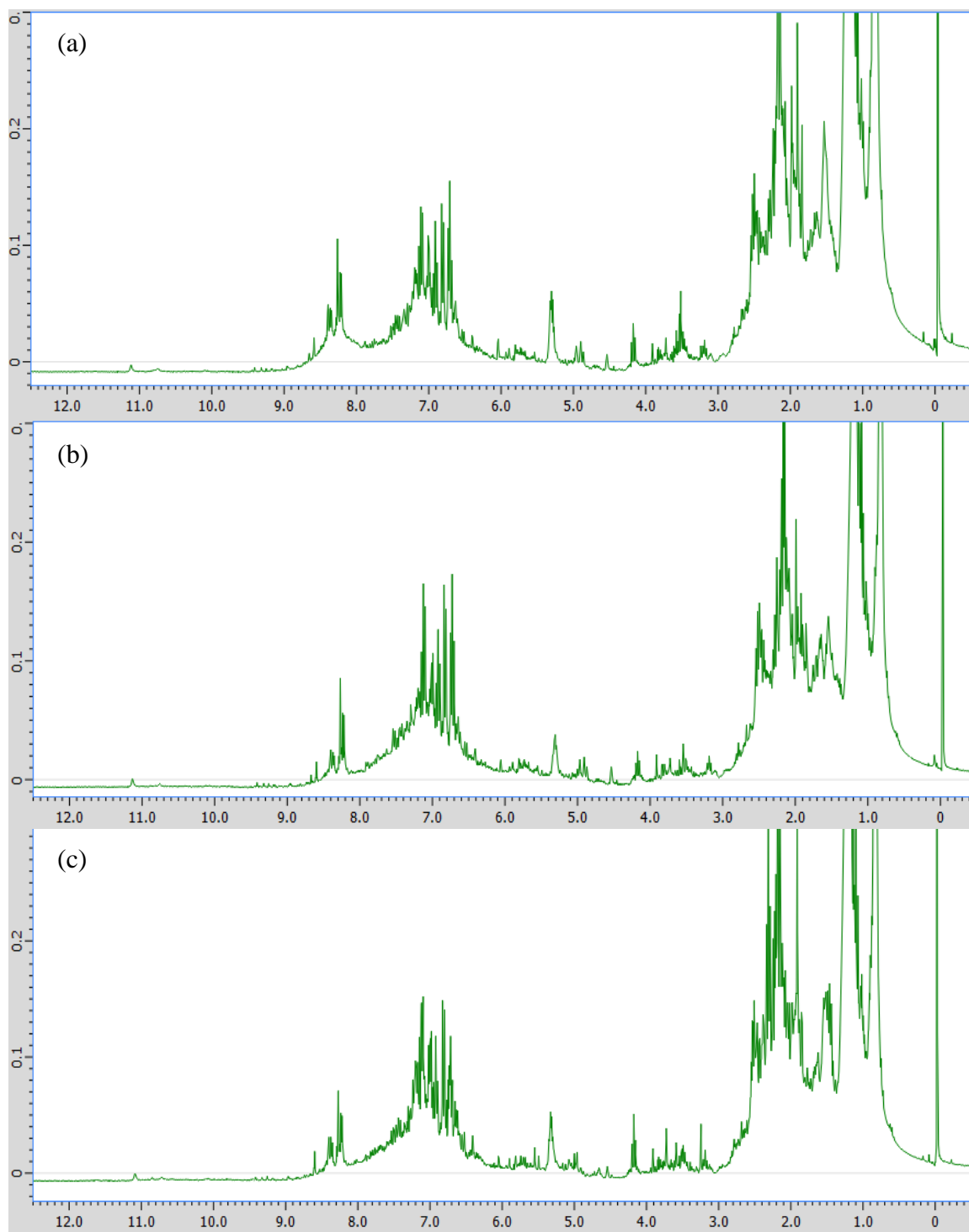


Figure 18. ^1H NMR spectra of the SR ESP oil from the (a) fast pyrolysis, (b) catalytic pyrolysis over regenerated red mud, (c) and catalytic pyrolysis over HZSM-5

The ^{13}C NMR spectra of the conventional and catalytic pyrolysis oils from the HSF are presented in Figure 19 a-c. The fast pyrolysis of the HSF produced an oil which was mainly aliphatic and aromatic. The integration of the ^{13}C NMR spectra is shown in Table 20. The signals of the aliphatic chains and aromatic compounds in the fast pyrolysis oil accounted for 88.22 % and 10.19 %, respectively. The aromatics could include chlorinated compounds such as chloromethane, dichloromethane. The signal at 179.7 ppm was attributed to carbonyl carbon in fatty acids that have survived the pyrolysis reaction.

The two peaks at 209.4 ppm and 211.7 ppm represented the carbonyl group in ketones and/or aldehydes. The catalytic pyrolysis of the HSF brought significant changes to the chemical composition of the bio-oil. When red mud was used, the aliphatics abundance decreased only by 5 %, whereas the olefins and aromatics signal increased by 52.3 %. The weak signal at 58.5 ppm could be attribute to CH_2 attached to hydroxyl group of an alcohol.

The signal of the carbonyl group in ketones decreased by 35.3 %, whereas the carbonyl group in carboxylic acids and/or esters was absent. These observations indicated that the use of regenerated red mud resulted in partial deoxygenation of the pyrolysis vapours. Farther, the decrease of the aliphatics signal and the increase of the olefins/aromatics signals could be explained by the dehydrogenation and aromatic cyclization of paraffins or the formation of aromatics from olefins by Diels-Alder reaction.

All of these reactions produce hydrogen as a by-product. The chemical composition of the bio-oil from the HZSM-5 catalyzed pyrolysis of the HSF was significantly different from that of the fast pyrolysis oil.

The aliphatic signals were significantly attenuated (41.3 %), whereas the intensity of the aromatic and alkene signals increased by 372.8 %. Interestingly, there was no carbonyl signals (160-180 ppm and 190-215 ppm) and no heteroatoms signal (50-110 ppm) in the spectrum of the bio-oil from the HSZM-5 catalyzed pyrolysis.

Table 20. Integration of the ^{13}C NMR spectra of bio-oils from the conventional/catalytic pyrolysis of the HSF

	fine sand	RRM	HZSM-5
Saturated aliphatics (0-50 ppm)	88.22	83.81	51.82
Aliphatic chains with heteroatoms (O and/or N) and methoxy group (50-110 ppm)	0	0.11	0
Olefins and aromatics (110-160 ppm)	10.19	15.52	48.18
esters, carboxylic acids (160-180)	0.75	0	0
Aldehydes and ketones (190-215 ppm)	0.85	0.55	0

The ^{13}C NMR spectra of the conventional and catalytic pyrolysis oils from the SR are presented in Figure 20. The DMSO- d_6 used to dissolve the SR bio-oil samples did not contain tetramethylsilane (TMS), therefore, the latter was added manually to the bio-oil sample dissolved in the DMSO- d_6 . The semi-quantification of the peaks is shown in Table 21 and was done relative to the TMS signal (~ 0 ppm). The ESP oil from the conventional pyrolysis of the SR exhibited dominance of aliphatic carbons (65.26 %), as well as olefinic and aromatic carbons (31.20 %). Heteroatoms (oxygen and or nitrogen) were also present in the oil (50-110 ppm) and accounted for 1.49 %. The carbonyl group signals attributed to ester and/or carboxylic acids (160-180 ppm) accounted for 1.97 %, whereas the signals corresponding to the ketones carbonyl group (205-220 ppm) accounted for 0.08 %.

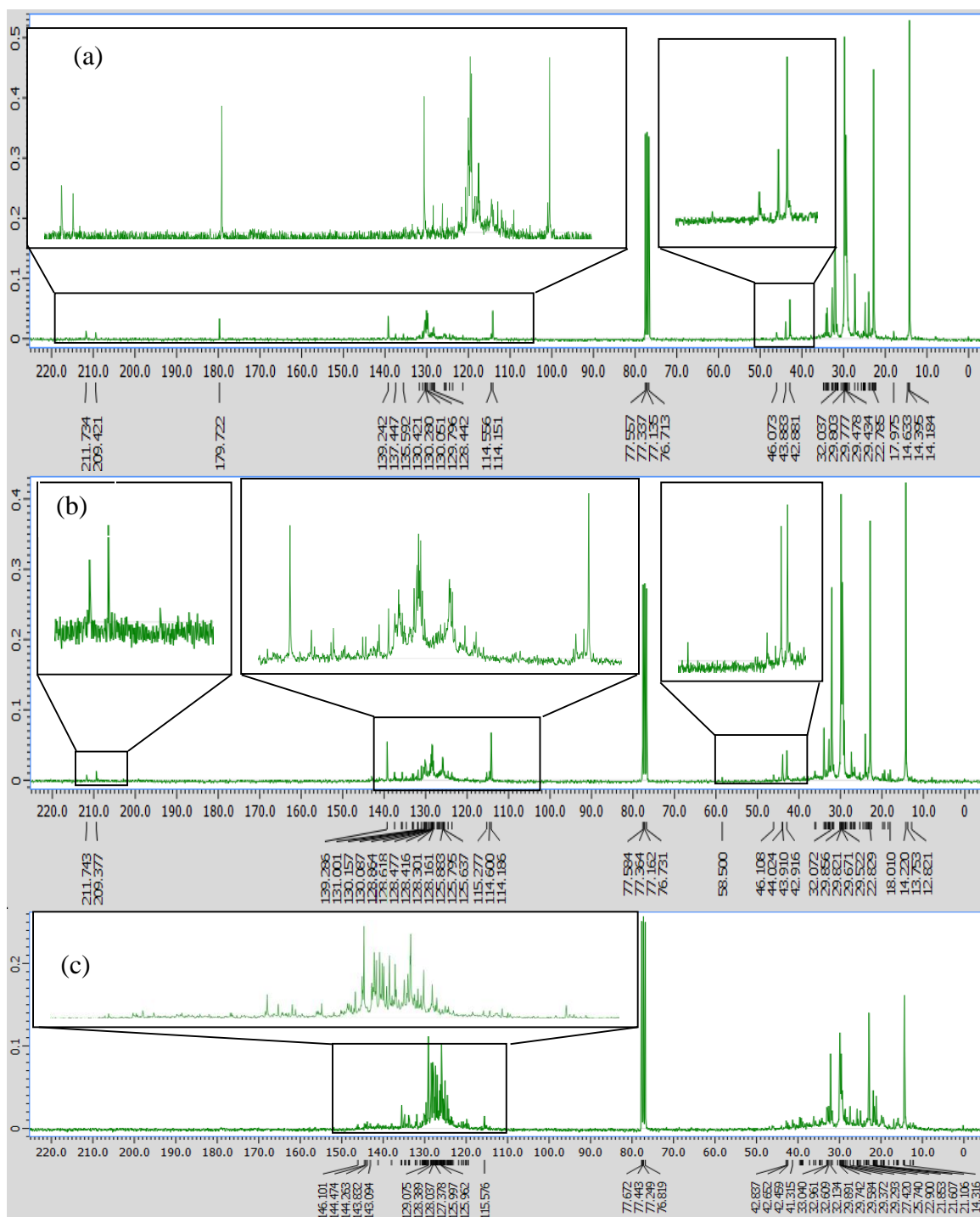
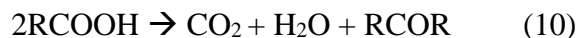


Figure 19. ^{13}C NMR spectra of the HSF ESP oil from the (a) fast pyrolysis, (b) catalytic pyrolysis over regenerated red mud, (c) and catalytic pyrolysis over HZSM-5

The catalytic pyrolysis of the SR influenced the chemical composition of the product bio-oil significantly. The RRM catalytic oil contained 24 % less aliphatics and 52.1 % more olefins and/or aromatics than the fast pyrolysis ESP oil. The signal corresponding to aliphatic chains substituted with a heteroatom (50-110 ppm) increased. The carbonyl signal corresponding to esters and carboxylic groups decreased by 39.6 %.

The ketones signal increased by 112.5 % compared to the non-catalytic oil, and that can be due to the fact that iron oxides as well as titanium oxide (TiO₂) are known to be active catalyst for ketonization.¹⁶

The HZSM-5 catalytic ESP oil had 10 % less aliphatic carbons and 26 % more aromatics compared to the fast pyrolysis oil. The signal of the aliphatic chains substituted with a heteroatom as well as the signal from the carbonyl group in esters and carboxylic acids, were significantly reduced (49.7 % and 56.3 %, respectively). The ketones signal increased by 312.5 %. The decrease in the carboxylic acid signal, the increase in ketones signals and pyrolytic water yield in the catalytic bio-oils were evidences of the ketonization reaction Equation 10. It is worth noting that the carboxylic acids/esters signal in the ESP oil from the RRM catalyzed pyrolysis of the SR was higher than that of the HZSM-5 experiment.



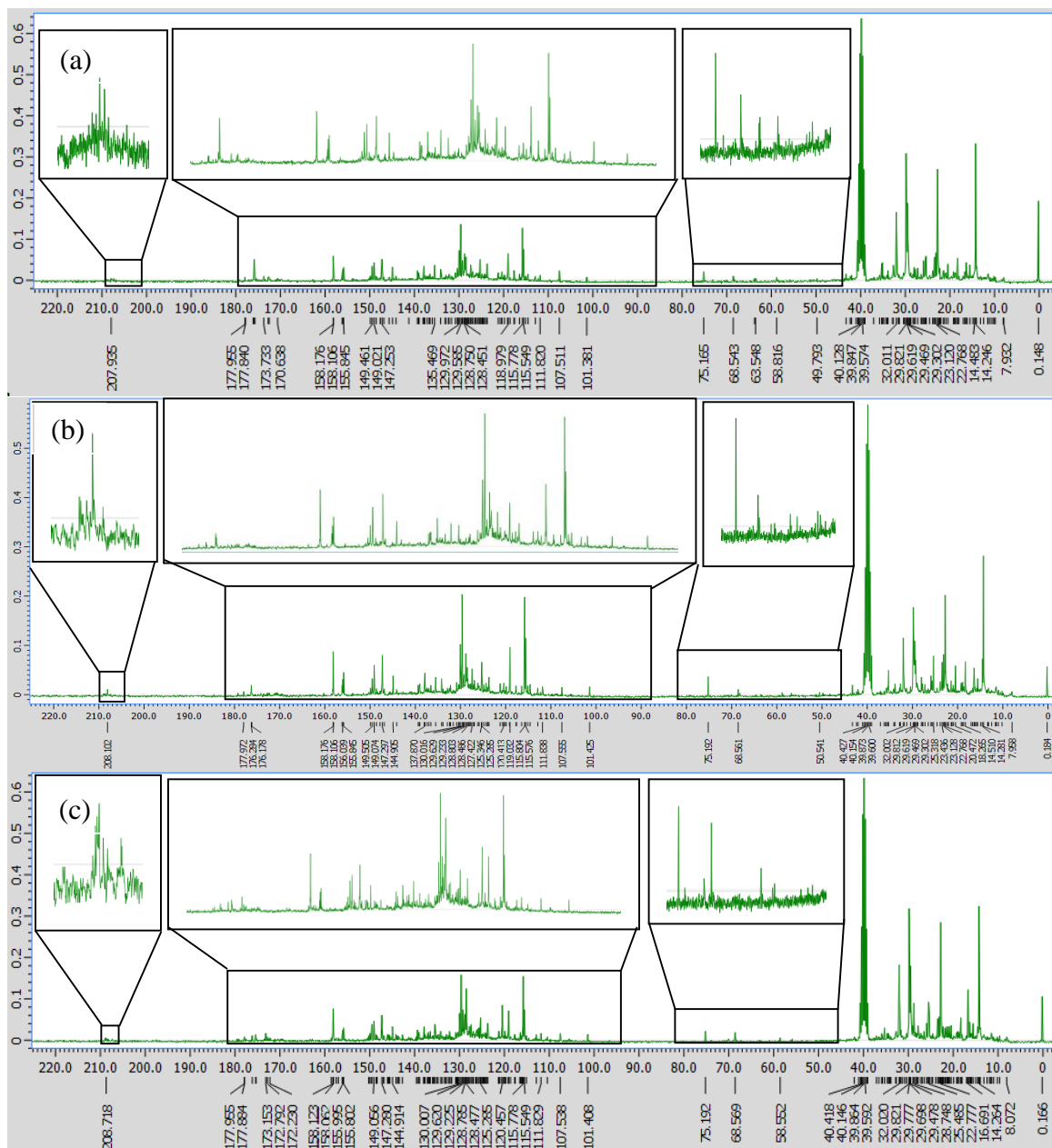


Figure 20. ^{13}C NMR spectra of the SR ESP oil from the (a) fast pyrolysis, (b) catalytic pyrolysis over regenerated red mud, (c) and catalytic pyrolysis over HZSM-5.

Table 21. Integration of the ^{13}C NMR spectra of bio-oils from the conventional/catalytic pyrolysis of the solid residue

	fine sand	RRM	HZSM-5
Saturated aliphatics (0-50 ppm)	65.26	49.62	58.74
Aliphatic chains with heteroatoms (O and/or N) and methoxy group (50-110 ppm)	1.49	1.55	0.75
Olefins and aromatics (110-160 ppm)	31.20	47.47	39.31
esters, carboxylic acids (160-180)	1.97	1.19	0.86
Aldehydes and ketones (190-215 ppm)	0.08	0.17	0.33

The ^{13}C NMR spectrum of the EVOO red mud catalyzed pyrolysis oil is shown in Figure 21-b. The spectra of the cracked HSF and EVOO indicated that both samples contained similar functional groups but with different abundance. The bio-oils from the catalytic pyrolysis of the HSF and the EVOO exhibited similar signal abundance in the aliphatic region, whereas aromatics and ketones signals were slightly higher for the cracked EVOO (Table 22). The weak signal at 58.5 ppm in the HSF bio-oil spectrum was absent in the cracked EVOO spectrum. This observation indicated that such peak did not correspond to a derivative of triglycerides or fatty acids.

Table 22. Integration of the ^{13}C NMR spectrum of the ESP oils from the regenerated red mud catalyzed pyrolysis of the HSF and the EVOO at 450 °C

	HSF	EVOO
Saturated aliphatics (0-50 ppm)	83.81	82.52
Aliphatic chains with heteroatoms (O and/or N) and methoxy group (50-110 ppm)	0.11	0
Olefins and aromatics (110-160 ppm)	15.52	16.79
esters, carboxylic acids (160-180)	0	0
Aldehydes/ketones (190-215 ppm)	0.55	0.69

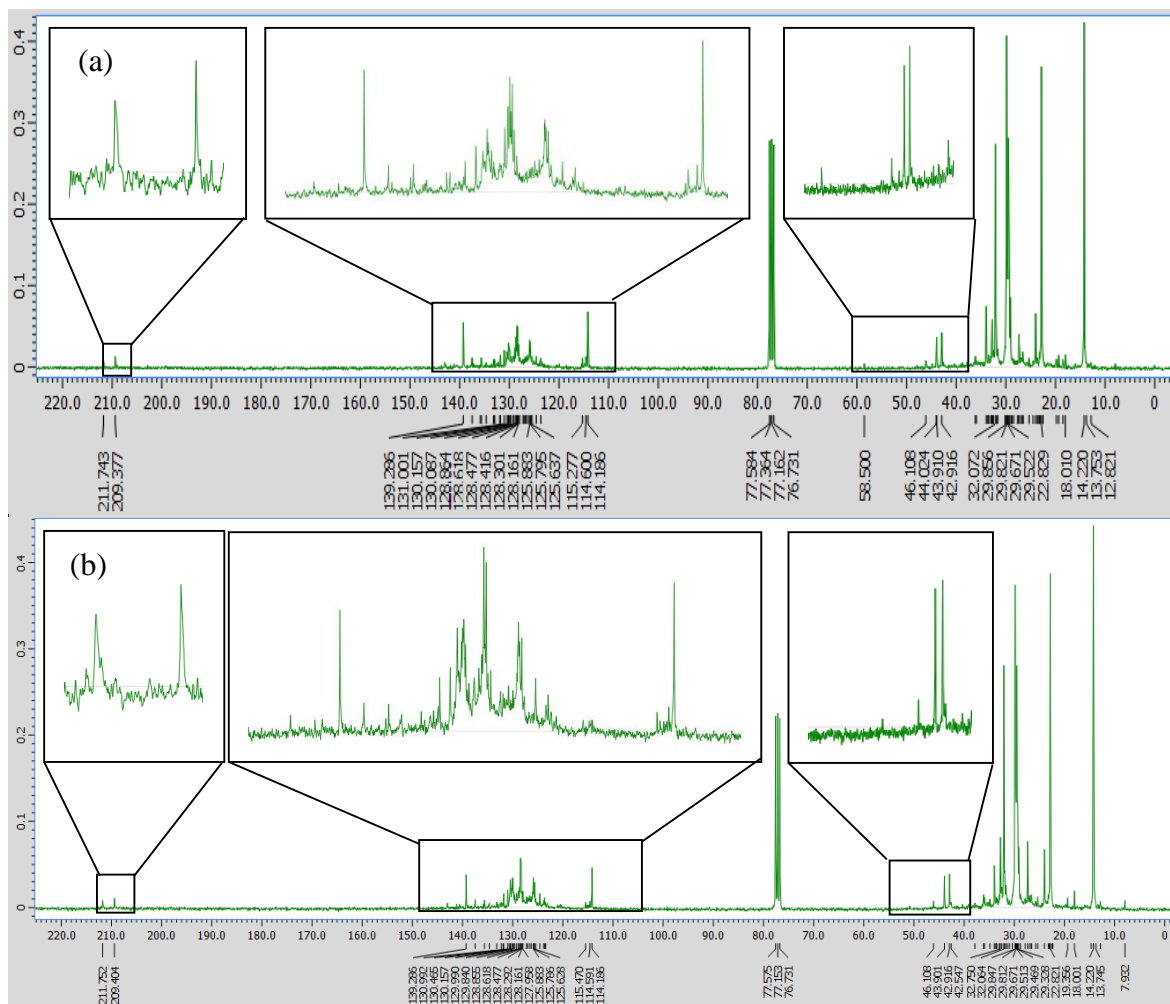


Figure 21. ^{13}C NMR of the ESP oil from the regenerated red mud catalyzed pyrolysis of the (a) HSF and (b) the EVOO at 450 °C.

4.3.3. Pyrolysis gas product composition

The gas product composition (wt. %, dry basis) from the conventional/catalytic pyrolysis of the HSF and the SR are shown in Table 23. During the thermal cracking of the HSF, the major gas products were carbon dioxide and $\text{C}_2\text{-C}_5$ hydrocarbons, which represented 44.16 % and 40.58 %, respectively, of the total gases. The CO and hydrogen accounted for 6 % and 1.5 % of the total gases. The gas product from the pyrolysis of the

SR consisted mainly of carbon dioxide (79.26 % of total gases). The C₂-C₅, CO, and H₂ accounted for 7.77 %, 6.95 %, and 0.71 %, respectively. The CO and CO₂ produced during the thermal cracking of the SR were 66.07 % and 157.09 % higher than those produced from the HSF. When considering the gas product composition from the fast pyrolysis of the OMWS, the hydrogen yield of the latter was higher than both yields from the HSF and the SR thermal cracking experiments. This observation implied that there was synergistic effect when both HSF and SR were pyrolyzed together as OMWS.

The catalytic pyrolysis of the HSF and the SR affected the gas product composition significantly. For the HSF, the use of red mud as catalyzed increased the hydrogen yield by 417.86 %. The CO and CO₂ yields increased by 64.29 % and 26.91 %, respectively. In addition to the water-gas-shift reaction, the high hydrogen yield could be due to the dehydrogenation, and/or aromatic cyclization⁵ of paraffins in the OMWS and/or the formation of aromatics from olefins by Diels-Alder reaction.¹⁷ During the RRM catalyzed pyrolysis of the HSF, the CO₂ yield increased by 26.91 % and the pyrolytic water yield increased by 30 % relative to the non-catalytic pyrolysis. The CO yield increased by 64.29 %. Therefore, the deoxygenation of the pyrolysis vapours over RRM occurred through decarbonylation, dehydration, and decarboxylation. As for the red mud catalyzed pyrolysis of the SR, the major gas was CO₂, and it accounted for 78.71 % of the total gases.

Compared to the conventional pyrolysis of the SR, the catalytic pyrolysis increased the hydrogen and CO₂ yields by 82.14 % and 197.94 %, respectively. The CO concentration increased by 133.04 %. During the RRM catalyzed pyrolysis of the SR, the pyrolytic water yield increased by 19.6 %, the CO₂ yield increased by 15.89 %, and the CO

yield increased by 40.32 %. Therefore, the deoxygenation of the SR pyrolysis vapours over RRM was through decarbonylation, decarboxylation, and dehydration. The non-condensable gas from the catalytic pyrolysis of the EVOO over RRM had similar composition as the gas from the HSF pyrolysis over RRM. The CO yield from the EVOO experiment was higher than that from the HSF, whereas the CO₂ yield was lower. This observation could be explained by the fact that the triglycerides in the EVOO give rise to acrolein and ketene after thermal cracking (~300 °C), these compounds produce CO and hydrocarbons at higher temperatures (400-500 °C) (Crossley et al., 1962). Since the triglycerides content of the EVOO is much higher than that of the HSF, the CO yield from the EVOO experiment was higher than that from the HSF one.

When HZSM-5 was used as the catalyst, the main gas product from the HSF was the C₂-C₅ hydrocarbons, which accounted for 82.75 %. Compared to the conventional pyrolysis, the HZSM-5 catalyzed pyrolysis of the HSF resulted in 666.36 % increase in the C₂-C₅, while the hydrogen yield decreased by 50 % compared to the fast pyrolysis. The CO increased by 410.71 %, and the CO₂ decreased by 67.64 %. It appears that the pyrolysis vapours of the HSF underwent severe cracking over HZSM-5, which was supported by the drastic increase in the gas yield (275.8 %) compared to the conventional pyrolysis. Furthermore, the pyrolytic water yield from the HZSM-5 experiment increased by 52.86 %. It appears that the deoxygenation of the HSF pyrolysis vapours over the HZSM-5 took place through decarbonylation and dehydration. The CO yield during the HZSM-5 experiment was 63.13 % higher than that from the RRM one, and the pyrolytic water yield was 76.2 % higher than that from the RRM one.

Consequently, the carbon and hydrogen losses were greater during the HZSM-5 experiment compared to the RRM one, hence the lower HHV of the HZSM-5 pyrolysis oil. The gas product from the catalytic cracking of the SR over the HZSM-5 consisted of CO₂ (51.71 %) and C₂-C₅ (20.49 %). Compared to the conventional pyrolysis, the HZSM-5 catalyzed pyrolysis of the SR resulted in the decrease in the CO₂ yield by 102.18 % and an increase in the C₂-C₅ yields by 176.44 % compared to the conventional pyrolysis experiment. The CO however increased by 19.89 %. It is worth noting that when the HZSM-5 was used, the hydrogen yield decreased by 21.05 % for the SR and by 50 % for the HSF compared to the conventional pyrolysis, probably because of the partial hydrocracking of the coke on the HZSM-5 and/or the hydrogenation of alkene on the Brønsted acid sites in the catalyst.

During the HZSM-5 catalyzed pyrolysis of the SR, the pyrolytic water yield increased by 4.52 %, the CO₂ yield decreased by 31.59 %, and the CO yield increased by 19.89 %. Therefore, the deoxygenation of the SR pyrolysis vapours over HZSM-5 occurred through decarbonylation and dehydration. During decarbonylation, for each oxygen atom rejected, a carbon atom is lost, whereas during decarboxylation only one carbon atom is lost per 2 atoms of oxygen (CO₂). On the other hand, the pyrolytic water produced during the RRM catalyzed pyrolysis of the SR was higher than that produced during the conventional pyrolysis and during the HZSM-5 catalyzed pyrolysis. During the dehydration reaction, for each oxygen atom rejected as water molecule, 2 hydrogen atoms are lost. Since the HHV is proportional to the hydrogen and carbon content of the bio-oil, the oil from the RRM catalyzed pyrolysis of the SR had its HHV slightly lower than that of the oil from the

HZSM-5 experiment. This explanation was supported by the elemental analysis of the ESP oils from the catalytic pyrolysis of the SR over RRM and HZSM-5.

The carbon content of the HZSM-5 oil was similar to that of the RRM oil, whereas the hydrogen content of the latter was slightly lower than the former. Farther, the oxygen and/or chlorine content of the RRM pyrolysis oil was similar to that from the HZSM-5 pyrolysis oil. Despite the minor differences in the HHV and the elemental composition, the RRM and HZSM-5 catalytic oils had roughly the same HHV which was slightly lower than the HHV of the non-catalytic oil.

The CO/CO₂ ratio of the conventional and catalytic pyrolysis of the HSF are shown in Figure 22 and those of the SR are presented in Figure 23. During the conventional pyrolysis of the HSF, the average CO/CO₂ ratio was stable at approximately 0.12. The catalytic pyrolysis of the HSF over HZSM-5 resulted in a higher CO/CO₂ ratio that was around 10 times higher than that of the fast pyrolysis for the first hour of the experiment then decreased gradually to stabilize around 1.5. Even after partial loss of the HZSM-5 activity, the corresponding CO/CO₂ ratio was still 7 times higher than that of the fast pyrolysis. As for the RRM catalyzed pyrolysis of the HSF, the CO/CO₂ was stable at around 0.22 for the 2 hours experiment. The CO/CO₂ was slightly higher than that of the conventional pyrolysis of the HSF. During the conventional pyrolysis of the SR, the CO/CO₂ ratio was roughly stable around 0.9. The catalytic pyrolysis resulted in an increase of the CO/CO₂ ratio. For the first hour of the experiments, the average CO/CO₂ ratio of the HZSM-5 experiment was around 0.16, whereas that of the RRM experiment was 0.1. The CO/CO₂ ratio was always higher for the catalytic pyrolysis compared to the conventional one.

Table 23. Gas product composition (wt. %) for the conventional/catalytic pyrolysis of the OMWS fractions and EVOO at 450 °C, using three times the minimum fluidization velocity

	Sand			HZSM-5			RRM			
	OMWS	HSF	SR	OMWS	HSF	SR	OMWS	HSF	SR	EVOO
H ₂	0.33	0.28	0.19	0.03	0.14	0.15	0.71	1.45	0.51	1.35
CO	1.37	1.12	1.86	1.31	5.72	2.23	2.26	1.84	2.61	2.09
CO ₂	13.22	8.25	21.21	14.22	2.67	14.51	18.45	10.47	24.58	9.96
CH ₄	0.81	0.47	0.53	0.17	0.06	0.29	0.67	0.42	0.64	0.44
C ₂ -C ₅	3.44	7.58	2.08	4.12	58.09	5.75	3.63	6.51	1.82	6.86
Unknown	0.67	0.98	0.89	1.23	3.52	5.13	0.93	1.04	1.07	1.99

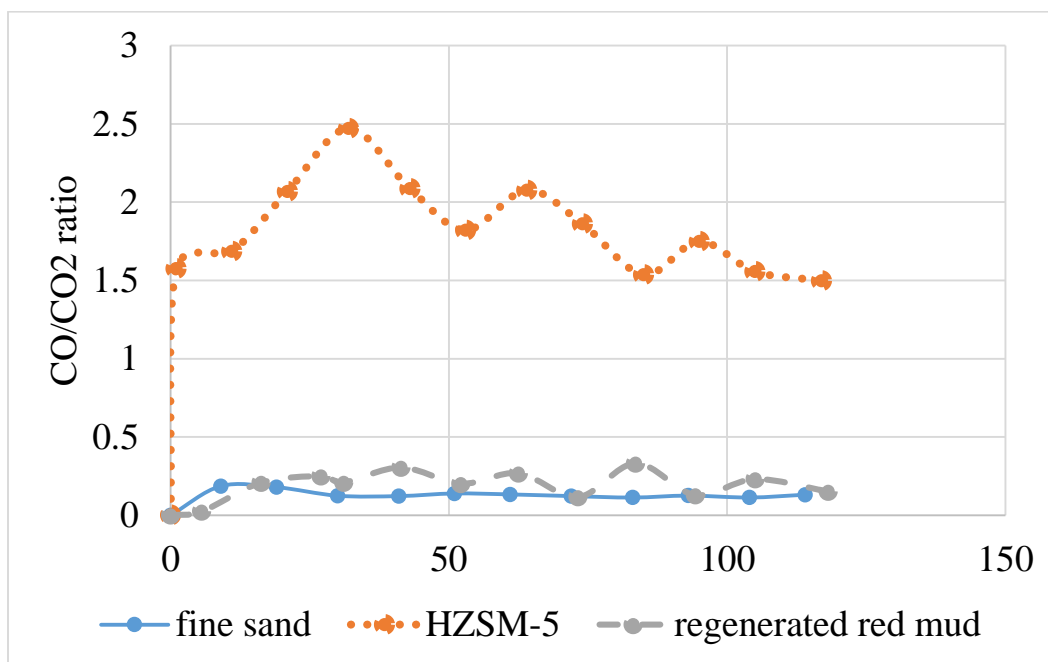


Figure 22. CO/CO₂ ratio of the conventional/catalytic pyrolysis of the HSF

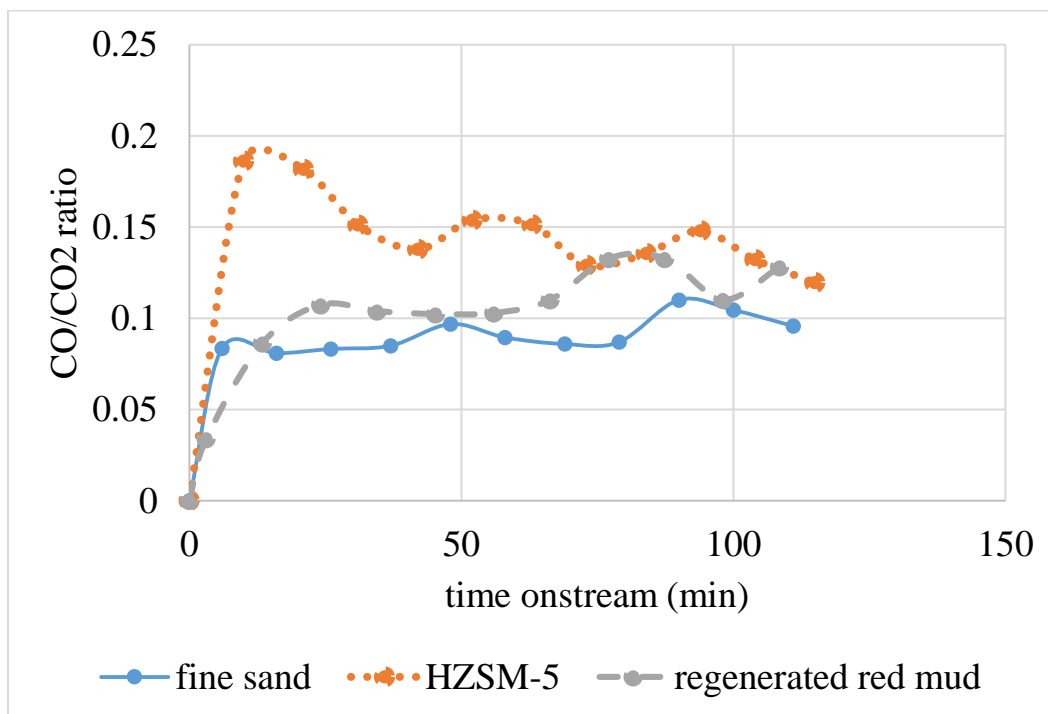


Figure 23. CO/CO₂ ratio of the conventional and catalytic pyrolysis of the SR

4.4. Conclusions

- The catalytic pyrolysis of the OMWS fractions produced bio-oils with significantly different physical-chemical properties. The catalytic pyrolysis of the HSF produced an acidic, low viscosity oil with high energy content, whereas the SR produced an oil with higher pH, higher viscosity and lower energy content. The HSF bio-oils were roughly nitrogen and sulfur free, whereas the SR bio-oils contained both of these undesirable elements.
- The bio-oil from the catalytic pyrolysis of the HSF and SR consisted of aliphatic and aromatic hydrocarbons. The SR bio-oil contained more heteroatoms (O and/or N) than the HSF bio-oil.
- The low viscosity and high energy content of the OMWS catalytic bio-oils were due to the HSF fraction, whereas the close to neutral pH as well as the nitrogen content were due to the SR fraction.

4.5. References

- (1) Brunetti, N.; Bonfitto, E.; Di Giacomo, G.; Del Re, G. In *European Cooperative Networks on Rural Energy. Workshop on Charcoal Production and Pyrolysis Technologies*; Roros, Norway, 1991, pp 91–97.
- (2) Demirbas, A. *Fuel* **2008**, 87 (8-9), 1743–1748.
- (3) Encinar, J. M.; González, J. F.; Martínez, G.; Román, S. *J. Anal. Appl. Pyrolysis* **2009**, 85 (1-2), 197–203.
- (4) Uzun, B. B.; Pütün, A. E.; Pütün, E. *J. Anal. Appl. Pyrolysis* **2007**, 79 (1-2 SPEC. ISS.), 147–153.
- (5) Chang, C. C.; Wan, S. W. *Ind. Eng. Chem.* **1947**, 39 (12), 1543–1548.

- (6) Crossley, A.; Heyes, T. D.; Hudson, B. J. F. *J. Am. Oil Chem. Soc.* **1962**, *39* (1), 9–14.
- (7) Benson, T. J. Elucidation of reaction pathways for catalytically cracked unsaturated lipids, Mississippi State University, 2008.
- (8) Bielansky, P.; Weinert, A.; Schönberger, C.; Reichhold, A. *Biomass Convers. Biorefinery* **2012**, *2* (1), 53–61.
- (9) Fahmi, R.; Bridgwater, A. V.; Donnison, I.; Yates, N.; Jones, J. M. *Fuel* **2008**, *87* (7), 1230–1240.
- (10) Chiaramonti, D.; Oasmaa, A.; Solantausta, Y. *Renew. Sustain. Energy Rev.* **2007**, *11* (6), 1056–1086.
- (11) Oasmaa, A.; Solantausta, Y.; Arpiainen, V.; Kuoppala, E.; Sipilä, K. *Energy and Fuels* **2010**, *24* (2), 1380–1388.
- (12) Amaral, C.; Lucas, M. S.; Coutinho, J.; Crespí, A. L.; do Rosário Anjos, M.; Pais, C. *Bioresour. Technol.* **2008**, *99* (15), 7215–7223.
- (13) Aviani, I.; Raviv, M.; Hadar, Y.; Saadi, I.; Dag, A.; Ben-Gal, A.; Yermiyahu, U.; Zipori, I.; Laor, Y. *Bioresour. Technol.* **2012**, *107*, 87–96.
- (14) Ntougias, S.; Gaitis, F.; Katsaris, P.; Skoulika, S.; Iliopoulos, N.; Zervakis, G. I. *Chemosphere* **2013**, *92* (4), 399–405.
- (15) Miranda, T.; Esteban, A.; Rojas, S.; Montero, I.; Ruiz, A. *Int. J. Mol. Sci.* **2008**, *9* (4), 512–525.
- (16) Lu, Q.; Zhang, Z. F.; Dong, C. Q.; Zhu, X. F. *Energies* **2010**, *3* (11), 1805–1820.
- (17) Schwab, A. W.; Dykstrab, G. J.; Selkeo, E.; Sorensonb, S. C.; Prydeo, E. H. *J. Am. Oil Chem. Soc.* **1988**, *65* (11), 1781–1786.

CHAPTER 5

SUMMARY AND CONCLUSIONS

The goal of this thesis was to valorize the olive mill wastewater sludge through its catalytic pyrolysis over two different catalysts i.e. red mud, a waste product from the Bayer process, and the synthetic catalyst HZSM-5. This goal was achieved through the elaboration of four chapters that included:

1. Characterization of the olive mill wastewater sludge.
2. Catalytic pyrolysis of the olive mill wastewater sludge.
3. Catalytic pyrolysis of the olive mill wastewater sludge fractions.

The characterization phase revealed that the OMWS was a potential feedstock for bio-fuels production because it consisted of 41.16 wt. % hexanes soluble fraction which had oleic acid and palmitic acid as the major compounds. The high ash content, however, would increase the char/coke yield at the expense of the organic yield. The high nitrogen content of the biomass was a nuisance because it will be collected in the bio-oil.

Compared to the conventional pyrolysis, the catalytic pyrolysis of the OMWS produced bio-oils that were at least 6 times less viscous and had at least 2 times less oxygen. Red mud had different cracking chemistry from the HZSM-5, however, the former produced bio-oil that was less viscous and had lower oxygen content than that produced over the latter.

450 °C was the optimal reaction temperature at which the maximum pyrolysis liquid product yield was obtained. The organic yield from the red mud experiments were higher than those from the HZSM-5 ones.

The char/coke yield of the red mud catalyzed pyrolysis was higher than that of the HZSM-5 one, however the activity of the former was less affected by the catalyst time on stream compared to the latter. The red mud promoted the water gas shift reaction as well as the Fisher-Tropsch reaction.

The red mud could be tuned depending on the desired outcome of the pyrolysis reaction. The reaction temperature had a significant effect on the pyrolysis yields and viscosity of the bio-oil. The deoxygenation of the pyrolysis primary vapors was mainly through dehydration. The red mud favored decarboxylation over decarbonylation, whereas the HZSM-5 promoted decarbonylation over decarboxylation.

The catalytic pyrolysis of the HSF produced an acidic, low viscosity oil with high energy content and was nitrogen and sulfur free, whereas the SR catalytic pyrolysis produced an oil with close to neutral pH, higher viscosity, lower energy content, traces of sulfur, and considerable nitrogen content. The HSF could be used as feedstock for the production of green diesel from catalytic pyrolysis. Based on the CO/CO₂ ratio evolution during the catalytic pyrolysis experiments, both catalysts exhibited higher activity during the cracking of the HSF compared to the cracking of the SR.